THERMAL EFFECTS IN LUBRICATION OF ROLLERS WITH A NON-NEWTONIAN FLUID

by

DHANESHWAR PRASAD

DEPARTMENT OF MATHEMATICS

INDIAN INSTITUTE OF TECHNOLOGY, KANPUP

DECEMBER, 1987

THERMAL EFFECTS IN LUBRICATION OF ROLLERS WITH A NON-NEWTONIAN FLUID

A Thesis Submitted
In Partial Fulfilment of the Requirements
for the Degree of

DOCTOR OF PHILOSOPHY

by

DHANESHWAR PRASAD

to the

DEPARTMENT OF MATHEMATICS

INDIAN INSTITUTE OF TECHNOLOGY, KANPUR

DECEMBER, 1987

Dedicated to
My Parents
As a token of
Love and Regards

CERTIFICATE

This is to certify that the matter embodied in the thesis entitled 'THERMAL EFFECTS IN LUBRICATION OF ROLLERS WITH A NON-NEWTONIAN FLUID' by Mr. Dhaneshwar Prasad for the award of the degree of Doctor of Philosophy of the Indian Institute of Technology, Kanpur, is a record of bonafide research work carried out by him under our supervision and guidance. The thesis has, in our opinions, reached the standard fulfilling the requirements of the Ph.D. degree. The results embodied in this thesis have not been submitted to any other University or Institute for the award of any degree or diploma.

(Punyatma Singh)
Thesis Supervisor
Department of Mathematics
Indian Institute of Technology,
Kanpur-208016, U.P.
INDIA

(Prawal Sinha)
Thesis Supervisor
Department of Mathematics
Indian Institute of Technology,
Kanpur-208016, U.P.
INDIA

December 1987

ACKNOWLEDGEMENTS

I wish to express my deep sense of gratitude to my thesis supervisors Prof. Punyatma Singh and Dr. Prawal Sinha, Department of Mathematics, Indian Institute of Technology, Kanpur, for their invaluable advice and guidance during the preparation of this thesis.

I am indebted to Prof. J.B.Shukla, Prof. M.R.M.Rao and Dr. P. Chandra for many interesting and useful discussions with them.

I am grateful to Prof. R. K. Jain and Prof. J.D. Borwanker, Head of the Department of Mathematics, I.I.T. Kanpur for providing me an excellent facilities to carry out this work. The affection and kindness shown to me by Prof. U.B.Tewari and Prof. O.P. Juneja is also sincerely acknowledged.

I am also grateful to Dr. S.S. Prasad, Department of Mathematics, Magadh University (Bodhgaya) and Dr. M. Prasad, Department of Mechanical engineering, I.I.T. Kanpur, who have been a source of inspiration and encouragement during the period of present work.

I am thankful to all my friends, in particular to Mr. A.K. Singh, Mr. P. Vellaisamy, Mr. J.K. Prasad and P. Abraham for their help and moral support.

I sincerely acknowledge the splendid company of Dr. J. Patel with whom I chatted and enjoyed a lot. The

association with Dr. J.K. Mishra has been a rich experience in itself and has made my stay here a remarkable event.

Whatever little I have done so far owes more than anyone to my dear parents , brothers and sister . I am **eter**nally indebted to them for their unfailing affection and care throughout my career as a scholar. And , of course , no list is complete without a word of appreciation to my wife and children for their forbearance throughout this venture.

Finally , I thank Mr. Ashok Kumar Bhatia for his extensive patience in excellent typing of this thesis, Mr. A.N. Upadhya for neat cyclostyling and Mr. B.N. Srivastava for drawing nice figures.

D. Prasad

Dec.1987 (DHANESHWAR PRASAD)

SYNOPSIS

of the

Ph.D. Thesis

on

THERMAL EFFECTS IN LUBRICATION OF ROLLERS WITH A NON-NEWTONIAN FLUID

by

DHANESHWAR PRASAD
Department of Mathematics
Indian Institute of Technology
Kanpur, INDIA

December, 1987

Lubrication is a part of tribology, the science and technology of interacting surfaces in relative motion and of related subjects and practices . In the process of interaction, part of the energy supplied to it is lost due to undesirable frictional forces opposing the motion. Lubrication practice is an art of controlling these frictional forces, reducing wear , distortion etc. by introducing some kind of lubricant in the separation gap formed by the interacting surfaces (bearing). This lubricant plays a vital role during the process of lubrication of bearings. Bearings are very important for the successful development of the modern science and engineering. It seems rather impossible to imagine the progress of the advanced technology without the application of bearings.

Separation between the bearing surfaces under the principle of hydrodynamic lubrication is achieved due to viscous shearing action of the fluid. This mechanism works very well in case of lubricated rolling bearings, which form an integral part of majority of machines.

The lubricant, under the hydrodynamic lubrication of heavily loaded rolling bearing, is subjected to very high shear stresses and velocity gradients. The resulting extremes of pressure and temperature act on the lubricant for a very short duration which may cause the lubricant to behave as a non-Newtonian fluid [12]. In addition increasing use of additives (high molecular weight polymers) in the lubricant is also responsible for the deviation of its behaviour from Newtonian [3]. A number of fluid rheological models have been postulated to account for the non-Newtonian behaviour. One such model is that of the power law which has found extensive applications in recent years [4].

The lubricant temperature field is the consequence of hydrodynamic lubrication process which consists essentially of two surfaces in relative motion shearing a thin layer of viscous fluid film. This temperature field becomes stronger in case of heavily loaded contacts. Since the lubricant viscosity is strongly dependent on temperature, it becomes necessary to acquire knowledge of temperature field in the lubricant [5].

There are several other factors which can influence the temperature and pressure field in the lubricant. The fluid inertia is one of them which is generally small and may be neglected in comparison to viscous force. However, with the current trend towards design of bearings operating with high speeds, and use of lubricants having low viscosities and high densities, the lubricant inertia may attain significance for some range of moderately large Reynolds numbers [6]. This effect may become stronger in case of thick film bearing under squeezing motions [7].

Another important factor affecting the bearing lubrication characteristics is the compressibility effect. The compressibility effect may not be neglected for high speed flows or flows with large variation of pressure and temperature [8]. In fact the density is also sensitive to exceedingly high temperatures and pressures.

The classical lubrication theory constitutes the solution to the standard form of Reynolds equation. However, much of the modern lubrication theory deals with the departure from it. This departure may be due to the thermal effects, inertia forces, compressibility, undetermined film thickness and non-Newtonian behaviour of the lubricant (as mentioned earlier). The present thesis work is devoted to the study of some of these important factors. The thesis consists of a general introduction and five chapters.

General introduction is introductory in nature. It starts from the field of terminology followed by history of lubricated bearings and a literature survey (theoretical and experimental) of lubricant rheology, fluid rheological models, thermal and inertia effects and compressibility. It may be noted that attention has been focussed mainly on the problem of lubricated rolling/sliding contacts.

In chapter I, a theoretical problem of pure rolling of two identical rigid cylindrical rollers moving with equal speed and lubricated with an incompressible power law fluid is considered under the usual assumptions of hydrodynamic lubrication. The lubricant consistency m is assumed to vary exponentially with pressure and temperature. The moving boundaries are assumed to be adiabatic. The modified Reynolds and energy equations are derived and are solved numerically for various values of the flow index n and the squeezing parameter q. Pressure, temperature and the film cavitation point are computed. It is observed that the effect of temperature on consistency is to shift the position of pressure peak slightly away from the centre line of contact. Pressure and temperature increase significantly with n, however both decrease as q increases. The consistency change in the pressure peak region is quite significant.

Chapter II deals with a similar geometry followed by a similar theoretical approach. The difference appears here due to the fact that the lubricant is assumed to be compressible. The lubricant density is assumed to vary with pressure as well as temperature. In view of the extra complication which arises due to the consideration of compressibility effect, squeezing effect has been dropped. Pressure , temperature, load and traction etc. are calculated for compressible as well as incompressible fluids. Compressible load and traction are found to be comparatively higher than those for incompressible case. The compressibility effect is found to be significant for Newtonian as well as dilatant fluids.

In chapter III also, the geometry of the problem and the mathematical formulation remain the same, as in chapter I, however, the adiabatic assumption is relaxed here. The heat of convection which is comparatively smaller to that of conduction is neglected. The lubricant consistency is assumed to be dependent on pressure and the mean film temperature. Various bearing characteristics such as pressure , the mean film temperature, load and traction are calculated as functions of n and q. The bearing characteristics depict a similar trend with respect to n and q as in chapter I.

The problem done in chapter IV is similar to that of chapter III. The difference here is that the fluid inertia and convection terms are retained in the momentum and the energy equations respectively. The presence of inertia and convection terms makes the solution very complicated. Thus averaged values of both the terms have been considered. The results for various bearing characteristics with and without inertia have been calculated. It is observed that the inclusion of inertia force leads to increase in pressure and thus also the load. Squeezing motion is found to have significant effect on inertia.

The last problem done in chapter V is also a generalized version of the problem formulated in chapter III. The major difference here is that both the rollers are assumed to have different dimensions and velocities, squeezing effect is here dropped. Various important results are calculated for various values of n and sliding parameter $\bar{U}$.

REFERENCES

[1] Yousif, A.E. and Bogi, K.D., The rheological behaviour of a new high temperature synthetic grease, Proc. Instn. Mech. Engrs., London, 1970.

[2] Rashid, M. and Seireg, A., Heat partition and transient temperature distribution in layered concentrated contacts: Part 1-Theoretical model, J. Tribology, 109(1987)487.

[3] Dayson, A., Thickness of very thin film in EHD lubrication, Discussion of the Faraday society, No.1(1971)231.

[4] Sinha P. and Singh C., Lubrication of cylinder on a plane with a non-Newtonian fluid considering cavitation, J. Lub. Tech., 104(1982)168.

[5] Safar, Z. and Szeri, A.Z., THD lubrication in laminar and turbulent regimes, J. Lub. Tech., 96(1974)48.

[6] You, H.I. and Lu, S., Inertia effect in hydrodynamic lubrication with film rupture, J. Tribology, 109(1987)86.

[7] Hashimoto, H. and Wada, S., The effects of fluid inertia forces in parallel circular squeeze film bearings lubricated with pseudo-plastic fluids, J. Tribology, 108(1986)282.

[8] Shih-I Pai, Viscous flow theory II, D. Van Nostrand company, Inc. (1957), P.252.

NOMENCLATURE

A	$(n/(2n+1))^n$
$\bar{A}$	$1/\alpha p_s$
A_n	$n^2/(2n+1)(3n+1)$
B_n	$2(2n+1)/(3n+2)$
c	specific heat of lubricant at constant volume
c_n	$((4n+2)/n)^n (U/h_o)^n (2R/h_o)^{1/2}$
c_p	specific heat of the lubricant at constant pressure
d_n	$n/((3n+1)2^{n+1})$
$\bar{D}$	a number as defined in (4.15)
E_t	dimensionless number ($= U^2\beta/c$)
f	$X^2-X_1^2+2q(X+X_1)$ (Chapter IV)
f	$H-\rho^* H^*/\rho_1$ (Chapter II)
$\bar{f}$	$X^2-X_1^2+2q(X+X_1)$ (Chapter I)
$\bar{f}$	$H-\bar{\rho}^* H^* e^{-\bar{A}\bar{p}_1+\bar{\varepsilon}(\bar{T}_1-\bar{T}_o)}$ (Chapter II)
F	$X^2-X_1^2+2q(X+X_1)$
G	$-F$
$\bar{F}$	a number as defined in (4.15)
g	$-H+\rho^* H^*/\rho_2$
$\bar{g}$	$-H+\bar{\rho}^* H^* e^{-\bar{A}\bar{p}_2+\bar{\varepsilon}(\bar{T}_2-\bar{T}_o)}$
h	film thickness
h_o	minimum film thickness
h^*, h_1	film thickness at the point of maximum pressure
h_2	film thickness at $x = x_2$
H	$1+X^2$
H^*	$1+X^{*2}$

H_1	$1+X_1^2$
$I_n(X)$	inertia term defined by relation (4.23)
$J_f(X)$	viscous term as defined in (4.23)
$J_{-f}(X)$	viscous term as defined in (4.33)
k	lubricant thermal conductivity
k_1	$(Uh_o/(4k\alpha))(h_o/2R)^{1/2}$
$\bar{K}$	βk_1
m	lubricant consistency
m_o	consistency at ambient pressure and temperature
$\bar{m}$	consistency $(=2mc_n^{\alpha})$
$\bar{m}_o$	consistency at ambient pressure and temperature $(=2m_o c_n^{\alpha})$
n	flow behaviour index
p	hydrodynamic pressure
$\bar{p}$	pressure$(=\alpha p)$
p_s	bulk modulus of compressibility
P_r	$(ch_o/4k\alpha U)(h_o/2R)^{1/2}$
q	squeezing parameter $(=\frac{V}{U}(R/2h_o)^{1/2})$
r	radius of the cylinder
R	equivalent radius
S	$1+X_1^2-2q(X+X_1)$
T	lubricant temperature
$\bar{T}$	temperature $(=\beta(T-T_o))$ (Chapter I)
$\bar{T}$	temperature $(=\beta T)$ (Chapter II, IV and V)
T_f	traction force

T_F	dimensionless traction force ($=-T_f/(h_o/2\alpha)$)
T_h	surface temperature (constant)
$\bar{T}_h$	temperature ($=T_h/k_1$) (Chapter III)
$\bar{T}_h$	($=\beta T_h$) (Chapters IV and V)
T_o	ambient temperature
$\bar{T}_o$	temperature ($=T_o/k_1$) (Chapter III)
$\bar{T}_o$	temperature ($=\beta T_o$) (Chapter IV and V)
T_{ol}	surface temperature at y = o
$\bar{T}_{ol}$	βT_{ol}
T_m	the mean film temperature as defined in relation (3.6)
$\bar{T}_m$	mean temperature ($=T_m/k_1$) (Chapter III)
$\bar{T}_m$	mean temperature ($=\beta T_m$) (Chapter IV and V)
u	lubricant viscosity in x-direction
$\bar{u}$	u/U
$\bar{u}_m$	the mean velocity as defined in (4.14)
U	velocity of the cylinder in pure rolling
$\bar{U}$	U_1/U_2
U_1	velocity of the plane surface
U_2	velocity of the cylinder under rolling/sliding contacts
v	velocity of the lubricant in y-direction
$\bar{v}$	velocity ($=(2v/U)(2R/h_o)^{1/2}$)
V	V/2 is the normal velocity of the cylinder
W_x	load in x-direction
W_X	dimensionless load ($=W_x/(2h_o/\alpha)$)

W_Y	dimensionless load $(=W_y/((2Rh_o)^{1/2}/\alpha))$
x, y	co-ordinate axes
x^*, x_1	$-x^*$ or $-x_1$ is the point of maximum pressure
x_2	cavitation point
X	dimensionless distance $(=x/(2Rh_o)^{1/2})$
Y	dimensionless distance $(=2y/h_o)$
X^*	$1+X^{*2}$
X_1	$1+X_1^2$
X_2	cavitation point $(=1+X_2^2)$
α	pressure coefficient
β	temperature coefficient
γ	$P_r E_t (n/(3n+1))$
$\bar{\gamma}$	$\beta/(\rho c \alpha)$ (Chapter I)
$\bar{\bar{\gamma}}$	$\beta/(\rho_o c_p \alpha)$ (Chapter II)
γ_1	$P_r E_t (n/(4n+1))$
$\bar{\gamma}_s$	$U_2 h_o \beta (h_o/2R)^{1/2}/(k\alpha)$
δ	locus of points at which lubricant velocity gradients vanish and is measured from y = o
$\bar{\delta}$	δ/h_o
$\bar{\delta}_2$	a value of $\bar{\delta}$ at $X = X_2$
δ^*	values of δ at $x = \pm x_1$
$\bar{\delta}^*$	δ^*/h_o
λ	$\rho U^2 \alpha$
ρ	lubricant density
ρ^*	lubricant density at $x = -x^*$
$\bar{\rho}$	ρ/ρ_o

ρ_o the lubricant density at ambient pressure and temperature

$\bar{\rho}$ ρ / ρ_o

ρ_2^* density of the lubricant $X = X_2$

ε temperature coefficient

$\bar{\varepsilon}$ ε / β

Subscripts :

1.2 Usually refer to the respective quantities in the inlet and the outlet regions separated by the point at which velocity gradient vanishes otherwise explicitely mentioned.

Bar denotes dimensionless number.

CONTENTS

GENERAL INTRODUCTION

1. LUBRICATION OF BEARING/FIELD TERMINOLOGY :

Lubrication is a part of 'tribology', the science and technology of interacting surfaces in relative motion and of related subjects and practices [1]. As the interaction between surfaces occurs during the process of sliding, rolling etc., part of the energy supplied to it is lost due to undesirable frictional forces opposing the motion. Lubrication practice is an art of controlling these forces, reducing wear, distortion etc., by introducing some kind of substance between these interacting surfaces having a relative motion. Insertion of such substance between the mating surfaces makes them operate more efficiently, i.e. it serves to separate rubbing surfaces, aids in the removal of heat, prevents rust formation, protects bearing from dirt and minimizes maintenance etc.. This substance is called a lubricant. The most commonly used lubricants are oils and greases. However, it is not unusual to use other liquid substances, as well as solid and air as lubricants.

Bearing is a machine component or a part whose function is to support a second member , preventing its motion in the direction of applied load but at the same time allowing motion in another predetermined direction [2]. It is not a matter of surprise that the longstanding appreciation of the importance and applications of bearings are quite unlimited.

It seems impossible to imagine the progress of modern science and technology without the application of bearing which forms an integral part of the majority of machines. One look at the devices and machines which typify present day civilization is enough for realizing how important successful bearing operation is to our daily living.

The general theme which runs through the consideration of bearings of whatever type is that a bearing must be considered from three aspects , no one of which is completely separable from others. These aspects are : (1) the design of bearing ; (2) the material of bearing ; and (3) the lubricant (used). No bearing is completely designed without proper consideration and integration of these three aspects [3]. Bearing analysis (especially rolling bearing) together with the third aspect will be the point of discussion within the frame work of this thesis.

The rolling contact bearings utilize the rolling action of balls and/or rollers having point or line contacts , and hence exercise minimum rolling frictional resistance. Rolling contact bearings are usually employed to allow either rotary motion or relative linear motion and sometimes a combination of both the types of motions [4]. A historical development has been given in the subsequent section.

2. HISTORY OF LUBRICATED BEARING AND RECENT DEVELOPMENTS :

The art of lubrication was known many centuries ago and lubricants such as animal fats , vegetable oils and even mineral oils were available. The chariot wheel, axle of which had been lubricated with a sticky greasy type substance (during the era of Egyptian Pharaohs), perhaps reminds of the early days of lubrication [5]. It was not until the end of 19th century that the true nature of lubrication mechanism was fully understood and a new branch of fluid mechanics , known as lubrication mechanics , was formed [6]. Hirn [7] who may be called the father of lubrication, discovered film lubrication in 1854. But the first research credit goes to Tower in England and Petroff in Russia [8]. An experiment on oil lubricated bearing conducted by Tower [9] in reply to a mistaken idea provided a break through in this field. He explained that the interacting surfaces might be separated by an oil film without metallic contact. He further concluded that a loaded oil bearing might be subjected to local pressure substantially higher than its mean pressure. This experiment attracted the attention of Prof. Reynolds [10] who was the first to give a complete mathematical formulation related to Tower's experiment. This was followed by Sommerfeld [11]. Ever since , this field has never lost its momentum because of its wide application in science and technology. Since the onset of the atomic age , bearing lubrication and other

scientific progress has occured virtually at an exponential pace. Today in the space age , continually increasing demands are being made on various sophisticated engineering equipments containing bearings. This has necessitated a reappraisal of the bearing design procedure in order to minimize frictional resistance and mitigate other undesirable phenomena.

Rolling element bearing is of relatively recent origin, so far as its common engineering application is concerned, dating back roughly to the year 1900 [3]. The principles involved were known many centuries ago but it is only with the advent of modern materials and techniques, the rolling element bearing has found extensive use. Since 1960, substantial attention has been given to the mechanism of rolling bearing lubrication and the rheology of lubricants. Manufacturers for world wide markets increased substantially in the seventies which have served to provide standard bearings of outstanding performance at relatively low cost to the consumers [4]. The advantages/disadvantages over other types of bearings are clear because rolling friction is far less than that of others. This has been discussed by Wilcock and Booser [3].

Mathematical treatment, of lubricated bearing is quite complicated. In the early days researchers working in this field were acquainted with the fact that the assumptions, such as no slip, isoviscous, isothermal, Newtonian lubricant

etc., are not valid for bearing under severe operating conditions. Consequently their theoretical results were not in good agreement with the experimental observations. It was thus realized that those assumptions cannot be made in order to get closer agreement with the experiment. With the advent of fast digital computers and various numerical techniques (FDM, FEM, BEM etc.), mathematical treatment became easier and analysts began to relax assumptions and more realistic solutions were obtained. However even today there exists no mathematical treatment which takes into account all the factors likely to influence lubrication characteristics. A theoretician must therefore resort to a gradual relaxation in the assumptions.

3. LUBRICANT RHEOLOGY :

Rheology is the science dealing with the deformation and flow of materials. Its significance in the field of lubrication has arisen in part from the realization that the lubricant, especially between gears and rollers, is subjected to quite high shear stresses and velocity gradients. The rheological properties of lubricant are therefore likely to have important effects on its actions [12]. Serious attention was paid to the rheology of lubricants in the sixties however the mechanism of bearing lubrication is not yet fully understood. It is also known that rheological properties of the lubricant in the proximity of the solid

surface change significantly. Particularly this phenomenon is evident when the additives in the lubricant are surface active in the EHD regime [13-14].

With the increasing demands being placed on lubricants for automotive engines, transmission and high speed loaded machinery much attention has been paid to the development of improved lubricants (mineral oils with additives). The first successful engine lubricant additive was produced by California Research Corporation in 1935 when the addition of Aluminium Naphthenate was successful in overcoming the sticking of Caterpilar diesel engine [15]. A small percentage of these chemical additives is incorporated to satisfy those demands that the natural properties of mineral oils cannot adequately cope with. Additives are used to fulfil specific requirements such as anti-oxidants (Sodium soap), anti-wear (Calcium soap), E P additives (Lithium soap), corrosion inhibitors (Aluminium soap), friction modifiers (Barium soap), metal deactivators (Aluminium complex), pour-point depressants (Bentonite clay), tackiness additives (Silica) and water repellants (Carbon/ Graphite) etc..

Kingsbury [16] may be considered to be the pioneer as far as the rheological abnormalities in lubrication is concerned. He observed enhancement of viscosity of the fluid in the region of attraction of the surface molecules of the metals. Needs' [17] experiment on rheological behaviour is

of great importance and interest. He squeezed fluids between two steel plates and found that a stable residual film was formed. Though some of his observations are questionable, it appears reasonable that an alteration of liquid film occurs near the bounding solid surface which makes it substantially more viscous compared to the bulk of the liquid. Fuks [18- 19] also conducted a number of experiments in support of Needs' observations, using an apparatus similar to that used by Needs. The works of Fuks and Needs were a matter of controversy and criticism, mainly by Hayward and Isdale [20]. They pointed out that the asperities on the solid surface might account for residual film. The dirt and the undissolved material in the fluid film have been also offered as an explanation. More recently Cameron et al [21-24] studied the influence of surface active compounds in viscous lubricating systems. The lubricants were pure Paraffins, mainly Hexadecane and other long chain polymer compounds. It was concluded that the oil film was influenced by the additive and solvent. Paul and his co-workers[25-27] and others [28] examined lubricant rheology experimentally on the basis of structural rearrangement under high shear stresses. It was convincingly demonstrated that the change in rheological properties comes out to be significant. Hirst and his co-workers [29-30] also examined lubricant rheology during impact theoretically and experimentally, using mineral oils and silicon fluids. He came up with a conclusion that these fluids

exhibited non-Newtonian behaviour (non-linear relation between shear stress and the rate of strain). Further, using a model for non-Newtonian fluid, he showed a good agreement with the experiment. Walter [31] presented a survey on the development on theoretical and experimental rheology which provides an adequate justification for the increasing importance of the rheology in lubrication studies.

4. FLUID RHEOLOGICAL MODELS :

It is well known that many mineral oils which are most commonly used as lubricants manifest non-Newtonian behaviour under severe operating conditions. The changes in the stress and the rate of strain are so rapid that the viscous linear model (Newtonian) is no longer adequate [32-35]. Johnson [36] pointed out that if the shear stress in a typical lubricant exceeds $\approx 10^6$ Pa, the fluid exhibits non-Newtonian behaviour. This behaviour is usually encountered under heavily loaded conditions. It was pointed out earlier that the additives (such as high molecular weight polymers) are used in mineral oils to obtain or enhance many properties that the ordinary mineral oils do not possess. The presence of these polymer additives in mineral oils is responsible for deviation from the Newtonian behaviour. Non-Newtonian behaviour may also be displayed due to the presence of impurity in the lubricant. Further the dirt particles collected during the process of lubrication and manufacturing may make the operating lubricant non-Newtonian.

A number of empirical fluid models have been suggested to account for non-Newtonian effects in lubrication. A Bingham plastic flow model, a first approximation to describe the behaviour of grease lubrication, has been used extensively. Milne [37] presented a theoretical study of grease lubricated slider bearing using this model. His analysis showed the existence of cored regions in the grease film. Sasaki et al [38] also used the same model and presented a theoretical study of grease lubricated roller bearing on the basis of cored regions. Wada et al [39] studied EHD lubrication between two cylinders using the same model where the plastic velocity and yield stress of the lubricant were assumed to be dependent on pressure. Experimental work on velocity determination in a grease lubricated cylindrical sliding/rolling contact has also been reported. Mutuli et al [40] made comparison between the theoretical results of a parabolic velocity distribution similar to that of a Newtonian fluid, derived from a Bingham plastic flow model.

Burton [41] studied the lubrication of rollers using Newtonian and non-Newtonian viscoelastic Maxwell model. A comparison of results (pressure distribution) for both the models indicates that shear elasticity can have effects of first order significance on both the magnitude and form of pressure distribution functions reducing load carrying capacity and maximum shear stress in the film by sizeable amounts. Walter [31] modeled the polymer thickened oil as elastoviscous

fluid and made various observations on lubrication of gears and rollers. Johnson and Tevaarwerk [42] formulated a new rheological equation on the lubricant by addition of a linear elastic element to non-linear viscous element. This model was further extended to include thermal effects by Houpert [43]. Bair and Winer [44] offered a modified Maxwell model that yields good agreement with the experiment. Heyes and Montrose [45] also made a theoretical study of EHD small strain behaviour of lubricant using viscoelastic model that involves reformulation of the Maxwell model in terms of Volterra convolution integral equation. Phan-Thien [46] studied flow of viscoelastic fluid squeezed between two parallel plates. It has been shown that the difference between two forces acting on the top and bottom plates is entirely an inertia phenomenon and arises due to the acceleration of the top plates (bottom plate is stationary). He and his co-workers also studied the squeezing problems with Maxwell fluid [47], Oldroyd fluid [48], and real elastic liquid [49].

Hsu and Saibel [50] used the constitutive relation (cubic) which is applicable to pseudoplastic and dilatant fluids. They found that for the pseudoplastic case the load capacity is less than that of Newtonian. Wada and Hayasi [51] analysed the hydrodynamic lubrication of a journal bearing by pseudo-plastic fluid both theoretically as well as experimentally. They also concluded that the load capacity, drag force and pressure distribution are reduced when compared to the

performance of Newtonian lubricant. Further Wada et al [52] applied the same model for cylindrical rollers including EHD effect and arrived at a similar conclusion. Very recently Wada and his co-workers [53] applied the same constitutive relation for a parallel circular squeezing film bearing including the effect of inertia and obtained various bearing characteristics considering sinusoidal squeezing motion.

Among the various models postulated to describe the flow behaviour of a non-Newtonian fluid, the power law model has perhaps found the most extensive application in various fields [54-58]. It is also probably the most criticized and most maligned model in all of rheology [59]. The appeal of this model is however evident when n, the flow behaviour index, is unity the model reduces to the Newtonian. For $0 < n < 1$, it describes a rheogram with the shape of a pseudoplastic fluid. For $n > 1$, the curve characteristic of dilatant behaviour is found. Furthermore, from the values of n one can readily obtain a qualitative picture of the degree of shear-rate dependence shown by a given material. The breadth of the application is shown in table 1 where a list of power law constants has been compiled [59-61].

Dayson and Wilson [62] were perhaps among the earliest researchers who used the power law model in lubrication. They examined the EHL capabilities of silicon fluids (modeled by power law) and concluded that they are poor lubricants for heavily loaded sliding surfaces due in part to the thinner EHD films formed as a result of their non-Newtonian behaviour. Safar and Shawki [63] studied a general solution for pressure distribution and load capacity for a hydrodynamic thrust bearing operating with power law lubricants. It was established that the load capacity of the bearing may be increased several folds with increasing value of the viscometric exponent n. Safar [64-65] applied the same model for journal bearing under steady and dynamic loading conditions and arrived at the same conclusion. Sinha et al [66] studied the lubrication of rollers under lightly loaded condition using this power law model and analysed load and traction ratios as functions of flow index n and squeezing velocity ratio q. A table for the points of cavitation was also presented with respect to n and q. Further Sinha and Raj [67] considered this problem for heavily loaded case where the consistency variation m was also accounted for. Salem et al [68-69] applied the same model for spherical bearing. They also emphasized on the consistency variation and extended the same problem for non-isothermal case. Dein and Elrod [70] formulated a generalized Reynolds equation for this model, applicable to journal bearing.

Elkouh et al [71] studied the laminar squeezing between two annular surfaces using this model. Further they generalized this to include the effect of difference in pressures at inner and outer boundaries [72]. A theoretical study of short journal bearings performance characteristics for the same fluid model was presented by Buckholz [73]. Fluid film pressure profiles in short bearing of arbitrary azimuthal length has been obtained using matched asymptotic expansions in the slenderness ratio. Further he and Hwang [74] discussed the accuracy of the short bearing approximation applicable to Newtonian as well as non-Newtonian power law lubricants. Raj [75] used this model for various geometries in his entire dissertation work. Nailwal [76] also used this model to study seal behaviour.

Apart from this, there are several other non-Newtonian models which have been used theoretically and experimentally and it is beyond the scope of this thesis to refer to all the non-Newtonian models.

5. THERMAL EFFECTS :

With the present day tendency towards limit design , it is becoming increasingly important that the bearing operating characteristics be predicted accurately. Because of the strong dependence of lubricant viscosity on temperature, it becomes necessary to acquire knowledge of the temperature field in the lubricant [77].

The temperature field in the lubricant is the consequence of hydrodynamic lubrication process which consists essentially of two surfaces in relative motion shearing a thin layer of viscous fluid film. With the exception of bearings running at low speeds, the heat balance is an important part of the analysis of bearing operating with fluid film. The operating temperature of the bearing is also of interest because the fatigue strength of the bearing material is a function of temperature.

In order to account for thermal effects, the classical isothermal theory of hydrodynamic lubrication has to be extended. Energy balance equation is required and has to be solved simultaneously along with the conservation equations of mass and momentum. Coupling of these governing equations makes the solution very complicated and further simplification (approximation) may be necessary.

Another approach for the consideration of thermal effects in lubrication has also been reported. Viscosity-temperature relation has been replaced by viscosity film thickness relation on the assumption that the highest temperature occurs in the zone where the film thickness is least [14,78]. This approach does not incorporate energy equation at all, so the complexity of the problem made by energy equation is overcome. But on the other hand, the temperature field in the lubricant is not fully known. It seems therefore that this way of approach has been used sparingly.

A number of papers [79-82] touched upon the effects of temperature on hydrodynamic bearing performance and requirements. Tipei and Nica [83-84] obtained the three dimensional temperature variation of journal bearing oil film. Separate relationship were established for both the convergent and divergent regions of the bearing taking into account viscosity variations and side leakage. The theory was found to be in good agreement with the experimental data obtained. McCallion et al [85] studied the thermal effects by obtaining solutions to momentum and energy equations for adiabatic and THD conditions. They compared the results with isothermal case and found that THD solution lies somewhere between isothermal and adiabatic. Crook [86-87] considered the effect of temperature on lubrication of rigid cylindrical rollers by a Newtonian incompressible fluid theoretically and experimentally. Pressure, temperature distributions, film thickness and traction curves were plotted for various parameters. Cheng and Sternlicht [88-89] considered very general case of non-isothermal lubricating layer, presenting an account of viscosity and density changes over the length and thickness of the film between two non-rigid cylinders rotating with unequal speeds. Numerical solutions to the coupled Reynolds and energy equations were presented for hydrodynamic conditions. Dayson [90] studied the effect of non-Newtonian linear and non-linear Maxwell fluid model on the rolling/sliding contact. He signified the region of contact in terms of linear, non-linear and thermal

regions and presented the variation of apparent viscosity with pressure and rolling speeds and made comparison between linear and non-linear models. A case of EHD traction for a very particular non-Newtonian model was analysed by Kannel and Walowit [91]. They compared their results for traction with Crook's results (considering viscosity variation with pressure and temperature). Johnson and Greenwood [92] extended Crook's result on the effect of shear heating on EHD traction, using an Eyring fluid rather than a Newtonian fluid. Conry [93] solved thermal EHD problem for some fluid to compare the predicted tractions with those obtained experimentally. Ghose and Hamrock [94] presented a numerical solution to the problem of thermal EHL of line contact using finite difference formulations. Pressure and temperature distributions and film shape for fully flooded conjunctions were obtained for a Paraffinic lubricant and various dimensionless speed parameters while the dimensionless load and material parameters were held constant. Houpert et al [95] analysed the rheological and thermal effects in lubricated elliptical Hertzian contacts with collinear speeds. Stress, temperature and shear strain rate distributions along and across the film were calculated for non-Newtonian visco-elastoplastic fluid including lubricant convection and conduction effects. Further Houpert [96] calculated traction force in EHD contact using Ree-Eyring fluid model and Roelands relationship [97] for

estimating lubricant viscosity. The Ree-Eyring shear stress is found to be greater when the Roelands viscosity relationship is used. Szeri [98] in his most recent paper emphasized on THD effect in lubrication of gear teeth. He suggested that in bearing under severe operating conditions, thermal effects may be significant to the extent that prediction of bearing performance is no longer possible when based on the assumption of a uniform film temperature. There are several other notable papers on thermal effects in lubrication for different geometries [99-101] and it is difficult to refer to all of them.

6. COMPRESSIBILITY EFFECT :

Lubricant compressibility is the measure of change of volume and density when the lubricant film is subjected to pressure and tension. This effect is caused by an abrupt change in pressure and temperature. Pai [102] pointed out that it cannot be neglected for high speed flows or flows with large variation of pressure and temperature. It was supported by Dowson et al [103] who also examined the influence of speed and lubricant compressibility on a theoretical solution to the EHD problem. Speed was shown to be the most important variable in the problem and the inclusion of the lubricant compressibility in the theory was found to have an appreciable influence on pressure distribution but a little effect on minimum film thickness. Since extremes of pressure

and temperature (together with large velocity) are often encountered in the lubrication of gear teeth and rolling contact, this effect or phenomenon attains increasing importance in heavily loaded contacts. The effect of compressibility is overcome by a reduction in the film thickness which modifies the pressure and temperature quite considerably. Change in density might be expected to reduce the magnitude of the pressure recovery near the periphery of the bearing, but accentuate phenomena near the inlet [104].

Houpert and Hamrock [105] who examined the compressibility effect of EHD lubricated line contact by Newtonian fluid emphasized on the point that the maximum density change could be about 35%. Even though this effect is not too significant, it would not be correct to assume incompressibility because a very high pressure in EHD lubricated films is encountered. The other significant contributions on this effect (of isothermal) of EHD lubricated line contact are due to Archard et al [106], Dowson and Whitaker [107], Adams and Hirst [108], Rodkiewicz and Srinivasan [109], Cheng [110], and Evans and Snidle [111] etc..

It was mentioned earlier that the density might change with temperature and pressure. This aspect was elaborated by Cheng and Sternlicht [88-89] using Newtonian lubricants. They studied the very complicated case of thermal EHD line contact and obtained pressure, temperature and film profiles in addition to frictional

force. Hirst and Moore [112] also studied the lubrication of similar geometry but they assumed the fluid to obey the non-Newtonian Maxwell model. They examined this problem using different fluid models and elaborated results through figures and tables. Apart from this there are several other publications regarding compressibility effect in lubrication [26,113-114].

7. INERTIA EFFECT :

The classical Reynolds equation is in general derived under the assumption that the thin lubricant film is laminar and lubricant inertia is negligible. However, with the current trend towards the design procedure for bearing operating with high speeds, and use of lubricants with lower viscosity and higher density, the fluid inertia becomes significant for some range of moderately large Reynolds numbers. This effect becomes even more significant in case of thick film bearing under squeezing motions.

Smalley and Vohr [115] studied the effect of inertia in hydrodynamic lubrication (of isothermal condition) theoretically and experimentally and elaborated the significance of fluid inertia. Wada et al [53] observed that in most of the squeeze film bearings, film thickness is developed due to the viscosity of lubricant. The fluid inertia attains considerable importance as the film thickness and squeezing motion increase. Elkouh [116] studied inertia effect in laminar flow of power law fluids

between two circular plates and concluded that load correction factor, defined as the difference of loads (with and without inertia) divided by absolute value of load without inertia, increases as n decreases. The non-Newtonian model has also been used by Salem et al [69] who incorporated inertia effect in a spherical bearing including thermal effects. They elaborated pressure and temperature as a function of n. Very recently Szeri [98] presented a brief survey on inertia effect in lubrication.

8. IN THIS WORK :

Classical lubrication mechanics constitutes the solution to the standard form of Reynolds equation (i.e. based on idealized conditions of isothermal , highly viscous Newtonian flow etc.) with various boundary conditions simulating various bearing configurations. However much of the modern lubrication theory deals with departure from standard form of Reynolds equation [6]. It was pointed out earlier that such departure may be due to thermal effects, inertia effects, undetermined film thickness and various types of non-Newtonian fluid behaviour etc.. Most recent information [117] about advances in hydrodynamic theory also suggests the incorporation of the following : thermal effects, use of accurate rheological models for the lubricant, evaluation of stress in the materials and considerations of unsteady conditions of loading. The work in this thesis is devoted to the study of some of these

important factors responsible for the departure.

The main factor which is responsible for the departure, in heavy loaded/high speed bearings, is the non-Newtonian aspect, which is invariably encountered. During the last few years, power law non-Newtonian model has found extensive applications. Keeping in view the motivation of recent research and the practical importance of this non-Newtonian model, the power law model is used throughout this thesis. In addition, roller bearing which has advantage over the other bearing configurations is chosen for study in this work.

Another factor responsible for the departure is the effect of temperature (and pressure) on the lubricant consistency m of the power law fluid. Hence for the entire work in the thesis, m is considered to vary with temperature (and pressure). Subsequently the consistency m is assumed to vary with the mean temperature (and pressure) [118]. Use of this mean temperature not only helps in reducing the complexity of the problems but also yields solutions for temperature in closed form.

Other factors considered here are the lubricant compressibility and the inertia effects. Squeezing motion of the rollers with and without inertia has also been incorporated. Finally the rollers are assumed to rotate with unequal speeds.

Table : 1 Representative power law constants

Material	m	n
54.3% Cement rock in water	25.1	0.153
23.3% Illinois yellow clay in water	55.5	0.229
Polystyrene at 300°F	1.6×10^6	0.400
1.5% Carboxymethylcellulose (CMC) in water	97	0.400
0.7% CMC in water	15	0.500
3% Polyisobutylene (Enjay Vistanex L-100) in decalin	9.4	0.770
3.5% Separan	1578	0.119
1% Hydroxyethyl Celulose in 50:50 Water glycerin mixture	128	0.400
2.5 Weight % polyacrylimide Suspension in a 35:65 water : glycerin mixture	86	0.545
Newtonian	0.75	1.000
Eth. glycol/H_2O/glycerine with Sp. gravity 1.240	0.56	1.150
Eth. glycol/H_2O with Sp. gravity 1.222	0.25	1.180

CHAPTER I

THERMAL EFFECTS IN LUBRICATION OF ROLLERS BY A POWER LAW FLUID

1.1 INTRODUCTION :

The isothermal form of Reynolds equation is commonly used to predict the performance of machine components like rolling and sliding element bearings. This standard form of Reynolds equation is valid for the lightly loaded bearing where material properties of the lubricant may be assumed to be constant [119-122].

However, in case of a heavily loaded bearing system under hydrodynamic and EHD conditions, where pressure is very high, material properties of the lubricant cannot remain constant but vary with pressure [123]. Hersey and Lodenslager [124] reported an investigation of the film thickness between rigid gear teeth lubricated by a fluid characterizing a parabolic viscosity-pressure relationship. Blok [125] used exponential viscosity-pressure relation for analysing gear lubrication and concluded that for the fluid following this exponential relation, there was a limiting film thickness at which the maximum pressure became infinite. A survey of the earlier works in this direction has been presented by Dowson and Higginson [126]. Recently, Cameron [127] presented a basic theory on lubrication stressing that the lubricant viscosity is an exponential function of pressure. Mostofi et al [128] also used the same viscosity-pressure relation to analyse the EHD lubricated point contact regime at moderate loads and concluded

that pressure and film thickness vary with material properties (in addition to load and squeeze velocity). Very recently, an isothermal theory of EHL of rollers having sinusoidal roughness, using the same viscosity-pressure relation has been presented by Karami et al [129]. It was observed that use of this relation results in a significant influence of roughness amplitude on the distribution of hydrodynamic pressure and film thickness at constant load and constant roughness wave length.

It has been pointed out earlier (section 4) that heat is generated during the process of lubrication. Imposition of squeezing velocity to the bearing surfaces is likely to generate considerably more heat inside the system [130-131]. Because of strong dependence of viscosity on temperature, it is also important to consider the effect of temperature on viscosity of the lubricant. Zienkiewicz [132] was perhaps the first who initiated the thermal effects in lubrication by assuming a temperature dependent viscosity. Dowson and Whitaker [133] described a numerical procedure for calculating the pressure and temperature distributions and lubricant film profiles at heavily loaded, line contact allowing for the consequence of viscous heating in the lubricant. Agrawal and Wilson [134] also presented a numerical analysis of the flow of a liquid lubricant (characterizing exponential viscosity-temperature relationship) under conditions where viscous

heating leads to a substantial viscosity variation across the film. More recently Heshmat and Pinkus [135] used a similar model in order to study mixing inlet temperatures in hydrodynamic bearings. Giordano and Boudet [136] studied the flow of lubricant between two parallel plates having unequal speeds, assuming the lubricant viscosity to vary with both pressure as well as temperature. He analysed a THD case and on comparing with the isothermal case, he found a significant difference between these results. The importance of thermal effects has also been verified experimentally [137-138].

In addition, the tendency towards 'limit design' increases the need for better tools to calculate bearing characteristics accurately. Thus the selection of an appropriate fluid model to analyse the operating characteristics in a better way, is also necessary. Although, Newtonian model with exponential viscosity variation with respect to pressure and temperature [139] is the simplest and the most widely used one. But it cannot meet the specific requirements of many engineering applications where different additives in the lubricating oils are used. These oils with long chain polymer additives have non-Newtonian behaviour i.e. the viscosity of the lubricant is not constant, but usually exhibits non-linear relation between shear stress and the strain rate [140]. One can therefore, assume the fluid to be non-Newtonian. The power law fluid is one of the

most viable and practical non-Newtonian models which has been used extensively in recent years [141].

Despite the fact that the fluid behaviour in lubrication may be non-Newtonian and variation of the material properties of the lubricant (especially apparent viscosity) is important, there are a very few published information [92,95-96,142] where these effects have been incorporated. However, following are probably the only publications where consistency (m) variation of the extensively used power law model has been accounted for : Salem et al [69] who analysed spherical bearing lubricated by power law fluids (characterizing exponential consistency-temperature relationship), did not consider the effect of pressure on m. Sinha and Raj [67] studied roller bearing considering consistency variation with regard to pressure. Raj [75] further extended his work to include thermal effects using the second approach [78]. This approach fails to provide any idea about the lubricant temperature field. Shukla and Isa [143] considered the effect of temperature and pressure on m. However only the squeezing motion of bearings was considered.

The present investigation endeavours to analyse the performance of thermal effects on the lubrication of rigid cylindrical solid by an incompressible non-thixotropic non-Newtonian power law fluid considering squeezing motion and cavitation. The modified Reynolds and energy equations allowing

exponential consistency variation along the film thickness, are obtained for pressure and temperature respectively and are solved numerically.

1.2 MATHEMATICAL ANALYSIS :

Basic Equations : To obtain an expression for rheodynamic study of lubrication, the Reynolds equation has to be reworked to take account of the abnormal viscosity properties of non-Newtonian power law lubricants. The non-linear relation between stress and the rate of strain for a power law fluid is given [33] by

$$\tau_{ij} = m \left| \sqrt{e_{ij} e_{ji}} \right|^{n-1} e_{ij} \quad , \; i,j = 1,2,3 \qquad (1.1)$$

where τ_{ij} is the stress tensor and e_{ij} is the rate of strain, m and n are experimental viscometric constants. For a steady state lubrication of identical rollers rotating with equal speed, as shown in fig. (1.1), and with the usual assumptions of hydrodynamic lubrication , the flow equations for a power law fluid are given [139] by

$$\frac{dp}{dx} = \frac{\partial \tau}{\partial y} \qquad (1.2)$$

$$\frac{\partial u}{\partial x} + \frac{\partial v}{\partial y} = 0 \qquad (1.3)$$

where τ (from(1.1)) takes the form

$$\tau = m \left| \frac{\partial u}{\partial y} \right|^{n-1} \frac{\partial u}{\partial y} \qquad (1.4)$$

u and v are the velocity components in the directions of x and y respectively and p is the hydrodynamic pressure.

The most difficult problem in lubricated bearings is the determination of th: operating viscosity. This difficulty arises from the fact that the viscosity of the lubricant varies rapidly with pressure and temperature. This variation does not lend itself to a simple expression in an analytical term. Various theoretical models have been postulated by different researchers. In this thesis, exponential relationship for viscosity has been used throughout. Hence one can write

$$m = m_o \, e^{\alpha p - \beta (T - T_o)} \tag{1.5}$$

where m_o is the value of m at p = 0 and temperature $T = T_o$ (ambient) ; α and β are the coefficients of pressure and temperature respectively.

The flow is assumed to be symmetric about x-axis. Thus, it is sufficient to consider the region for $y \geq 0$. The boundary conditions for the problem are

$$\begin{aligned} u &= U \text{ at } y = \frac{h}{2} \\ \frac{\partial u}{\partial y} &= 0 \text{ at } y = 0 \end{aligned} \tag{1.6}$$

h is the variable film thickness given [107] by

$$h = h_o + x^2/2R \tag{1.7}$$

where h_o is the minimum film thickness and R = r/2, r being the radius of the either cylinder.

Reynolds Equation : Considering the appropriate sign for pressure and velocity gradients [33] for two different

regions as indicated in fig.(1.1), integration of equation (1.2) yields[1]

$$u = U-(\frac{1}{m_1}\frac{dp_1}{dx})^{1/n}(\frac{n}{n+1})\{(\frac{h}{2})^{(n+1)/n}-y^{(n+1)/n}\},\ -\infty\leq x\leq -x_1 \tag{1.8}$$

$$u = U+(-\frac{1}{m_2}\frac{dp_2}{dx})^{1/n}(\frac{n}{n+1})\{(\frac{h}{2})^{(n+1)/n}-y^{(n+1)/n}\},$$

$$-x_1\leq x\leq x_2 \tag{1.9}$$

where $x = -x_1$ and $x = x_2$ are respectively the point of maximum pressure and the point of cavitation.

Integration of equation (1.3) with boundary conditions

$$\begin{aligned} v &= 0 \quad \text{at } y = 0 \\ v &= v_h \text{ at } y = \frac{h}{2} \end{aligned} \tag{1.10}$$

gives [139]

$$-v_h = \frac{\partial}{\partial x}\int_0^{h/2} u\,dy - \frac{U}{2}\frac{dh}{dx} \tag{1.11}$$

where v_h is the resultant of the squeezing velocity $V(\frac{V}{2}$ is the velocity of the either cylinder) and the normal component of rolling velocity U i.e.

$$v_h = \pm\frac{V}{2}+\frac{U}{2}\frac{dh}{dx} \tag{1.12}$$

Substituting u from equation (1.8) in equation (1.11), the Reynolds equation is obtained as

$$\frac{d}{dx}\{(\frac{2n}{2n+1})(\frac{h}{2})^{(2n+1)/n}(\frac{1}{m_1}\frac{dp_1}{dx})^{1/n}-Uh\} = V,\ -\infty\leq x\leq -x_1 \tag{1.13}$$

---

1. m is a function of x-alone because under adiabatic condition T is assumed to be a function of x only (see energy equation).

A similar expression is found for the other region i.e.

$$\frac{d}{dx}\{(-\frac{2n}{2n+1})(\frac{h}{2})^{(2n+1)/n}(-\frac{1}{m_2}\frac{dp_2}{dx})^{1/n} + Uh\} = -V, \quad -x_1 \leq x \leq x_2 \tag{1.14}$$

Equations (1.13) and (1.14) are the modified Reynolds equations for the two specified regions.

Pressure Equation : To solve the above Reynolds equations, the following pressure conditions are used [33]:

$$\left.\begin{aligned} p_1 &= 0 \text{ at } x = -\infty \\ p_1 &= p_2 \\ \frac{dp_1}{dx} &= \frac{dp_2}{dx} = 0 \end{aligned}\right| \text{ at } x = -x_1,\ h = h_1$$

$$p_2 = \frac{dp_2}{dx} = 0 \text{ at } x = x_2,\ h = h_2 \tag{1.15}$$

Integration of equations (1.13) and (1.14) using the above conditions yields

$$\frac{dp_1}{dX} = 2m_1 c_n (X^2 - X_1^2 + 2q(X+X_1))^n / (1+X^2)^{2n+1} \tag{1.16}$$

$$\frac{dp_2}{dX} = -2m_2 c_n (X_1^2 - X^2 - 2q(X+X_1))^n / (1+X^2)^{2n+1} \tag{1.17}$$

where

$$c_n = (\frac{4n+2}{n})^n (\frac{U}{h_o})^n (\frac{2R}{h_o})^{1/2}, \quad q = \frac{V}{U}(\frac{R}{2h_o})^{1/2}$$

$$X = \frac{x}{(2Rh_o)^{1/2}}, \quad X_1 = \frac{x_1}{(2Rh_o)^{1/2}}, \quad X_2 = \frac{x_2}{(2Rh_o)^{1/2}} \tag{1.18}$$

Further, use of the condition $\frac{dp_2}{dx} = 0$ at $x = x_2$ in (1.17) gives

$$X_2 = X_1 - 2q \tag{1.19}$$

With the non-dimensional scheme

$$H = \frac{h}{h_o} = 1 + X^2 \ , \ \bar{m} = 2m\, c_n\, \alpha \ , \ \bar{p} = \alpha p \tag{1.20}$$

equations (1.16) and (1.17) can be rewritten as

$$\frac{d\bar{p}_1}{dX} = \bar{m}_1 (\bar{f})^n / H^{2n+1} \tag{1.21}$$

$$\frac{d\bar{p}_2}{dX} = -\bar{m}_2 (-\bar{f})^n / H^{2n+1} \tag{1.22}$$

where

$$\bar{m}_1 = \bar{m}_o\, e^{\bar{p}_1 - \bar{T}_1} \ ; \ \bar{m}_2 = \bar{m}_o\, e^{\bar{p}_2 - \bar{T}_2} \tag{1.23}$$

and $$\bar{f} = X^2 - X_1^2 + 2q(X + X_1). \tag{1.24}$$

Energy Equation : Heat generation by viscous heating and heat transfer from (or to) bearing both serves to create large temperature variation in the lubricant film. However, in most cases, almost all of the work done on the lubricant is stored in it as internal energy [139], i.e. system may be assumed to be adiabatic. This adiabatic assumption also serves to reduce the complexity of the energy equation.

The steady-state energy equation for an incompressible power law fluid under adiabatic condition may be written as [144]

$$\rho \frac{dE}{dt} = \tau_{ij}\, e_{ij} \tag{1.25}$$

where E is the specific internal energy of the system and ρ is the density of the lubricant. The conduction terms of the energy equation have been ignored completely under adiabatic condition [143,146].

In a generalized thermodynamic approach, the internal energy must be modified. However the basic ideas concerning thermodynamics of systems undergoing deformations are still in the developmental stage [59]. Besides in non-isothermal analysis of power law fluids, it is customary to use the conventional expression for the internal energy [145]. Thus, the energy equation (1.25) for the system under consideration and with the assumptions already discussed, in one dimensional case reduces to

$$\rho c u \frac{dT}{dx} = m \left|\frac{\partial u}{\partial y}\right|^{n-1} \left(\frac{\partial u}{\partial y}\right)^2 \qquad (1.26)$$

where c is the specific heat of the lubricant which is assumed to be constant. Averaging the energy equation (1.26) over the film thickness , one can obtain

$$\rho c \frac{dT}{dx} \int_0^{h/2} u\,dy = m \int_0^{h/2} \left|\frac{\partial u}{\partial y}\right|^{n-1} \left(\frac{\partial u}{\partial y}\right)^2 dy$$

or
$$\frac{d\bar{T}_1}{d\bar{X}} = \bar{\gamma}\bar{m}_1 (\bar{f})^{n+1}/(SH^{2n+1}), \qquad -\infty \leq X \leq -X_1 \qquad (1.27)$$

$$\frac{d\bar{T}_2}{d\bar{X}} = \bar{\gamma}\bar{m}_2 (-\bar{f})^{n+1}/(SH^{2n+1}), \qquad -X_1 \leq X \leq X_2 \qquad (1.28)$$

where

$$\bar{T}_1 = \beta(T_1 - T_o), \quad \bar{T}_2 = \beta(T_2 - T_o)$$

$$S = 1 + X_1^2 - 2q(X + X_1), \quad \bar{\gamma} = \beta/\rho c\alpha$$

Equations (1.27) and (1.28) are the main equations for temperature for the two specified regions.

Solutions : For the first region , $-\infty \leq X \leq -X_1$, logarithmic differentiation of (1.23) implies

$$\frac{1}{\bar{m}_1}\frac{d\bar{m}_1}{dX} = \frac{d\bar{p}_1}{dX} - \frac{d\bar{T}_1}{dX} \tag{1.29}$$

Integration of (1.29) after substituting the expressions for $\frac{d\bar{p}_1}{dX}$ and $\frac{d\bar{T}_1}{dX}$ from (1.21) and (1.27) results in

$$\bar{m}_1(X) = \frac{1}{\frac{1}{\bar{m}_o} - \int_{-\infty}^{X} \left(1 - \frac{\bar{\gamma}\bar{f}}{\bar{S}}\right) \frac{(\bar{f})^n}{H^{2n+1}}\, dX} \quad , \quad -\infty \leq X \leq -X_1 \tag{1.30}$$

Similarly, for the next region, the expression corresponding to (1.30) is

$$\bar{m}_2(X) = \frac{1}{\frac{1}{\bar{m}_o} - \left\{ \int_{-\infty}^{-X_1} \left(1 - \frac{\bar{\gamma}\bar{f}}{\bar{S}}\right) \frac{\bar{f}^n dX}{H^{2n+1}} - \int_{-X_1}^{X} \left(1 - \frac{\bar{\gamma}\bar{f}}{\bar{S}}\right) \frac{(-\bar{f})^n dX}{H^{2n+1}} \right\}}$$

$$-X_1 \leq X \leq X_2 \tag{1.31}$$

Finally the pressure is obtained from equations (1.21) and (1.22) as follows :

$$\bar{p}_1(X) = \int_{-\infty}^{X} \frac{\bar{m}_1(X)\bar{f}^n dX}{H^{2n+1}} \quad , \quad -\infty \leq X \leq -X_1 \tag{1.32}$$

$$\bar{p}_2(X) = \int_{-\infty}^{-X_1} \frac{\bar{m}_1(X)\bar{f}^n dX}{H^{2n+1}} - \int_{-X_1}^{X} \frac{\bar{m}_2(X)(-\bar{f})^n dX}{H^{2n+1}} \quad , \quad -X_1 \leq X \leq X_2 \tag{1.33}$$

These expressions for pressure contain an unknown X_1 which can be determined by using conditions :

$$\bar{p}_1 = 0 \text{ at } X = -\infty \text{ and } \bar{p}_2 = 0 \text{ at } X = X_2 \qquad (1.34)$$

in (1.32) and (1.33), and one can obtain an integral equation

$$\int_{-\infty}^{-X_1} \frac{\bar{m}_1(X)\bar{f}^n dX}{H^{2n+1}} - \int_{-X_1}^{X_2} \frac{\bar{m}_2(X)(-\bar{f})^n dX}{H^{2n+1}} = 0 \qquad (1.35)$$

where X_2 and X_1 are related from equation (1.19).

This integral equation (1.35) can be solved by numerical method giving the value of X_1 and thereafter pressure can be obtained from equations (1.32) and (1.33). Similarly temperature can be obtained from solving equations (1.27) and (1.28).

1.3 RESULTS AND DISCUSSION :

Expressions for various bearing characteristics, (equations (1.21-1.22), (1.27-1.28)), are functions of the flow behaviour index n, velocity ratio $q(= \frac{V}{U}(\frac{R}{2h_o})^{1/2})$ and thermal factor $\bar{\gamma}(= \beta/\rho c\alpha)$. For numerical calculations, the following values are used :

$\alpha = 1.16 \times 10^{-9}$ dyne^{-1} cm^2 , $\beta = 6 \times 10^{-3}$ deg c^{-1},

$\rho c = 2 \times 10^{7}$ erg cm^{-1} degc^{-1}, R = 2.54 cm ; U = 400 cm sec^{-1} ;

$h_o = 10^{-4}$ cm.

Results are computed for pseudoplastic and Newtonian fluids only i.e. for $n \leq 1$. Results for dilatant fluids ($n > 1$) can

also be obtained, provided the initial value of the consistency m corresponding to n > 1 is known. The values of q are not straightforward but one may expect q lying between the two given ranges: (a) $-10^{-2} \leq q \leq 10^{-2}$, which is valid for steady-state lightly loaded condition [148] (b) $-1 \leq q \leq 1$, which is valid for unsteady-state lightly loaded condition [121]. In accordance with our expectation for steady state heavily loaded bearing, q may be assumed to lie in the range : $-.1 \leq q \leq +.1$.

Numerical Method : To evaluate pressure and temperature which develop inside the fluid film, we use equations (1.21-1.22) and equations (1.27-1.28) respectively which contain an unknown X_1. This X_1 is calculated by solving the integral equation (1.35) numerically for various values of n and q, using Simpson rule and bisection method. The point of cavitation X_2 is then calculated by using the formula given in (1.19) and these values are listed in tables (1.1) and (1.2). Finally, the simultaneous equations for pressure and temperature are solved numerically by Runga-Kutta method. The results for dimensionless pressure, temperature and consistency are elaborated through figures.

Pressure Distribution : The dimensionless pressure $\bar{p}$ is plotted versus X , in fig. (1.2) for various values of n and q . It is observed from the figure that for a fixed n , a

numerical increase in -q results in the shift of the position of pressure peak towards the centre line of contact, whereas a numerical increase in +q causes the reversal of the trend. Physically, one may interpret that as the surfaces approach each other with increasing normal velocity, more pressure is generated. The obtained pressure profile as a function of q is quite similar to that of Dowson et al [121].

The variation of pressure with respect to n is similar to that obtained by Safar and Shawki [63]. Pressure increases significantly as n increases whereas the position of pressure peak does not change significantly.

Temperature Distribution : The non-dimensional temperature $\bar{T}$ is depicted in fig. (1.3) versus X for various values of n and q and the location of the point of maximum pressure is marked by X_1 on each curve . The temperature profile shows that there are two temperature dominant regions , one is near the inlet and other near the outlet. These temperature regions show that heat of convection plays an important role there. The existence of the temperature dominant regions in the proximity of the inlet and outlet, only conforms to expectations, since the viscous heating which is caused by non-zero velocity gradients exists in these regions. The importance of heat of convection in the inlet region has been established by Crook [86] and Murch [149].

The velocity gradient at the point of maximum pressure is zero. This causes the temperature to be almost constant in the vicinity of that point. The temperature variation with respect to n and q is almost similar to that of pressure in the region $-\infty \leq X \leq -X_1$. In the other region $-X_1 \leq X \leq X_2$, pressure decreases whereas temperature increases. The effect of temperature on pressure peak is elaborated in Tables (1.1) and (1.2). It is observed from the tables that the effect of temperature is to shift the position of pressure peak towards the left which is in accordance with that of obtained by Cheng and Sternlicht [89].

Consistency Distribution : The main aspect of this analysis is to study the variation of consistency $\bar{m}$ under heavily loaded conditions. The interesting pattern of this variation versus X is clearly demonstrated in fig. (1.4) for various values of n and q. In this figure also the point of maximum pressure is marked on each curve as X_1. For a fixed value of q, consistency decreases with n. This decrease is almost arrested as n reaches the value 0.545. It should be emphasized at this stage that for values of $n \leq 0.545$, a change in q fails to produce a significant variation in pressure, temperature and hence consistency . These curves therefore could not be plotted. For fixed n and for all $q > 0$, the nature of $\bar{m}$ is quite similar to that of pressure (fig. (1.2)) i.e. $\bar{m}$ goes on increasing/decreasing throughout the regions

$-\infty \leq X \leq -X_1$ / $-X_1 \leq X \leq X_2$. In this sense the behaviour of $\bar{m}$ for all $q \leq 0$, is similar to that of mentioned above except near the inlet where temperature dominates pressure. Because of the temperature dominance in this small region, $\bar{m}$ starts decreasing and continues to decrease till the fluid reaches the extreme pressure region. The consistency $\bar{m}$ increases with q in the temperature dominant regions, however in the pressure dominant region , $\bar{m}$ increases as q decreases.

1.4 CONCLUSION :

In this chapter, a generalized Reynolds equation is derived for a power law fluid which lubricates two identical rollers having the same speed. The effects of pressure and temperature (i.e. often encountered in heavily loaded lubricated bearings) on the lubricant consistency is taken into account. The squeezing motion of the bearing surfaces is also accounted for.

The effect of temperature on consistency is to shift the position of pressure peak slightly away from the centre line of contact. However, the pressure peak is found always near the exit of the film (with and without thermal effects).

Squeezing motion of the surfaces also has a significant effect on pressure peaks, the points of cavitation (see tables (1.1-1.?) on pressure and on temperature (see fig.(1.2) and fig. (1.3)). Pressure and temperature increase as squeezing velocity decreases. In addition, the consistency change, especially in the zone where pressure is maximum, is also quite significant.

Table 1.1

Fluids	$\beta = 6 \times 10^{-3}$ X_1	X_2	q
9% hydroxyethyl cellulose in a 50:50 water : glycerin mixture	.40055608	.66055608	-.09
	.44349815	.60349815	-.05
	.49377480	.49377480	0.00
	.54949037	.38949037	0.05
	.57935908	.33935908	0.09
2.5 wt. polyacrylimide suspension in a 35:65 Water:Glycerin mixture	.4429683	.66968331	-.09
	.45148758	.61148758	-.05
	.49848193	.49848193	0.00
	.55133610	.39133610	0.05
	.57953154	.33993154	0.09
Newtonian	.44522361	.68522361	-.09
	.47300519	.63300917	-.05
	.52157510	.52157510	0.00
	.57015684	.41015683	0.05
	.59562448	.35562448	0.09

Table 1.2

Fluids	$\beta = 0$ X_1	X_2	m_o	n
9% hydroxyethyl cellulose in a 50:50 water : glycerin mixture	.40385648	.64385648	128	0.400
	.42665444	.58665444		
	.47597905	.47597905		
	.53022216	.37022160		
	.55913316	.31913316		
2.5 wt. polyacrylimide suspension in a 35:65 Water:Glycerin mixture	.40338498	.64338498	86	0.545
	.42599088	.58599088		
	.47498265	.47498265		
	.52896864	.36896864		
	.55778085	.31778085		
Newtonian	.40019437	.64019437	0.75	1.000
	.42247506	.58247506		
	.47090303	.47090303		
	.52445795	.36445795		
	.55310822	.31310822		

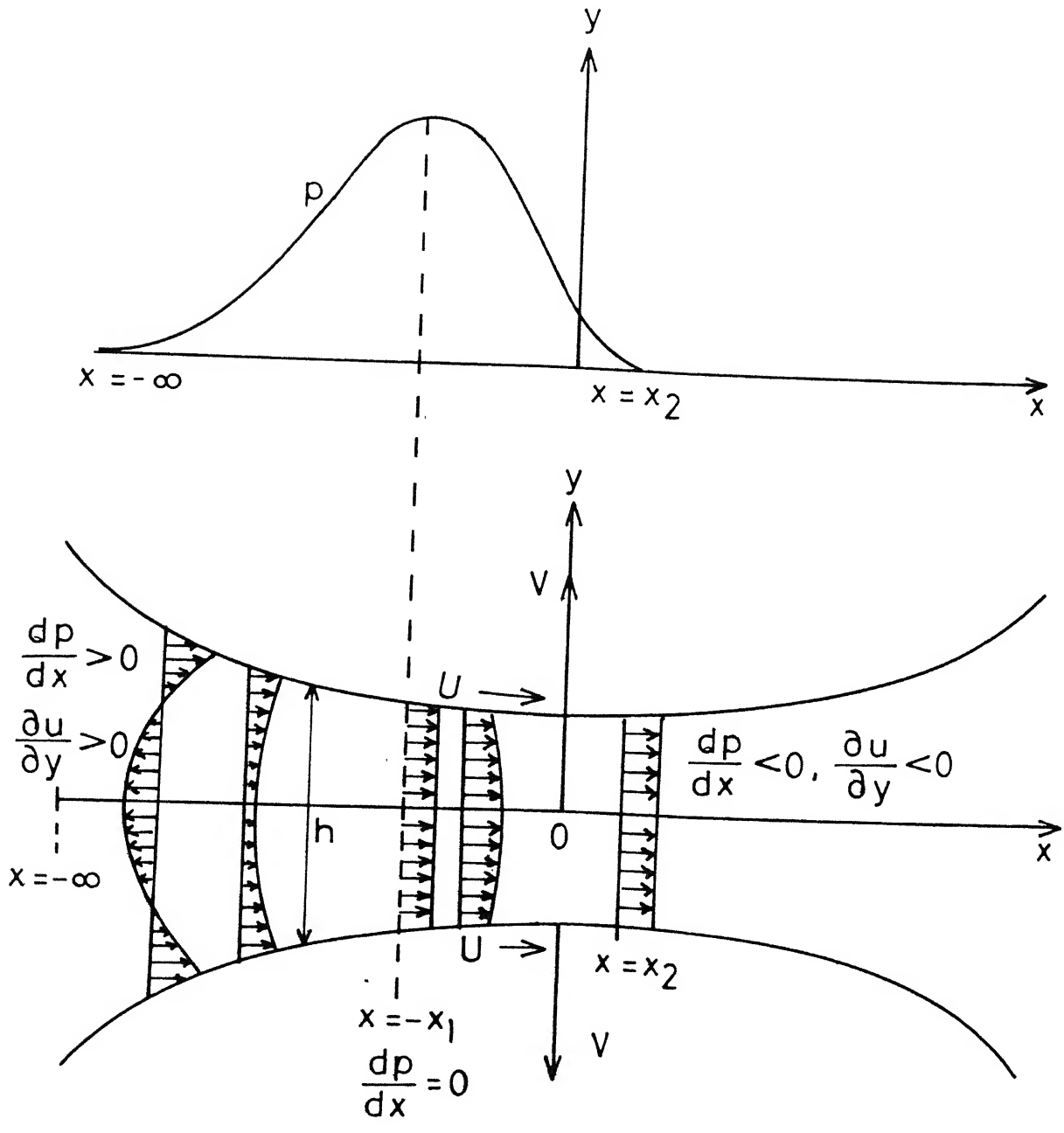

Fig. 1.1 Lubrication of two identical cylindrical rollers together with velocity and pressure profiles.

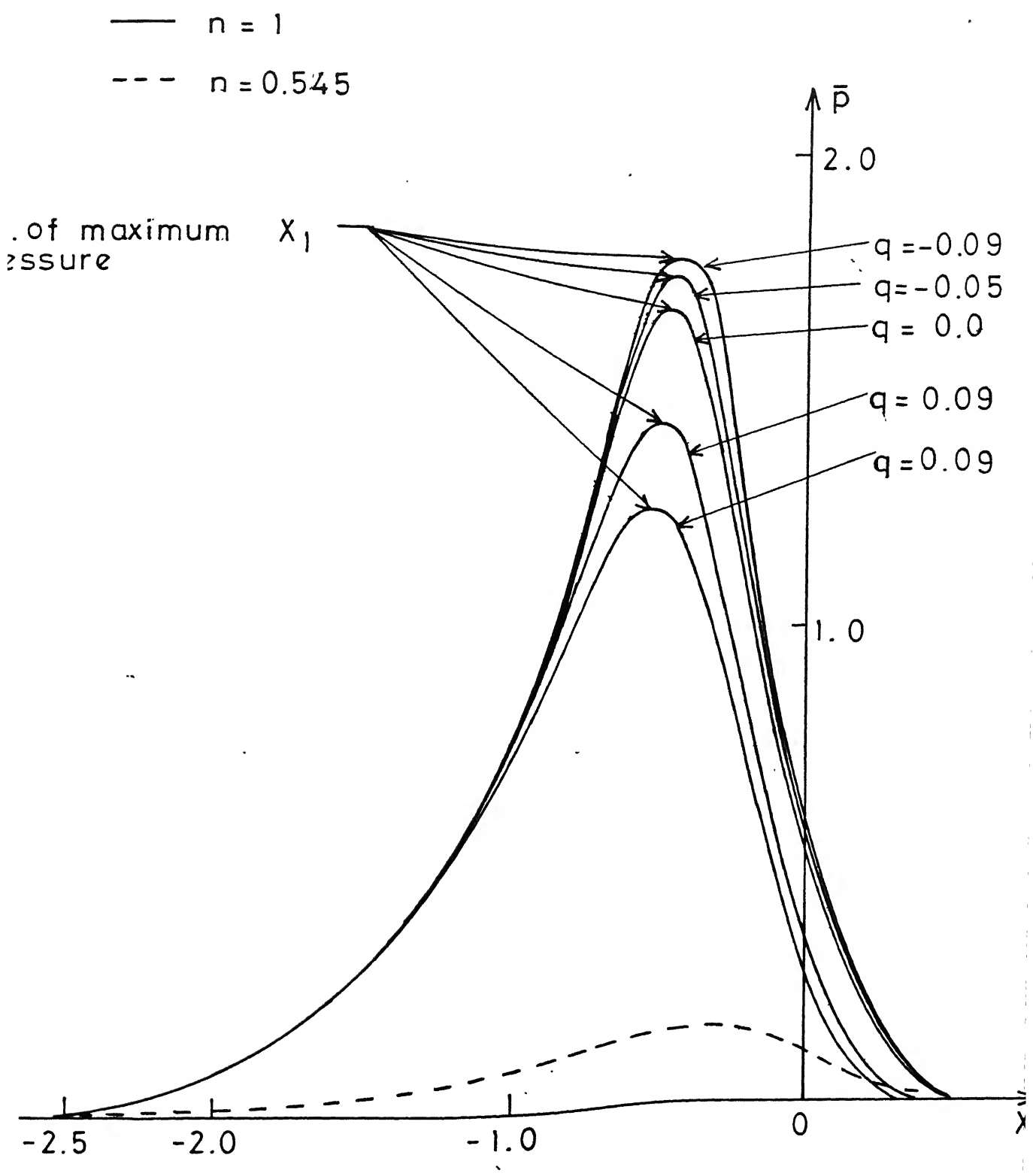

Fig.1.2 Distribution of $\bar{p}$ vs. X.

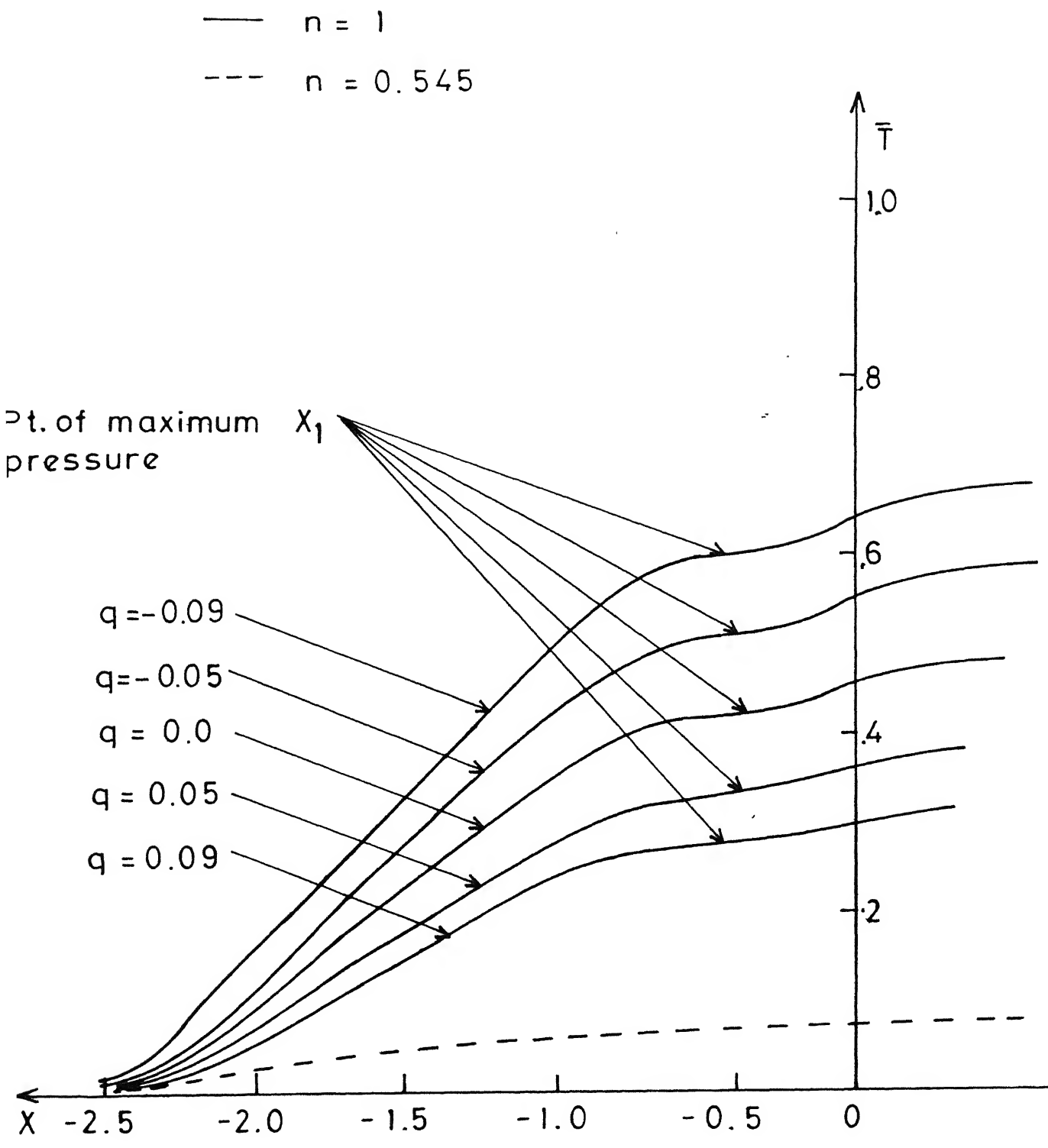

Fig. 1.3 Distribution of $\bar{T}$ vs. X.

CHAPTER[+] II

NON-UNIFORM TEMPERATURE IN NON-NEWTONIAN FLUID FILM LUBRICATION OF ROLLERS

2.1 INTRODUCTION :

It has been emphasized in the previous chapter that extremes of pressures and temperatures are encountered in heavily loaded bearings and material properties of the lubricant do not remain constant. Attention has been focussed mainly on lubricant consistency variation with regard to film pressure and film temperature and a number of references in support of it have been presented. However , another significant property i.e. density also plays an important role in determining lubrication characteristics [129]. The density ρ of the lubricant is also a function of pressure and temperature [150]. In fact ρ increases with pressure and decreases with temperature if the lubricant is liquid. For a gas lubricant ρ increases with temperature. Density ρ may increase by about 20% at exceedingly high pressures [126]. Since the liquid lubricant density ρ increases with pressure and decreases with temperature, the effective density is expected to lie somewhere between the maximum increase due to pressure and the maximum decrease due to temperature. Therefore the compressibility effect assumes a significant importance.

Dowson and Whitaker [107] examined the isothermal lubrication of rigid as well as elastic cylinders by lubricants having pressure-dependent profiles. They observed that the

[+]Accepted by Journal of Tribology, Trans. A.S.M.E.

relevant lubricant properties which were influenced by high pressure were viscosity and density. They made a comparison among pressure curves for compressible fluid (with variable viscosity) and incompressible fluid (with and without variable viscosity) and found appreciable differences among them. Isothermal EHL problem for the case of two rolling cylinders, at different speeds has been presented by Rodkiewicz and Srinivasan [109] where lubricant has been assumed to be compressible throughout the region. Pressure and film thickness profiles have been presented for different rolling velocities. Evans and Snidle [111] studied the isothermal EHL of spheres including compressibility effect and viscosity variation. They also obtained pressure and film thickness profiles. Hamrock and Jacobson [151] outlined a numerical solution of the isothermal EHL problem for line contacts assuming variable viscosity and density. This result was found in good agreement with that of Dowson and Higginson [152]. Lubrecht et al [153] also studied the same problem for isothermal case considering viscosity and density variation with pressure but they applied multigrid method in order to calculate film thickness and pressure profiles. Influence of the compressibility of the lubricant on the minimum film thickness and on pressure spike has been examined. Experimental result on the compressibility of the lubricant has also been reported [26].

In addition, variation of lubricant density with respect to temperature has also been studied [114]. One of the most important observations made by Cheng [88] has already been referenced in which the lubricant density change with respect to pressure as well as temperature was incorporated. Mazumdar [113] presented a THD solution of oil journal bearing where he considered the viscosity and density to be functions of temperature and concluded that this consideration leads to a small decrease in the load capacity when compared with that using constant lubricant properties. Very recently Lebeck [154] also considered the effect of temperature on lubricant significant properties, when he examined lubrication analysis of parallel slider bearing theoretically and experimentally. In his theoretical analysis, an exponential relationship for viscosity and a linear relationship for density has been used. Both the results (theoretical and experimental) have been found in good agreement. Non-Newtonian lubrication of EHD line contacts together with the compressibility effect has also been studied by Houpert and Hamrock [105]. Gross [155] presented a brief survey (of the early work) on thermal effects in lubrication where he concluded that changes in density and viscosity along and across the film can result in a load capacity for the otherwise non-load supporting parallel film. Apart from them there are several informations dealing with variations in lubricant properties and it is difficult to recall all of them.

The present analysis focuses on thermal effects in lubrication of rigid cylindrical rollers by a compressible power law fluid considering cavitation. The properties such as density and viscosity of the lubricant are assumed to vary with pressure as well as temperature. The modified Reynolds and energy equations, allowing exponential consistency and density variation along the fluid film are obtained and are solved numerically. The non-dimensional pressure and temperature profiles, load capacity and traction etc. are obtained and are compared with those for incompressible case.

2.2 MATHEMATICAL FORMULATION :

Basic Equations : Governing equations similar to (1.2) and (1.3) including the lubricant compressibility effect can be written as follows :

$$\frac{dp}{dx} = \frac{\partial}{\partial y}\left(m\left|\frac{\partial u}{\partial y}\right|^{n-1} \frac{\partial u}{\partial y}\right) \tag{2.1}$$

$$\frac{\partial \rho u}{\partial x} + \frac{\partial \rho v}{\partial y} = 0 \tag{2.2}$$

where the consistency m and the density ρ of the lubricant are assumed to vary with pressure and temperature as per the following relationships [86,89]

$$m = m_o \, e^{\alpha p - \beta (T-T_o)} \tag{2.3}$$

$$\rho = \rho_o \, e^{p/p_s - \varepsilon (T-T_o)} \tag{2.4}$$

where ρ_o is the density at the ambient pressure and temperature, p_s is the bulk modulus of compressibility and ε is the coefficient of thermal expansion. Assuming that the flow of the lubricant through the bearing clearence (shown in fig. (1.1)) is symmetric about the x-axis i.e. both rollers are identical and moving with the same speed and T is a function of x-alone (see section 1.2), one may consider fluid flow in the region $y \geq 0$ only.

Using the boundary conditions given in equation (1.6), one can solve equation (2.1) and can obtain

$$u_1 = U - \left(\frac{n}{n+1}\right)\left(\frac{1}{m_1}\frac{dp_1}{dx}\right)^{1/n}\left\{\left(\frac{h}{2}\right)^{(n+1)/n} - y^{(n+1)/n}\right\}, \quad -\infty \leq x \leq -x^* \tag{2.5}$$

$$u_2 = U + \left(\frac{n}{n+1}\right)\left(-\frac{1}{m_2}\frac{dp_2}{dx}\right)^{1/n}\left\{\left(\frac{h}{2}\right)^{(n+1)/n} - y^{(n+1)/n}\right\}, \quad -x^* \leq x \leq x_2 \tag{2.6}$$

where $x = -x^*$ corresponds to the point of maximum pressure, u_1, m_1 and u_2, m_2 correspond the respective quantities in the regions $-\infty \leq x \leq -x^*$ and $-x^* \leq x \leq x_2$. Making use of the conditions (1.10), integration of the continuity equation (2.2) gives

$$-\rho_1 v_h = \int_o^{h/2} \frac{\partial}{\partial x}(\rho_1 u_1)\, dy$$

or $$-\rho_1 v_h = \frac{\partial}{\partial x}\int_o^{h/2} \rho_1 u_1\, dy - \frac{\rho_1 U}{2}\frac{dh}{dx} \tag{2.7}$$

where v_h is the velocity in y-direction at $y = h/2$ and may be written as [67]

$$v_h = \frac{U}{2}\frac{dh}{dx} \tag{2.8}$$

A further simplification of equation (2.7) on substituting u_1 from (2.5) yields

$$\frac{d}{dx}\left[\frac{\rho_1 Uh}{2} - \rho_1\left(\frac{n}{2n+1}\right)\left(\frac{1}{m_1}\frac{dp_1}{dx}\right)^{1/n}\left(\frac{h}{2}\right)^{(2n+1)/n}\right] = 0,$$

$$-\infty \leq x \leq -x^* \qquad (2.9)$$

Similarly for the other region, one can also get

$$\frac{d}{dx}\left[\frac{\rho_2 Uh}{2} + \rho_2\left(\frac{n}{2n+1}\right)\left(-\frac{1}{m_2}\frac{dp_2}{dx}\right)^{1/n}\left(\frac{h}{2}\right)^{(2n+1)/n}\right] = 0,$$

$$-x^* \leq x \leq x_2 \qquad (2.10)$$

Integrating equations (2.9) and (2.10), using the following conditions:

$$\frac{dp_1}{dx} = 0 \qquad x = -x^* \ , \ h = h^* \qquad (2.11)$$
$$\rho = \rho^*$$

One may write

$$\frac{dp_1}{dX} = 2m_1 c_n (f)^n / H^{2n+1} \ , \ -\infty \leq X \leq -X^* \qquad (2.12)$$

$$\frac{dp_2}{dX} = -2m_2 c_n (g)^n / H^{2n+1}, \ -x^* \leq X \leq X_2 \qquad (2.13)$$

where $f = H - \rho^* H^* / \rho_1$ (2.14)

$g = -H + \rho^* H^* / \rho_2$ (2.15)

The dimensionless quantities occuring in equations (2.12) and (2.13) have already been defined in equations (1.18) and (1.20).

The boundary and the matching conditions for the pressure equations (2.12) and (2.13) together with the cavitation boundary conditions are

$$\begin{aligned} p_1 &= 0 \ , \ X = -\infty \\ \rho_1 &= \rho_2 \ ; \ p_1 = p_2 \ , \ X = -X^* \end{aligned} \tag{2.16}$$

$$p_2 = \frac{dp_2}{dX} = 0 \ , \ X = X_2 \tag{2.17}$$

Energy Equation : Assuming that the fluid is compressible and the convection term of the energy equation is dominant (see section 1.2), then the energy equation reduces to the following (see page 706, ref.[89]) under adiabatic condition :

$$\rho c_p u \frac{dT}{dx} = m \left|\frac{\partial u}{\partial y}\right|^{n-1} \left(\frac{\partial u}{\partial y}\right)^2 + \varepsilon T u \frac{dp}{dx} \tag{2.18}$$

where c_p is the specific heat at constant pressure which is assumed to be a constant.

Integrating the energy equation (2.18) with respect to y over the film thickness h and simplifying it, one may obtain

$$\rho_1 c_p \frac{dT_1}{dX} = \frac{2m_1 c_n \left[\varepsilon T_1 H^* + \frac{\rho_1}{\rho^*} f\right]}{H^* H^{2n+1}} (f)^n, \quad -\infty \leq X \leq -X^* \tag{2.19}$$

$$\rho_2 c_p \frac{dT_2}{dX} = \frac{2m_2 c_n \left[-\varepsilon T_2 H^* + \frac{\rho_2}{\rho^*} g\right]}{H^* H^{2n+1}} (g)^n, \quad -X^* \leq X \leq X_2 \tag{2.20}$$

Use of the condition $dp_2/dX = 0$ at $X = X_2$ in equation (2.13) results in

$$H_2 = \rho^* H^* / \rho_2^* \tag{2.21}$$

$$\frac{dT_2}{dX} = 0 \text{ at } X = X_2 \tag{2.22}$$

where ρ_2^* is the density of the lubricant at $X = X_2$, $H = H_2$.

Making use of the dimensionless scheme given below, equations (2.12-2.13) and (2.19-2.20) may be written as

$$\frac{d\bar{p}_1}{dX} = \bar{m}_1 (\bar{f})^n / H^{2n+1} \tag{2.23}$$

$$\frac{d\bar{p}_2}{dX} = -\bar{m}_2 (\bar{g})^n / H^{2n+1} \tag{2.24}$$

$$\frac{d\bar{T}_1}{dX} = \bar{\gamma}\bar{m}_1 (\bar{f})^n [\bar{f} + \bar{\varepsilon}\bar{T}_1 \bar{\rho}^* H^* e^{-\bar{A}\bar{p}_1 + \bar{\varepsilon}(\bar{T}_1 - \bar{T}_o)}] / (\bar{\rho}^* H^* H^{2n+1}) \tag{2.25}$$

$$\frac{d\bar{T}_2}{dX} = \bar{\gamma}\bar{m}_2 (\bar{g})^n [\bar{g} - \bar{\varepsilon}\bar{T}_2 \bar{\rho}^* H^* e^{-\bar{A}\bar{p}_2 + \bar{\varepsilon}(\bar{T}_2 - \bar{T}_o)}] / (\bar{\rho}^* H^* H^{2n+1}) \tag{2.26}$$

where

$$\bar{T} = \beta T, \ \bar{\rho}^* = \rho^* / \rho_o, \ \bar{\gamma} = \beta / (\rho_o c_p \alpha), \ \bar{\varepsilon} = \varepsilon / \beta, \ \bar{A} = 1 / \alpha p_s \tag{2.27}$$

$$\bar{f} = H - \bar{\rho}^* H^* e^{-\bar{A}\bar{p}_1 + \bar{\varepsilon}(\bar{T}_1 - \bar{T}_o)}$$

$$\bar{m}_1 = \bar{m}_o e^{\bar{p}_1 - (\bar{T}_1 - \bar{T}_o)} \tag{2.28}$$

$$\bar{g} = -H + \bar{\rho}^* H^* e^{-\bar{A}\bar{p}_2 + \bar{\varepsilon}(\bar{T}_2 - \bar{T}_o)}$$

$$\bar{m}_2 = \bar{m}_o \, e^{\bar{p}_2 - (\bar{T}_2 - \bar{T}_o)} \tag{2.29}$$

Equations (2.23-2.26) are the final forms of Reynolds and energy equations giving pressure and temperature distributions. These equations have to be solved under the following boundary and matching conditions :

$$\bar{p}_1 = 0 \ , \ \bar{T}_1 = \bar{T}_o \text{ at } X = -\infty$$

$$\bar{p}_1 = \bar{p}_2 \ , \ \bar{T}_1 = \bar{T}_2 \text{ at } X = -X^* \qquad (2.30)$$

$$\bar{p}_2 = 0 = \frac{d\bar{p}_2}{dX} \text{ at } X = X_2$$

The pressure and temperature equations (2.23-2.26) contain an unknown X_2 which can be determined as follows [139]: with an assumed X_2 , equation (2.23-2.26) can be solved to give indepence of $\bar{p}$ on X. If the assumed X_2 is correct, then $\bar{p}$ will vanish at $X = X_2$, if it is not, then another value of X_2 is taken and the process is repeated as often as is necessary to make $\bar{p} = 0$ at $X = X_2$ to the required order of accuracy. Finally , these equations are solved simultaneously for pressure and temperature using fourth order Runga-Kutta method.

Load : The normal force component in the direction of x is given [75] by

$$W_x = -2 \int_{h_1}^{h_2} p \, dh = -2 \int_{-\infty}^{x_2} \frac{px}{R} \, dx = \left(\frac{2h_o}{\alpha}\right) \int_{-\infty}^{x_2} X^2 \frac{d\bar{p}}{dX} \, dX$$

The dimensionless load component W_X , defined as $W_X = W_x/(2h_o/\alpha)$, may be obtained as

$$W_X = \left[\int_{-\infty}^{-X^*} \frac{\bar{m}_1 X^2 (\bar{f})^n}{H^{2n+1}} \, dX - \int_{-X^*}^{X_2} \frac{\bar{m}_2 X^2 (\bar{g})^n}{H^{2n+1}} \, dX \right] \qquad (2.31)$$

Similarly, the y-component of the normal force is

$$W_y = \int_{-\infty}^{x_2} p \, dx$$

$$\text{or} \quad W_y = -\left[\int_{-\infty}^{-X^*} \frac{\bar{m}_1 X (\bar{f})^n}{H^{2n+1}} \, dX - \int_{-X^*}^{X_2} \frac{\bar{m}_2 X (\bar{g})^n}{H^{2n+1}} dX \right] \qquad (2.32)$$

where $W_Y = W_y/(\sqrt{2Rh_o}/\alpha)$.

Traction force : The traction force T_f may also be defined by

$$T_f = -\int_{-\infty}^{x_2} \frac{h}{2} \frac{dp}{dx}\, dx$$

which comes out in dimensionless form to be

$$T_F = \left[\int_{-\infty}^{-X^*} \frac{\bar{m}_1(\bar{f})^n}{H^{2n}}\, dX - \int_{-X^*}^{X_2} \frac{\bar{m}_2(\bar{g})^n}{H^{2n}}\, dX \right] \quad (2.33)$$

where $T_F = T_f/(-h_o/2a)$.

2.3 RESULTS AND DISCUSSION :

Theoretical aspects of numerically computed results for various bearing characteristics are elaborated through figures and tables which follow. These characteristics are functions of the flow behaviour index n. The index n plays a very prominent role in the present context. Results are calculated for the following values of n, i.e.

$$0.4 \leq n \leq 1.15$$

For numerical calculation, the following set of values are used :

$R = 2.54$ cm, $U = 300$ cm sec^{-1}, $h_o = 5 \times 10^{-4}$ cm,
$\alpha = 1.6 \times 10^{-9}$ $dyne^{-1}$ cm^2 and $p_s = 8.125 \times 10^8$ dyne cm^{-2},
$\bar{\gamma}$ and $\bar{\varepsilon}$, defined as $\bar{\gamma} = \beta/(\rho_o c_p \alpha)$ and $\bar{\varepsilon} = \varepsilon/\beta$ are dimensionless numbers, values of which are taken as 0.4 and 0.5 respectively.

In order to study the qualitative behaviour of consistency variation of the compressible lubricant, pressure and temperature

must be computed first. This is achieved by solving the simultaneous equations (2.23-2.26). These equations contain an unknown X_2 which is evaluated by the method described in the analysis. Further, $-X^*$, the point of maximum pressure, is determined from the relation

$$X^* = \sqrt{(1 + X_2^2)\, e^{-\bar{p}_{max}/\alpha p_s + \bar{\varepsilon}(\bar{T}_{max} - \bar{T}_o)} - 1} \qquad (2.34)$$

where $\bar{p}_{max}$ and $\bar{T}_{max}$ are the maximum pressure and the temperature at $X = -X^*$. The density of the fluid at the exit $X = X_2$ is assumed to be equal to that of the ambient.

Subsequent to the computation of X^* and X_2, the simultaneous eqs. (2.23-2.26) are solved numerically for dimensionless pressure $\bar{p}$ and temperature $\bar{T}$ by Runga-kutta method. This finally yields dimensionless consistency $\bar{m}$, using empirical relations given in (2.28) and (2.29).

The variation of $\bar{p}$, $\bar{T}$ and $\bar{m}$ with X for various values of n are presented in figs. (2.1), (2.2), and (2.3) respectively. All these curves have one feature in common that variation in n does not change the general shape of the profiles. The compressible and incompressible curves, denoted by continuous and broken lines respectively, are presented for several values of n. Curves in these two cases are hardly distinguishable for values of $n \leq 1$. Furthermore, for $n \leq 1$, there is a fixed trend between compressible and the corresponding incompressible curves, i.e. incompressible curves for $\bar{p}$ and $\bar{T}$ lie below the compressible curve. Whereas for $n \geq 1.15$ such a fixed trend does not exist.

Pressure Distribution : The pressure distribution $\bar{p}$ versus X for various values of n has been depicted in fig. (2.1) for compressible as well as incompressible fluids. $\bar{p}$ increases continuously in the inlet region and decreases in the outlet. Once the pressure peak is attained, $\bar{p}$ falls down very rapidly to the ambient as the fluid moves towards the outlet. The behaviour of $\bar{p}$ against X for each n is similar to that of Dowson et al [121]. It is seen from fig. (2.1) that $\bar{p}$ increases with n. This is in conformity with the results of Safar and Shawki [63]. One may also observe that for values of $n \leq 1$ the $\bar{p}$ curves for incompressible fluid, denoted by dotted lines in fig. (2.1) , always lie below the corresponding curves for compressible fluid. A similar trend was observed by Dowson and Whitaker [107] for Newtonian fluid. However, for $n = 1.15$, this particular trend exists only near the outlet followed by reverse trend in the inlet zone.

Temperature Distribution : The temperature distribution $\bar{T}$ for various values of n is presented in fig. (2.2). It is interesting to note that $\bar{T}$ increases in the inlet zone. This increase is arrested at the point of maximum pressure, $X = -X^*$. $\bar{T}$ subsequently decreases, rather slowly to the outlet. An increase in $\bar{T}$ in the region $-\infty \leq X \leq -X^*$ indicates that heat of convection is dominant in the inlet region [86,149]. This increase in $\bar{T}$ in the inlet region is also in accordance with the view point that the dragging action of

the faster layers in the high pressure region causes more viscous dissipation in the convergence zone and hence results in more temperature there.

$\bar{T}$ increases as n increases, this can be seen from fig. (2.2). An increase in $\bar{T}$ with n can be physically interpreted. An increase in n signifies an enhanced effective viscosity. Thus the resistance to the motion would increase, leading to a higher viscous dissipation.

Incompressible fluid film temperature $\bar{T}$ is also presented in fig. (2.2) (by dotted lines). It is observed that incompressible film temperature is comparatively less than the compressible one for all values of n, except when $n \geq 1.15$. In this case the incompressible temperature $\bar{T}$ in the inlet zone is slightly higher than that for the compressible one. The difference is, however, not very significant, both for Newtonian as well as non-Newtonian fluids.

Consistency Distribution : The main objective of this analysis is to study the behaviour of consistency variation of a compressible non-Newtonian fluid with respect to pressure and temperature. The consistency $\bar{m}$ varies with pressure and temperature according to relations (2.28) and (2.29). The general trend of $\bar{m}$ versus X for various values of n is shown in fig. (2.3). It is clear from the figure that $\bar{m}$ decreases near the inlet where temperature $\bar{T}$ (caused by heat

of convection) dominates. This decrease continues until such time that the pressure $\bar{p}$ starts dominating. From this point and onwards, $\bar{m}$ increases rather rapidly, and becomes maximum at $X = -X^*$. For heavy loads under consideration, consistency peak near $X = -X^*$ is not unexpected. If one looks at the definition of $\bar{m}$ given in (2.28) and (2.29), it is obvious that in the high pressure region, $\bar{m}$ must be high because pressure $\bar{p}$ developed inside the film through hydrodynamic action is more than compensated by $\bar{T}$. In the region $-X^* \leq X \leq X_2$, $\bar{m}$ decreases continuously up to the cavitation point. It is because, the dominant factor $\bar{p}$ on which $\bar{m}$ depends, decreases rather abnormally in this region.

It is also possible to discuss the behaviour of $\bar{m}$ versus n from fig. (2.3). This might throw some light on the possible dependence of n on pressure and temperature. It is seen that $\bar{m}$ increases as n increases. For values of $n \leq 1.0$ there is no significant change in $\bar{m}$. It may thus be safe to assume that for low values of n, neither m nor n may depend upon pressure and temperature. For dilatant fluids no conclusive statement can be made.

The behaviour of consistency $\bar{m}$ for incompressible fluid is also depicted along with compressibility effect. Though its qualitative behaviour is quite similar to that of compressible one. But there are minor quantitative differences,

especially for values of $n \leq 1$. However, for $n = 1.15$, compressibility effect seems to be observable.

Film Rupture : Points of cavitation and maximum pressure for compressible as well as incompressible fluid film are given in Table (2.1) for various values of n. Mathematically these points are related by relation (2.34). For incompressible fluid it reduces to

$$X_2 = X^* \tag{2.35}$$

It is evident from the relation (2.34) that $X_2 \geq X^*$ or $H_2 \geq H^*$ [107]. It is seen that the difference between X^* and X_2 for $n \geq 1$ is large, i.e. significant departure from incompressible result. One may thus infer that compressibility effect is significant for $n \geq 1$, but for $n < 1$, this difference is not much, i.e. $X^* \approx X_2$. Thus for $n < 1$, density change may be neglected. This is also in accordance with the physical situation that density of a liquid changes only in case of high pressure which is true for $n \geq 1$.

For compressible fluids, the point of cavitation X_2 moves away from the center line of contact (origin O) as n increases. However, in the case of incompressible fluids , X_2 moves closer to origin as n increases [33].

Load and Traction : Load capacity and the traction force, which are the most important bearing characteristics, are presented in Tables (2.2) and (2.3), for various values of n. It is

seen from these tables that both the dimensionless load components $\bar{W}_X$ and W_Y and the dimensionless traction force T_F increase with n ; which confirms the enhancement in effective viscosity with n [63].

It is observed that there are no significant differences between the values of W_X, W_Y , T_F for incompressible and their corresponding values for compressible fluid when $n \leq 1$ (pseudoplastic). For dilatant fluid the compressibility effects are more obvious.

2.4 CONCLUSIONS :

The problem of heavily loaded rollers, lubricated by a compressible power law fluid is considered. The consistency and density are assumed to vary with temperature and pressure. It is further assumed that the flow index n does not vary with pressure and temperature. Though this is customary [145], it nevertheless imposes restrictions on the applicability of the analysis. Another important issue that remains unresolved is the variation of the internal energy for power law fluids.

From the present analysis, it is observed that for low values of n there is no significant effect of pressure and temperature on the consistency. Even the compressibility effects are not significant. It might be thus safe to assume that both m as well as n do not vary with temperature

and pressure for low values of n. The same may perhaps be said about the internal energy. However, for values of $n > 1$, nothing can be said.

A careful assessment of these assumptions is highly desirable. Experiment conducted in view of this analysis might prompt researchers to investigate further and resolve these issues.

Table 2.1

Compressible		Incompressible		
X^*	X_2	X^*, X_2	m_o	n
0.1712024	0.8730804	0.4706875	0.560	1.150
0.3901324	0.5011706	0.4725625	0.750	1.000
0.4520124	0.4826696	0.4795813	0086	0.545
0.4700024	0.4825070	0.4825000	0128	0.400

Table 2.2 : Compressible

W_X	W_Y	T_F	m_o	n
1.735096	0.1305279	1.762750	0.560	1.150
0.4525186	0.2562538	0.4589417	0.750	1.000
0.1546492	0.0757574	0.1552770	0086	0.545
0.03553886	0.0167051	0.0355398	0128	0.400

Table 2.3 : Incompressible.

W_X	W_Y	T_F	m_o	n
2.0906140	1.1104130	2.117660	0.560	1.150
0.4615181	0.2424701	0.4671063	0.750	1.000
0.1553269	0.0747965	0.1559035	0086	0.545
0.0355680	0.0166580	0.0356004	0128	0.400

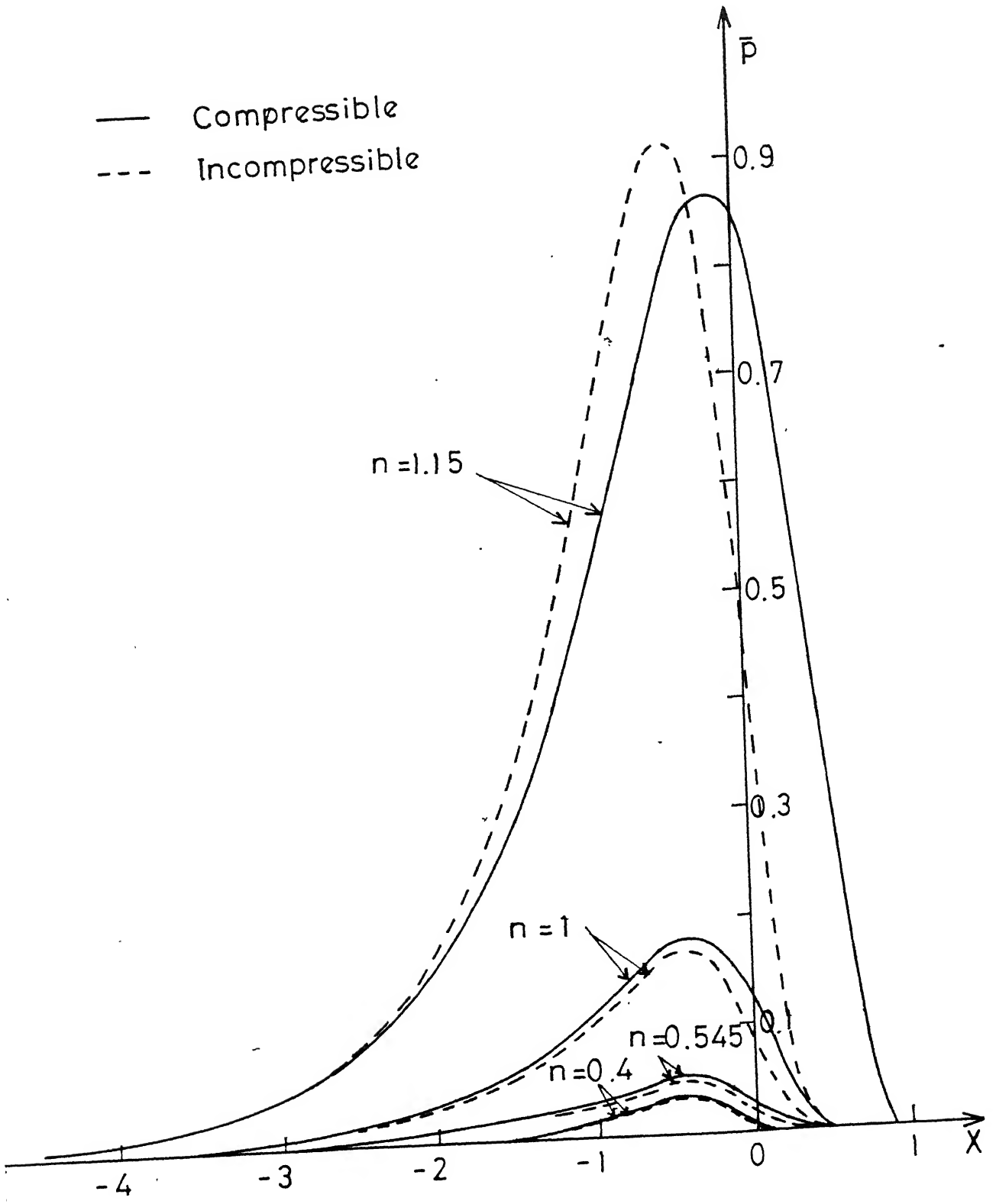

Fig. 2.1 Distribution of $\bar{p}$ vs. X.

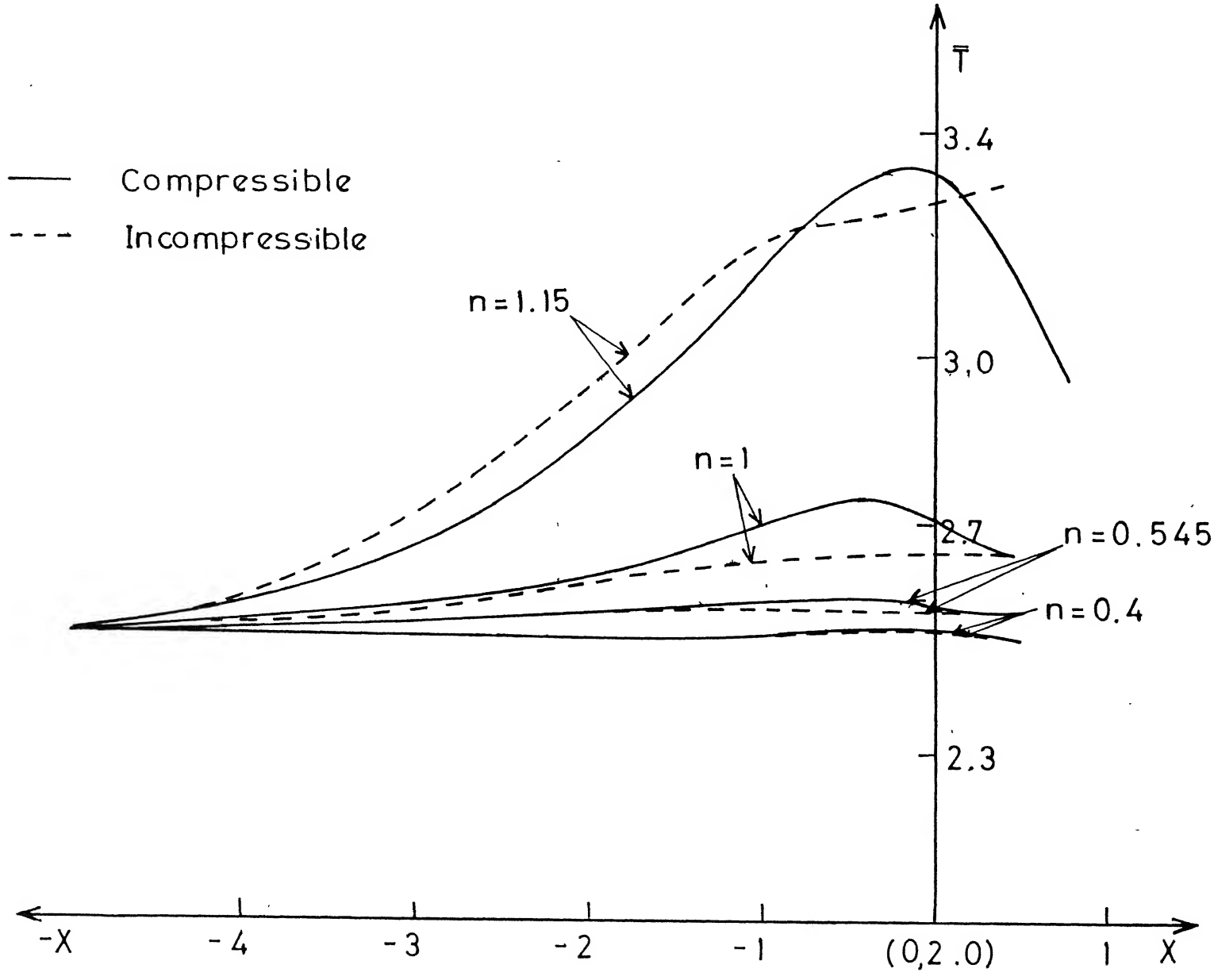
Compressible
Incompressible
n = 1.15
n = 1
n = 0.545
n = 0.4
T̄
3.4
3.0
2.7
2.3
-X
-4
-3
-2
-1
(0,2.0)
1
X

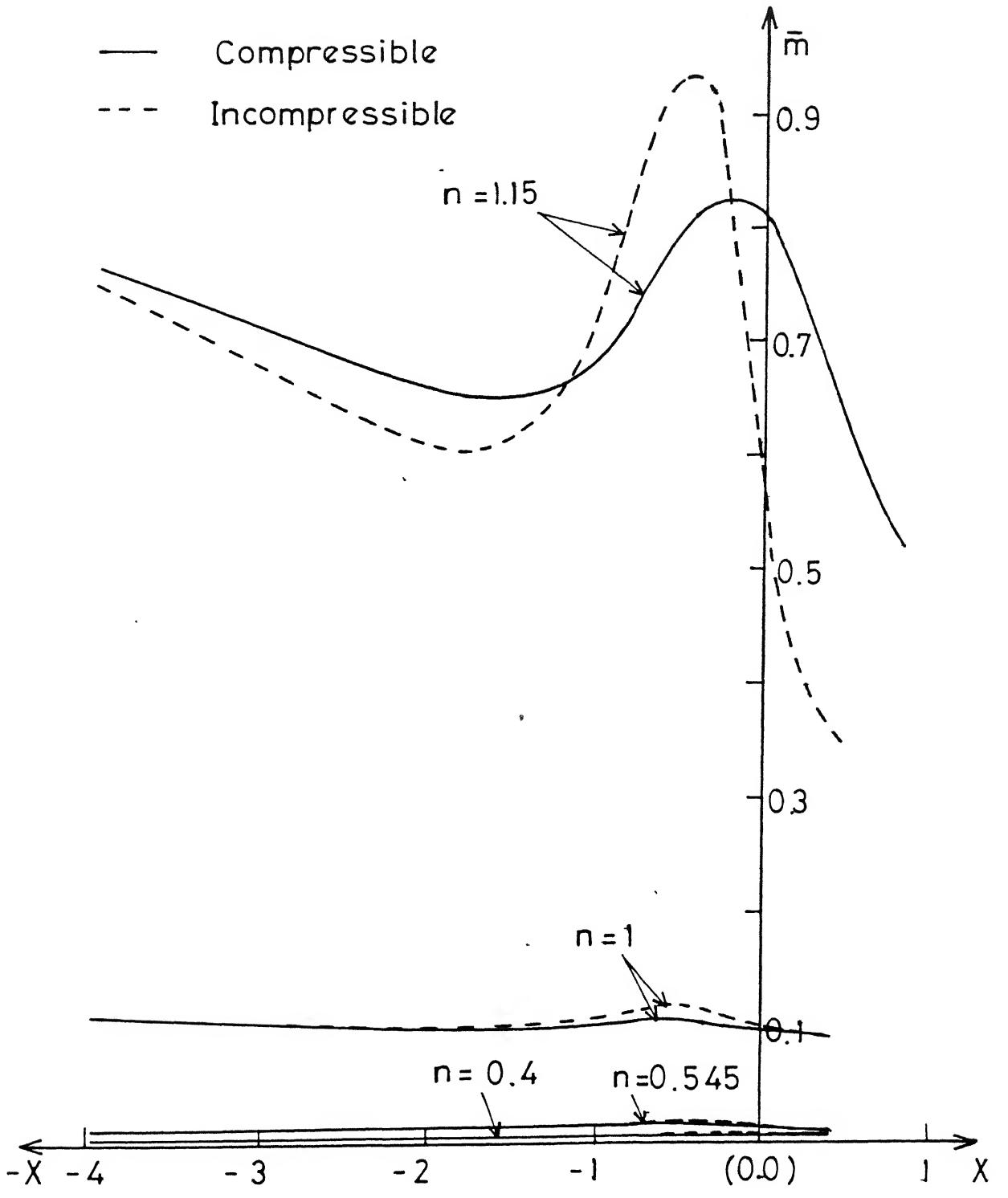

Fig. 2.3 Distribution of $\bar{m}$ vs. X.

CHAPTER* III

THERMAL AND SQUEEZING EFFECTS IN NON-NEWTONIAN FLUID FILM LUBRICATION OF ROLLERS

3.1 INTRODUCTION :

It is a matter of fact that in a heavily loaded lubricated bearing, high pressure and temperature are experienced. The lubricant properties do not remain constant but become pressure and temperature dependent. However, coupling of energy and Reynolds equations makes the solution very complicated and one has to work out numerically using fast digital computer. Moreover, sometimes convergence of solution is so poor that a lot of computer time is consumed and the application of more accurate solution becomes less feasible. In view of these uncertainties, one is tempted to make some extra assumptions which may result solutions in closed form or semi-analytical.

In the first and the second chapters, energy equation was coupled through consistency and density of the lubricant. Temperature was assumed to be a function of x-alone. This assumption under adiabatic condition may be reasonable for qualitative purpose , but for non-adiabatic case it is not accurate because the temperature gradient across the fluid film is not small [131]. If one relaxes this assumption , solutions of the coupled Reynolds and energy equations become complicated. Analytical solution is not possible unless one

---

*Published in Wear volume 119(1987) 175-190.

makes some other reasonable approximations.

In this regard, Radzimoviskey [2] mentioned that due to mathematical difficulties which arise when analysing such a bearing, the influence of temperature change and pressure change along (and across) the fluid film is generally ignored and viscosity corresponding to the mean film temperature and pressure is assumed in the computation. Cheng and Sternlicht [89] solved THD lubrication of elastic rollers where viscosity variation with film pressure as well as the mean film temperature was mentioned. Recently Pascovici [156] applied the exponential viscosity variation with the mean temperature of the lubricant and compared the theoretical results with those obtained experimentally [157]. Both the results were found in good agreement. More recently Malik et al [158] presented an isothermal analysis of hydrodynamic journal bearings using non-Newtonian lubricants by 'viscosity averaging across the film'. The performance characteristic results obtained in this analysis for a plane journal bearing with lubricant following cubic shear strain rate law, compare very well with the experimental and theoretical results available in the published literature. Very recently Hashimoto and Wada [118] examined turbulent lubrication problems of a sector-shaped tilting-pad thrust bearings with thermal and elastic deformations of a pad using the exponential relationship for viscosity-mean

temperature. Lubrication and energy equations have been solved simultaneously giving film pressure and temperature distributions, thermal and elastic deformations and inclinations of a pad.

Another reasonable approximation to avoid mathematical complication is to neglect the heat-convection of the energy equation in comparison to the heat of conduction across the film . Crook [86] pointed out that except for a region far removed from the pressure zone, convection plays little part in dissipation of the frictional heat and the temperatures in the pure rolling are effectively those needed to dissipate the heat by conduction across the film. Johnson and Greenwood [92], and Heyes and Montroso [159] studied the influence of temperature on viscosity in the thermal analysis of non-Newtonian lubricant under EHD line contacts . They too had neglected the convection term in the energy equation.

Thus the present analysis deals with the problem of two inelastic heavily loaded rollers, lubricated by non-Newtonian power law fluids under rolling and squeezing motions, considering cavitation where both the approximations mentioned above have been made i.e. the consistency of the lubricant is assumed to vary exponentially with film pressure and the mean temperature and the convection term of the energy equation is dropped . Subsequently the Reynolds equation and the energy equation are solved simultaneously. This results into a closed form solution for the temperature field.

3.2 MATHEMATICAL FORMULATION :

Basic Equations : Referring to the previous section , two kinds of approximations have been made : (a) viscosity of the lubricant varies with the pressure and the mean film temperature, and (b) convection term of the energy equation may be dropped in comparison to the heat of conduction across the film. Keeping in view these approximations, energy equation for an incompressible power law fluid (with the usual assumptions) may be written as [92,156]

$$k\frac{\partial^2 T}{\partial y^2} + m\left|\frac{\partial u}{\partial y}\right|^{n-1}\left(\frac{\partial u}{\partial y}\right)^2 = 0 \qquad (3.1)$$

where k is the lubricant conductivity and the consistency m characterizes the following exponential relationship :

$$m = m_o \cdot e^{\alpha p - \beta (T_m - T_o)} \qquad (3.2)$$

Here T_m is the mean film temperature defined as

$$T_m = \frac{1}{h}\int_{-h/2}^{h/2} T \, dy \qquad (3.3)$$

The other quantities occuring in the above equations together with the other governing equations have already been defined in section (1.2).

The boundary conditions for the energy equation (3.1) are

$$\frac{\partial T}{\partial y} = 0 \text{ at } y = 0 \qquad (3.4)$$

$$T = T_h \text{ at } y = \pm \frac{h}{2} \qquad (3.5)$$

where T_h is the surface temperature which may be assumed to be a constant (isothermal boundary).

The first boundary condition (3.4) may be called the symmetric condition (about x-axis) for temperature. Using the symmetry of the flow about x-axis and the condition (3.4), the relation given in (3.3) can be rewritten as

$$T_m = \frac{2}{h} \int_0^{h/2} T \, dy \tag{3.6}$$

Solutions : It is obvious from the relations (3.2) and (3.3) that m is a function of x only. Therefore the Reynolds equations (for the two different regions) remain the same as those given in section (1.2). Hence the energy equation only will be reconsidered.

Since the fluid flow is symmetric about x-axis, the velocity gradient $\frac{\partial u}{\partial Y}$ can be evaluated by integrating equation (1.2) once, using the symmetric condition given in (1.6), one can obtain

$$\frac{\partial u}{\partial Y} = \left(\frac{Y}{m_1} \frac{dp_1}{dx} \right)^{1/n}, \quad -\infty \leq x \leq -x_1 \tag{3.7}$$

$$\frac{\partial u}{\partial Y} = -\left(\frac{-Y}{m_2} \frac{dp_2}{dx} \right)^{1/n}, \quad -x_1 \leq x \leq x_2 \tag{3.8}$$

Integration (twice) of the equation (3.1) , using the conditions given in (3.4) and (3.5) and relations (3.7-3.8), yields

$$T_1 = T_h + \frac{m_1 n^2}{k(2n+1)(3n+1)} \left(\frac{1}{m_1} \frac{dp_1}{dx} \right)^{(n+1)/n} \left\{ \left(\frac{h}{2} \right)^{(3n+1)/n} - y^{(3n+1)/n} \right\} \tag{3.9}$$

$$T_2 = T_h + \frac{m_2 n^2}{k(2n+1)(3n+1)} \left(-\frac{1}{m_2}\frac{dp_2}{dx}\right)^{(n+1)/n} \left\{\left(\frac{h}{2}\right)^{(3n+1)/n} - y^{(3n+1)/n}\right\} \tag{3.10}$$

where m_1 , T_1 and m_2 , T_2 correspond to the respective quantities in the regions $-\infty \leq x \leq -x_1$ and $-x_1 \leq x \leq x_2$. The mean temperature in these two regions can be obtained by substituting the values of temperatures T_1 and T_2 from the expressions (3.9) and (3.10) into (3.6). Thus

$$T_{m_1} = T_h + \frac{m_1 n^2}{k(2n+1)(4n+1)} \left(\frac{1}{m_1}\frac{dp_1}{dx}\right)^{(n+1)/n} \left(\frac{h}{2}\right)^{(3n+1)/n}, \quad -\infty \leq x \leq -x_1 \tag{3.11}$$

$$T_{m_2} = T_h + \frac{m_2 n^2}{k(2n+1)(4n+1)} \left(-\frac{1}{m_2}\frac{dp_2}{dx}\right)^{(n+1)/n} \left(\frac{h}{2}\right)^{(3n+1)/n}, \quad -x_1 \leq x \leq x_2 \tag{3.12}$$

Substituting the expressions for $\frac{dp_1}{dx}$ and $\frac{dp_2}{dx}$ from (1.16) and (1.17) into (3.11) and (3.12), one can write

$$T_{m_1} = T_h + \left(\frac{2n\alpha}{4n+1}\right) m_1 k_1 c_n F^{n+1}/H^{2n} , \quad -\infty \leq X \leq -X_1 \tag{3.13}$$

$$T_{m_2} = T_h + \left(\frac{2n\alpha}{4n+1}\right) m_2 k_1 c_n G^{n+1}/H^{2n} , \quad -X_1 \leq X \leq X_2 \tag{3.14}$$

where $k_1 = \frac{Uh_o}{4k\alpha} \left(\frac{h_o}{2R}\right)^{1/2}$, $F = \bar{f}$ (see section (1.2)) and $G = -F$.

Again using the same non-dimensional scheme as given in section (1.2) together with

$$\bar{T}_m = T_m/k_1 \quad \text{etc.}$$
$$\bar{K} = \beta k_1 \tag{3.15}$$

equations (3.13) and (3.14) can be rewritten as

$$\bar{T}_{m_1} = \bar{T}_h + \left(\frac{n}{4n+1}\right) \bar{m}_1 F^{n+1}/H^{2n}, \quad -\infty \leq X \leq -X_1 \tag{3.16}$$

$$\bar{T}_{m_2} = \bar{T}_h + \left(\frac{n}{4n+2}\right) \bar{m}_2 G^{n+1}/H^{2n}, \quad -X_1 \leq X \leq X_2 \tag{3.17}$$

where $\bar{m} = \bar{m}_o e^{\bar{p}} - \bar{K}(\bar{T}_m - \bar{T}_o)$ etc. (3.18)

Finally, differentiation of the above equations (3.16) and (3.17) with respect to "X", gives[2]

$$\frac{d\bar{T}_{m_1}}{dX} = \frac{\left(\frac{n}{4n+1}\right)\bar{m}_1 \left[\bar{m}_1 \frac{F^{n+1}}{H^{2n}} + 2\{H(n+1)(X+q) - 2nXF\}\right] F^n}{H\left[H^{2n} + \left(\frac{n}{4n+1}\right) \bar{K}\bar{m}_1 F^{n+1}\right]},$$

$$-\infty \leq X \leq -X_1 \tag{3.19}$$

$$\frac{d\bar{T}_{m_2}}{dX} = -\frac{\left(\frac{n}{4n+1}\right)\bar{m}_2 \left[\bar{m}_2 \frac{G^{n+1}}{H^{2n}} + 2\{H(n+1)(X+q) + 2nXG\} G^n\right]}{H\left[H^{2n} + \left(\frac{n}{4n+1}\right) \bar{K}\bar{m}_2 G^{n+1}\right]},$$

$$-X_1 \leq X \leq X_2 \tag{3.20}$$

The equations (3.19) and (3.20) are ordinary differential equations having initial conditions

$$\begin{aligned} \bar{T}_{m_1} &= \bar{T}_o \text{ at } X = -\infty \\ \bar{T}_{m_2} &= \bar{T}_{m_1} \text{ at } X = -X_1 \end{aligned} \tag{3.21}$$

respectively, which are coupled with the Reynolds equations (1.21) and (1.22) viz.

$$\frac{d\bar{p}_1}{dX} = \bar{m}_1 F^n/H^{2n+1} \tag{3.22}$$

---

2. $\frac{d\bar{T}_h}{dX} = 0$ is assumed for isothermal boundaries.

$$\frac{d\bar{p}_2}{dX} = -\bar{m}_2 G^n / H^{2n+1} \qquad (3.23)$$

The pressure conditions for the last two equations are the same as those given in section (1.2) (see condition (1.34)). Equations (3.19), (3.20), (3.22) and (3.23) are the required equations for temperature and pressure distributions which have to be solved simultaneously using the same technique given in the last of the section (2.2).

Load and Traction : The non-dimensional load W_Y and the traction force T_F, as defined earlier, may be obtained as follows :

$$W_Y = -\left[\int_{-\infty}^{-X_1} \frac{X\bar{m}_1 F^n}{H^{2n+1}}\, dX - \int_{-X_1}^{X_2} \frac{X\bar{m}_2 G^n}{H^{2n+1}}\, dX \right] \qquad (3.24)$$

$$T_F = \int_{-\infty}^{-X_1} \frac{\bar{m}_1 F^n}{H^{2n}}\, dX - \int_{-X_1}^{X_2} \frac{\bar{m}_2 G^n}{H^{2n}}\, dX \qquad (3.25)$$

where $\bar{m}_1$, $\bar{m}_2$ are calculated using the relation (3.18).

3.3 RESULTS AND DISCUSSION :

The present analysis is devoted to the study of consistency variation in a steady-state thermal lubrication of heavily loaded cylindrical roller bearings. The semi-analytical solutions for pressure, temperature and the frictional force generated inside the fluid film are obtained.

Parametric Values : All the bearing characteristics, which specify the lubrication behaviour of the system, depend upon the various parameters: n (flow behaviour index), q (squeezing ratio defined as $\frac{V}{U}\frac{\sqrt{R}}{\sqrt{2h_o}}$) and $\bar{K}$ (thermal factor defined as $\frac{\beta U h_o^{3/2}}{4k\alpha\sqrt{2R}}$). n is assumed to vary from 0.4 to 1.15. The values of q for the system under consideration (steady-state heavily loaded) are chosen in the range $-.1 \leq q \leq +1$. The thermal factor $\bar{K}$ is introduced to study the behaviour of lubricant consistency with temperature and the value of which is chosen to be 0.5. A particular value of $\bar{K}$ (=o) corresponds to no effect of temperature on consistency [67] and α = o, $\bar{K}$ = o correspond to the case of constant consistency throughout the region [66]. For numerical calculation, the following set of values are used :

$R = 2.54$ cm , $U = 400$ cm sec^{-1} , $h_o = 6\times10^{-4}$ cm ,
$\alpha = 1.6\times10^{-9}$ $dyne^{-1}$ cm^2.

Numerical Calculation : In order to study the qualitative behaviour of the consistency $\bar{m}$ which is a function of pressure $\bar{p}$ and the mean temperature $\bar{T}_m$, the simultaneous equations (3.19, 3.22) and (3.20, 3.23) have to be solved first, to compute $\bar{p}$ and $\bar{T}_m$. These equations contain an unknown X_1 which is evaluated by an iterative process (see section 3.2) using conditions $\bar{p}_1 = o$ at $X = -\infty$ and $\bar{p}_2 = o$ at $X = X_2 = X_1 - 2q$.

Having found X_1 and hence X_2, the resulting simultaneous equations (3.19, 3.22) and (3.20, 3.23) are solved numerically for $\bar{p}$ and $\bar{T}_m$ using the Euler-modified method. Subsequently $\bar{m}$ is calculated from the empirical relation (3.18).

The results thus obtained are elaborated through the figures and table which follow. All these curves have one feature in common that variations in n and q do not change the general shape of the profiles. Moreover, for all $n < 1$, these profiles hardly vary, thus only a few values of n and q are considered for these profiles.

Pressure Profiles : Curves for pressure $\bar{p}$ versus X for various values of n and q are presented in fig. (3.1) and a few related results are given in the table (3.1). It is clear from the figure that for fixed n and q, $\bar{p}$ starts rising from $X = -\infty$ and continues to do so till it reaches the point $X = -X_1$. Beyond this, it starts decreasing with a very steep slope and reduces to the ambient pressure $\bar{p} = 0$ at the point of cavitation $X = X_2$.

For a fixed q, $\bar{p}$ increases significantly with n, especially for $n \geq 1$, which is in accordance with Safar and Shawki [63]. From the table one can observe that for a fixed q, the points of maximum pressure and the points of cavitation both tend to go nearer to the centre line of contact, (the origin O) as n increases [67]. For a fixed

n, $\bar{p}$ increases remarkably as q decreases and the cavitation points move slowly towards the centre line of contact as q increases [66]. This significant change in pressure with respect to q accounts for the observation that as the surfaces approach each other with increasing velocity, comparatively more pressure is generated. The pressure curves presented in this analysis for various values of q are similar to those obtained by Dowson et al [121] for a Newtonian fluid.

Temperature Profiles : The influence of n and q on $\bar{T}_m$ has been illustrated in fig. (3.2). It is clear from the figure that for a fixed value of n (= 1) and q , $\bar{T}_m$ decreases throughout the inlet region up to the point $X = -X_1$, then it increases upto the origin O, and thereafter decreases up to the point $X = X_2$. However, increase or decrease in $\bar{T}_m$ beyond the point $X = -X_1$ is hardly discernible and may be treated as constant. The same trend is true for $n < 1$ also though it has not been shown in the figure. The Newtonian curve (n=1) for $\bar{T}_m$, shown in fig. (3.2), is almost similar to that obtained by Crook [86] , $\bar{T}_m$ follows a similar trend for $n > 1$ and $q > o$. However, for $n > 1$ and $q \leq o$, $\bar{T}_m$ increases initially (though only marginally) then decreases and finally follows the Newtonian behaviour. This trend is almost similar to the experimental result obtained by Pascovici [157].

Letting n (≤ 1) fixed and varying q in the specified interval $(-.1, +.1)$, $\bar{T}_m$ decreases as q increases near the inlet while in the proximity of the surfaces $\bar{T}_m$ increases with q. However for a fixed $n > 1$, $\bar{T}_m$ decreases as q increases throughout the region except in the proximity of the surface (i.e. in the range, $-7 \leq X \leq X_2$) where $\bar{T}_m$ increases with q. The behaviour of $\bar{T}_m$ with n can be interpreted from fig. (3.2). It is observed that $\bar{T}_m$ for Newtonian (n=1) and non-Newtonian are not significantly different in the inlet region, however, as one proceeds towards the point $X = -X_1$, the behaviour of $\bar{T}_m$ is markedly different for both dilatant ($n > 1$) as well as Newtonian fluids.

The mean temperature $\bar{T}_{m_i}$ for $\bar{K} = 0$ is also calculated for various values of n and q. Since the general behaviour of $\bar{T}_{m_i}$ with respect to n and q remains the same as that of $\bar{T}_m$, so only selected values of n and q have been considered for $\bar{T}_{m_i}$. From fig. (3.3), it is clear that for $n \leq 1$, $\bar{T}_{m_i}$ is less than $\bar{T}_m$ except in the n'hood of the point $X = -X_1$. For $n > 1$, values of $\bar{T}_{m_i}$ near the inlet are larger (though only marginally) than the corresponding values of $\bar{T}_m$. While in the remaining portion, $\bar{T}_{m_i}$ is less than $\bar{T}_m$. Over all $\bar{T}_{m_i}$ is quantitatively less than $\bar{T}_m$ for all n and q. One may, thus, conclude that the assumption of temperature independent consistency leads to under-estimation of temperature.

Consistency Profiles : The curves for consistency $\bar{m}$ are presented in fig. (3.4) for various values of n and q. For fixed values of $n(\leq 1)$ and q , qualitative behaviour of $\bar{m}$ is identical to that of pressure. The same trend is followed for $n > 1$ and $q > 0$. However, for $n > 1$ and $q \leq 0$, $\bar{m}$ decreases initially as a consequence of increased temperature $\bar{T}_m$ near the inlet. Thereafter, $\bar{m}$ increases and follows the pressure ($\bar{p}$) trend. This is an immediate consequence of the profiles for $\bar{p}$, $\bar{T}_m$ (given in figures (3.1) and (3.2)) and the empirical relation (3.18). For a fixed n , $\bar{m}$ increases with q near the inlet while in the proximity of the surface $\bar{m}$ decreases as q increases. However, for a fixed q, $\bar{m}$ increases with n. It is interesting to note that significant changes in $\bar{p}$ and $\bar{T}_m$ which appear in the neighbourhood of the point $X = -X_1$, cause a corresponding change in consistency. It is also noted from the table and figure that the effect of temperature on consistency is (i) to shift the position of pressure peak and the cavitation points slightly towards the centre line of contact and (ii) to make the slope of $\bar{m}$ very sharp. The change in consistency for dilatant and Newtonian fluids, especially in the neighbourhood of the point $X = -X_1$, is very remarkable which justifies the inclusion of consistency variation in the treatment of the lubrication of a heavily loaded system.

The consistency $\bar{m}_i$ (for $\bar{K} = 0$) is also computed for various values of n and q. It was seen that the behaviour of $\bar{m}_i$ in relation to $\bar{m}$ was similar for all n and q, hence only one value of q has been chosen for the graph of $\bar{m}_i$ (fig.(3.5)). For all $n(\leq 1)$ and q, $\bar{m}_i$ is quantitatively less than the corresponding values of $\bar{m}$ throughout the region. The same trend is followed for $n > 1$ except near the inlet where $\bar{m}_i \geq \bar{m}$ (though only marginally).

Load and Traction : The non-dimensional load component W_Y for the system under consideration is presented in the table (3.1) for different values of n and q. It is observed from the table that the load component W_Y increases with n for a fixed value of q [63,66]. However, it decreases as q increases for a fixed n, which is expected, since $\bar{p}$ increases as q decreases.

The load component W_{Y_i} (for $\bar{K} = 0$) is also presented in the same table for all the considered values of n and q. The qualitative behaviour of W_{Y_i} for all n and q is also the same as that of W_Y. However, W_{Y_i} is quantitatively less than W_Y. This follows from the fact that value of consistency $\bar{m}$ is higher than that of $\bar{m}_i$, so is pressure and thus the load.

The non-dimensionalized traction T_F is also presented along with load component in the same table. Its behaviour with respect to n and q is the same as that of load component for both the cases $\bar{K} = 0$ and $\bar{K} \neq 0$.

3.4 CONCLUSION :

The problem of pure rolling of two inelastic identical cylinders lubricated with an incompressible power law fluid is considered including squeezing motion and cavitation. The heat of convection which is small as compared to that of conduction is neglected. The lubricant consistency is assumed to vary exponentially with pressure and the mean temperature, Reynolds and energy equations for pressure and temperature are derived and are solved numerically for various bearing characteristics with and without consistency variation with temperature.

The effect of temperature on the lubricant consistency is to shift the position of pressure peak slightly towards the centre line of contact. However, the cavitation goes away from that contact. The flow index n and the squeezing parameter q are found to have pronounced effects on various lubrication characteristics such as pressure, the mean temperature, consistency , load and traction (see figures and table). The consistency variation, particularly in the pressure peak region, for the Newtonian and the dilatant fluids is quite significant.

Table 3.1 : Comparison of bearing characteristics

		Thermal factor $\bar{K} \neq 0$			
n/m_o	q	X_1	X_2	W_Y	T_F
1.15/0.56	-0.09	0.389453	0.569453	2.49206	1.79640
	-0.05	0.415625	0.515622	2.30833	1.55546
	0.00	0.449420	-	2.10661	1.31386
	+0.05	0.484844	0.384844	1.92642	1.11804
	+0.09	0.514453	0.334453	1.79434	0.98627
1.0/0.75	-0.09	0.413750	0.593750	0.363025	0.215015
	-0.05	0.436875	0.536875	0.348435	0.197837
	0.00	0.468125	-	0.330036	0.177845
	+0.05	0.502187	0.402187	0.311594	0.159402
	+0.09	0.529375	0.349375	0.297275	0.146149
0.545/86	-0.09	0.423750	0.603750	0.120024	0.063030
	-0.05	0.447187	0.547187	0.117723	0.059685
	0.00	0.478750	-	0.114665	0.055638
	+0.05	0.511719	0.411719	0.111471	0.051769
	+0.09	0.540312	0.360312	0.108768	0.048802
0.4/12.6	-0.09	0.426250	0.606250	0.027369	0.013770
	-0.05	0.451250	0.551250	0.027009	0.013137
	0.00	0.485000	-	0.026503	0.012374
	+0.05	0.518750	0.418750	0.025970	0.011644
	+0.09	0.545000	0.365000	0.025534	0.011091

Continued

n/m_o	q	X_1	X_2	W_{Y_i}	T_{F_i}
		Thermal factor $\bar{K} = 0$			
	-0.09	0.416797	0.596797	2.22211	1.45908
	-0.05	0.439922	0.539922	2.05843	1.27704
1.15/0.56	0.00	0.470703	-	1.87781	1.08956
	+0.05	0.503906	0.403906	1.71653	0.93476
	+0.09	0.531719	0.351719	1.59946	0.82987
	-0.09	0.418750	0.598750	0.352244	0.205313
	-0.05	0.442500	0.542500	0.337798	0.188885
1.0/0.75	0.00	0.473750	-	0.319833	0.169906
	+0.05	0.504370	0.404370	0.302528	0.152991
	+0.09	0.532500	0.352500	0.288468	0.140203
	-0.09	0.424687	0.604687	0.117500	0.0612635
	-0.05	0.448594	0.548524	0.115256	0.0580430
0.54/86	0.00	0.480625	-	0.112295	0.0541050
	+0.05	0.513750	0.413750	0.109188	0.0504130
	+0.09	0.541562	0.361562	0.106607	0.0475800
	-0.09	0.429150	0.609150	0.027196	0.013661
	-0.05	0.451875	0.551875	0.026860	0.013044
0.4/126	0.00	0.486125	-	0.026381	0.012000
	+0.05	0.519500	0.419500	0.025846	0.011577
	+0.09	0.546500	0.366500	0.025426	0.011037

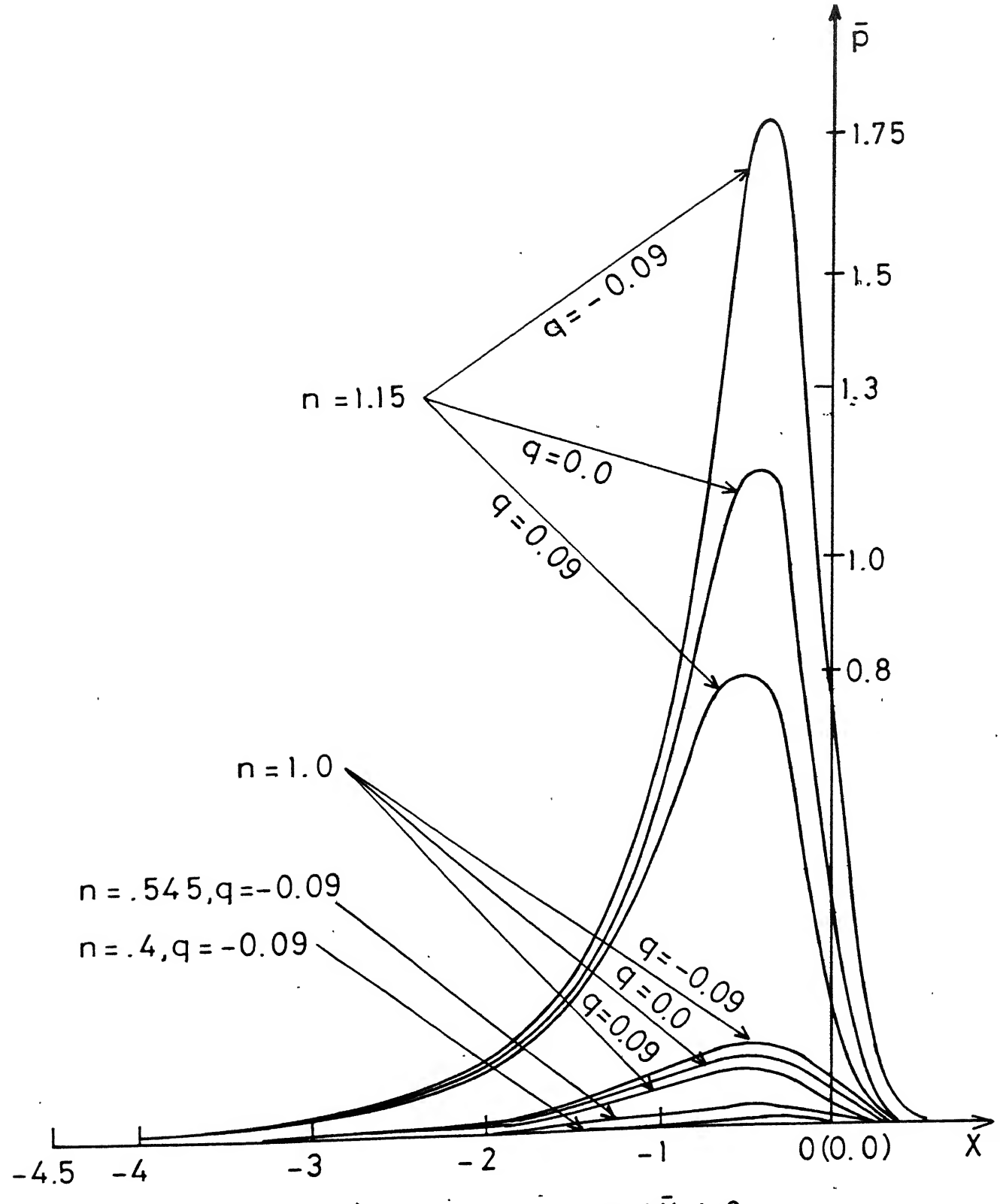

Fig. 3.1 Pressure $\bar{p}$ vs. X for $\bar{K} \neq 0$.

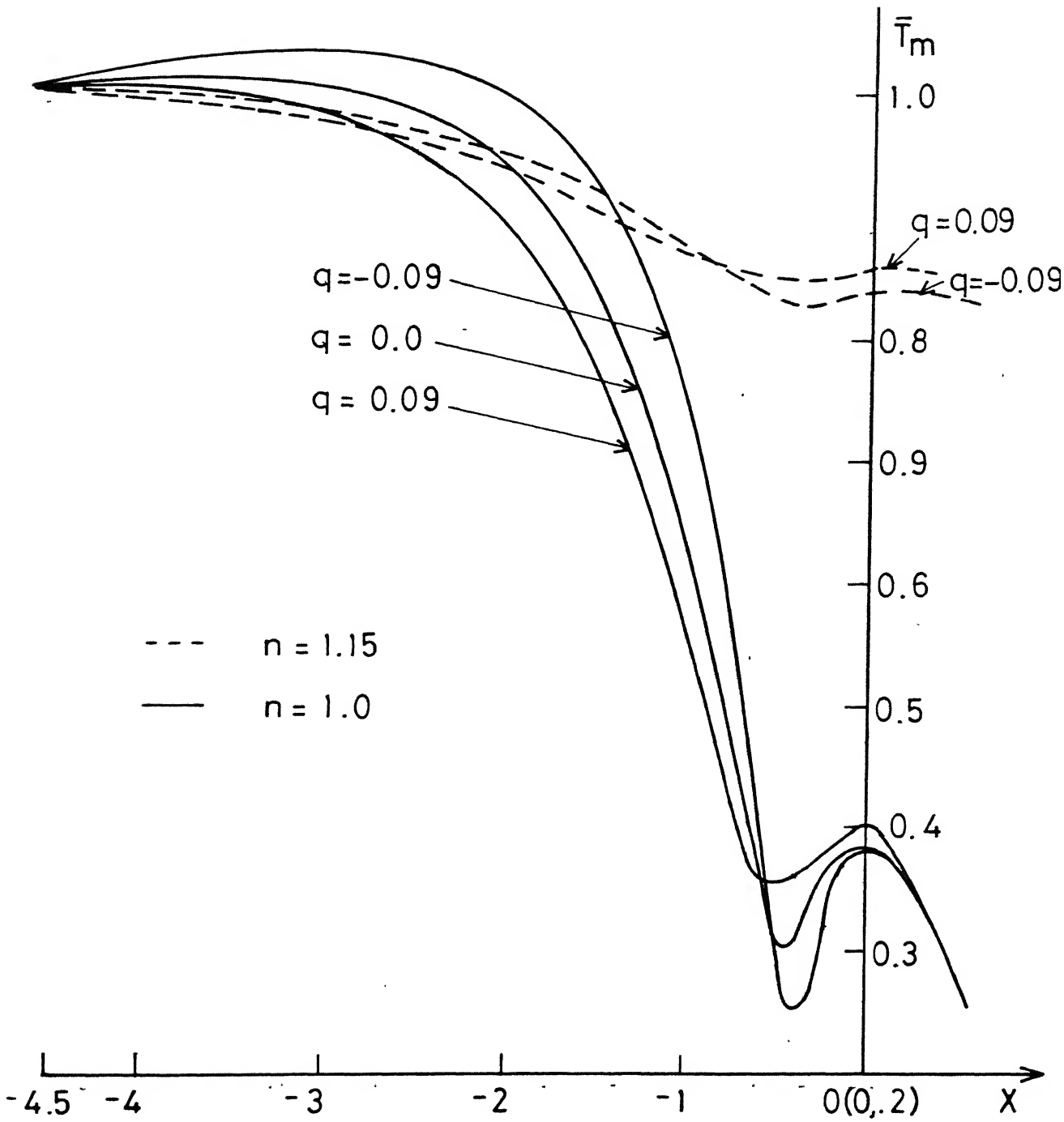

Fig.3.2 The mean temperature $\bar{T}_m$ vs.X for $\bar{K} \neq 0$.

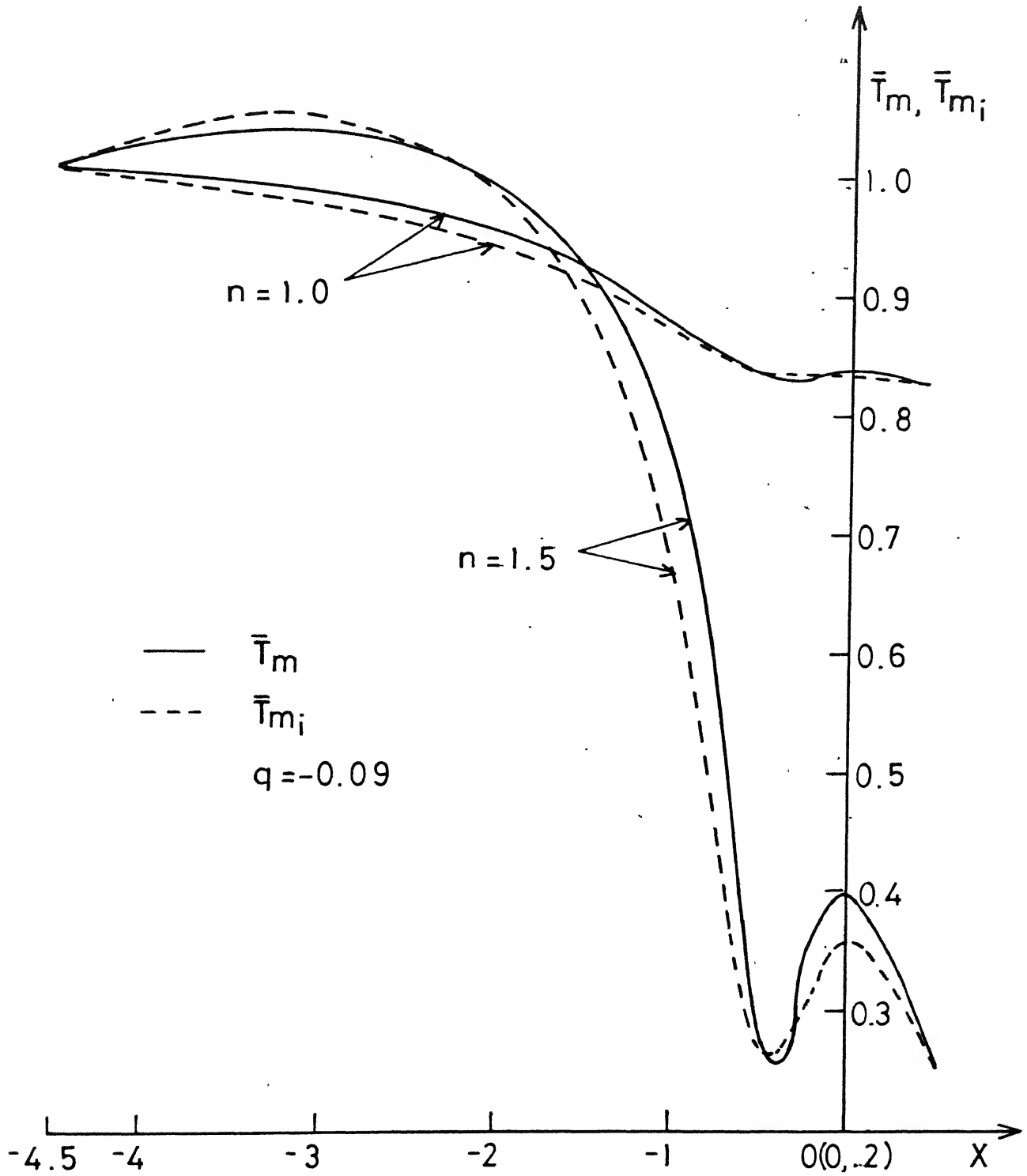

Fig. 3.3 Comparison between $\bar{T}_m$ and $\bar{T}_{m_i}$

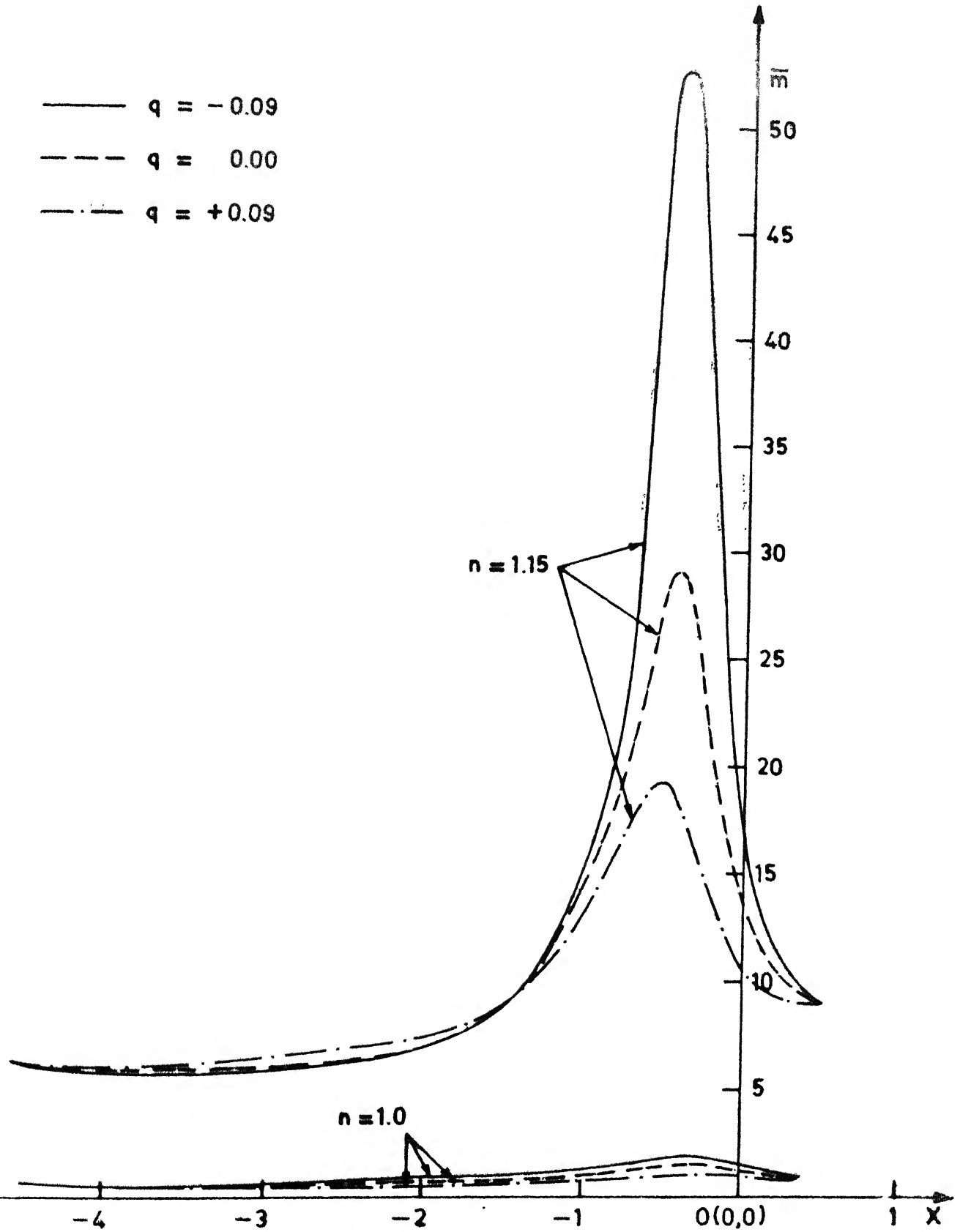

Fig. 3.4 The consistency distribution $\bar{m}$ vs. X for $\bar{K} \neq 0$.

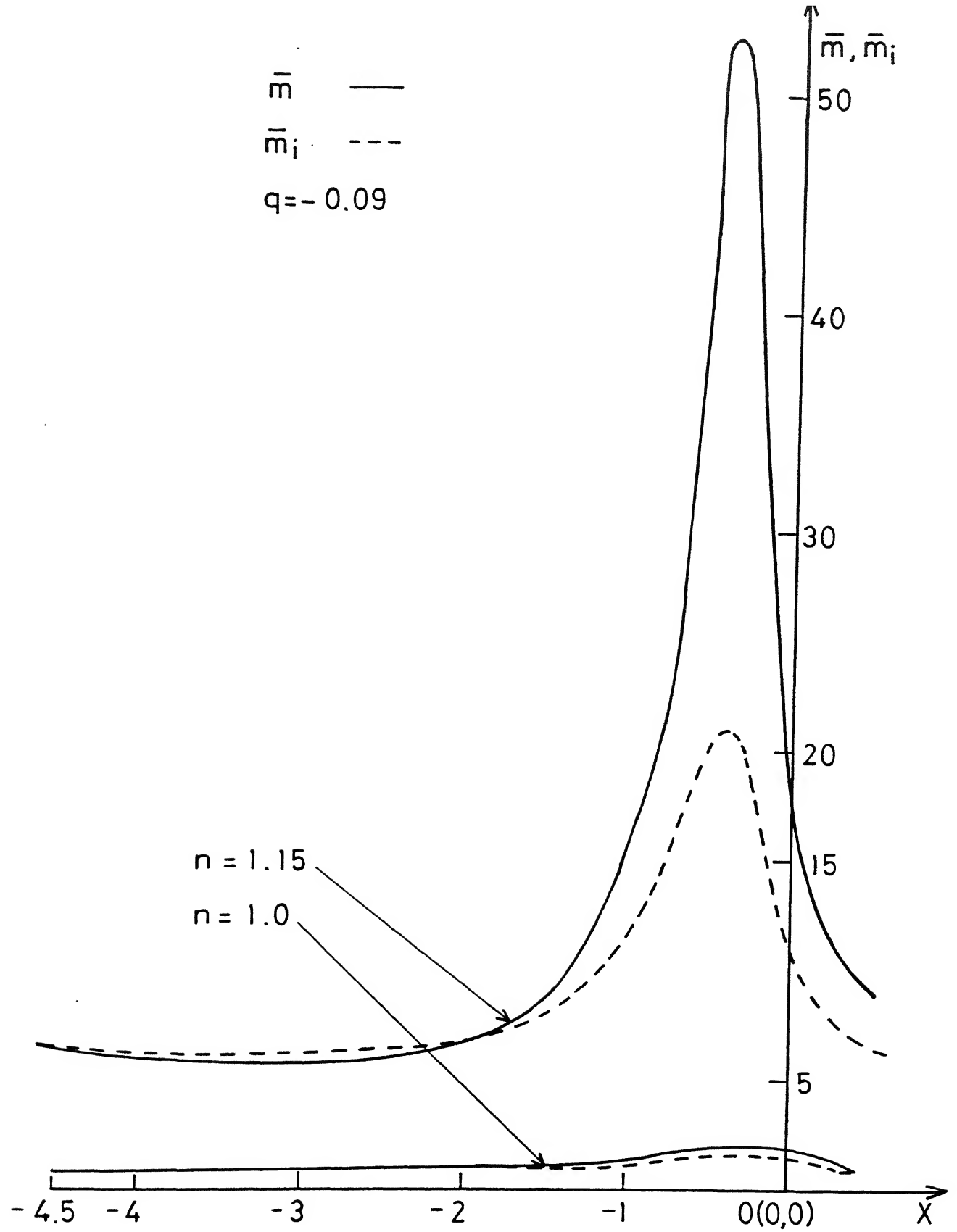

Fig. 3.5 Comparison between $\bar{m}$ and $\bar{m}_i$.

CHAPTER IV

THERMAL AND INERTIA EFFECTS IN HYDRODYNAMIC LUBRICATION OF ROLLERS BY A POWER LAW FLUID

4.1 INTRODUCTION :

In the preceding chapters, various aspects of thermal effects in lubrication of roller bearings have been studied. Lubricant inertia was assumed to be very small in comparison to the viscous force. However, to meet the present day requirements in science and technology, bearings are subjected to a variety of situations such as high operating speeds, the use of lubricants with low viscosity and high density etc.. Under these circumstances fluid inertia is likely to be significant [161,162]. This effect is important even in case of laminar flow [163-165] where an increase in load capacity is observed [166]. Inertia forces attain greater significance if the bearing surfaces are also subjected to squeezing motion [167]. An increase in hydrodynamic film thickness may also sometimes compel one to consider this effect. Milne [168] conducted an order of magnitude analysis of the terms in the Navier-stokes equations. It was observed that the influence of the lubricant inertia is most prominent in the region of large clearence and for rapid changes in velocity. Ting and Mayer [169] investigated inertia and thermal effects simultaneously in a parallel surface step thrust bearing. They found a correlation between their theory

and the experiment performed by Coombs and Dowson [170]. Smalley and Vohr [115] studied lubricant inertia for a very arbitrary geometry and demonstrated convincingly its significance in lubrication. Dowson et al [171] conducted a wide range of experiments using a cylinder on a plane. It was observed that, for a moderately large Reynolds number, the experimental data deviated substantially (due to inertia effect) from the Coyne-Elrod rupture conditions. Very recently You and Lu [172] presented a cylinder-plane bearing and a journal bearing analysis theoretically, and showed that the lubricant inertia had a profound effect even at moderate value of the Reynolds number.

In recent years researchers have directed their efforts to analyse inertia effects in fluid film lubrication using non-Newtonian fluids. Elkouh [116] analysed the effects of inertia forces in non-Newtonian squeeze films using power law fluids. It has been shown that inertia correction in load capacity is more significant for pseudoplastic fluids ($n < 1$). In another paper Elkouh [173] used the same non-Newtonian model to analyse this effect in squeeze film between two plane annuli and presented various other bearing characteristics. The same non-Newtonian model was also used by Salem et al [69] who presented a spherical rolling bearing analysis including inertia and thermal effects simultaneously. They illustrated frictional power as a function of n in addition to pressure and temperature distributions. Tichy [174] investigated

circular plates-squeeze film using non-Newtonian viscoelastic lubricants and elaborated the effect due to inertia on various bearing characteristics. Hashimoto and Wada [53] also investigated theoretically the effects of fluid inertia forces in parallel circular squeeze film bearings lubricated with pseudoplastic fluids and observed that these effects become considerably significant with increase in squeezing velocity as well as the film thickness.

In view of the present specific requirements where the bearings operate with high speedsand under extreme conditions of pressure and temperature, the consideration of inertia effect seems to be important. In the work presented here, inertia and thermal effects in a squeeze film roller bearing lubricated with a power law fluid are examined theoretically. The fluid consistency m is assumed to vary with pressure and the mean film temperature. The modified Reynolds and energy equations obtained here are solved simultaneously.

4.2 MATHEMATICAL FORMULATION :

Basic Equations : Making use of the constitutive relation for a power law fluid (given in (1.4)), applying the usual assumptions of hydrodynamic lubrication for the geometry shown in fig. (4.1) and retaining the fluid inertia term, one obtains the following equation of motion [116] :

$$\rho\left(u \frac{\partial u}{\partial x} + v \frac{\partial u}{\partial y}\right) + \frac{dp}{dx} = \frac{\partial}{\partial y}\left(m\left|\frac{\partial u}{\partial y}\right|^{n-1} \frac{\partial u}{\partial y}\right) \tag{4.1}$$

The first term in the left hand side of this equation is the fluid convective inertia which is usually neglected in hydrodynamic lubrication.

The equation of continuity is

$$\frac{\partial u}{\partial x} + \frac{\partial v}{\partial y} = 0 \tag{4.2}$$

The temperature within the lubricant film resulting from viscous dissipation is defined by the energy equation [143]

$$\rho c\left(u \frac{\partial T}{\partial x} + v \frac{\partial T}{\partial y}\right) = k \frac{\partial^2 T}{\partial y^2} + m \left|\frac{\partial u}{\partial y}\right|^{n-1} \left(\frac{\partial u}{\partial y}\right)^2 \tag{4.3}$$

Boundary conditions for these governing equations are considered to be the same as given earlier by equations (1.6), (1.10), (3.4) and (3.5). The relation connecting m, p and T is also taken to be the same viz.

$$m = m_o \, e^{\alpha p - \beta (T_m - T_o)} \tag{4.4}$$

with

$$T_m = \frac{2}{h} \int_o^{h/2} T \, dy \tag{4.5}$$

Making use of the following non-dimensional scheme :

$$Y = 2y/h_o \, , \; \bar{u} = u/U \, , \; \bar{v} = \frac{2v}{U}\left(\frac{2R}{h_o}\right)^{1/2}, \; \bar{T} = \beta T \tag{4.6}$$

$$\lambda = \rho U^2 \alpha \, , \; P_r = \frac{c h_o}{4Uk\alpha}\left(\frac{h_o}{2R}\right)^{1/2} \, , \; E_t = U^2 \beta / c \, , \; \bar{T}_m = \beta T_m$$

Equations (4.1-4.5) reduce to

$$\lambda\left(\bar{u} \frac{\partial \bar{u}}{\partial X} + \bar{v} \frac{\partial \bar{u}}{\partial Y}\right) + \frac{d\bar{p}}{dX} = A \frac{\partial}{\partial Y}\left(\bar{m} \left|\frac{\partial \bar{u}}{\partial Y}\right|^{n-1} \frac{\partial \bar{u}}{\partial Y}\right) \tag{4.7}$$

$$\frac{\partial \bar{u}}{\partial X} + \frac{\partial \bar{v}}{\partial Y} = 0 \tag{4.8}$$

$$\lambda P_r\left(\bar{u}\frac{\partial\bar{T}}{\partial X}+\bar{v}\frac{\partial\bar{T}}{\partial Y}\right)=\frac{\partial^2\bar{T}}{\partial Y^2}+\bar{m}\,P_r\,E_t A\,\left|\frac{\partial\bar{u}}{\partial Y}\right|^{n-1}\left(\frac{\partial\bar{u}}{\partial Y}\right)^2 \tag{4.9}$$

$$\bar{m}=\bar{m}_o\,e^{\bar{p}-(\bar{T}_m-\bar{T}_o)} \tag{4.10}$$

$$\bar{T}_m=\frac{1}{H}\int_o^H \bar{T}\,dY \tag{4.11}$$

where $A=(n/(2n+1))^n$. The other quantities occuring in equations (4.7-4.11) have already been defined in chapter I.

The presence of inertia and convection terms in equations (4.7) and (4.9) respectively makes them complicated. Therefore their average values are considered. Consequently equation (4.7) may be written as

$$\frac{\lambda}{H}\int_o^H\left(\bar{u}\frac{\partial\bar{u}}{\partial X}+\bar{v}\frac{\partial\bar{u}}{\partial Y}\right)dY+\frac{d\bar{p}}{dX}=A\frac{\partial}{\partial Y}\left(\bar{m}\,\left|\frac{\partial\bar{u}}{\partial Y}\right|^{n-1}\frac{\partial\bar{u}}{\partial Y}\right) \tag{4.12}$$

The contribution of the second term $\bar{v}\frac{\partial\bar{T}}{\partial Y}$ is small[3] as compared to $\bar{u}\frac{\partial\bar{T}}{\partial X}$ and therefore it is neglected from (4.9). Further if one assumes $\frac{\partial\bar{T}}{\partial X}\approx\frac{d\bar{T}_m}{dX}$ [89]. Equation (4.9) now becomes

$$\lambda\,P_r\,\bar{u}_m\frac{d\bar{T}_m}{dX}=\frac{\partial^2\bar{T}}{\partial Y^2}+\bar{m}\,P_r\,E_t A\,\left|\frac{\partial\bar{u}}{\partial Y}\right|^{n-1}\left(\frac{\partial\bar{u}}{\partial Y}\right)^2 \tag{4.13}$$

where the velocity $\bar{u}_m$ is taken as

$$\bar{u}_m=(\bar{u}|_{Y=o}+\bar{u}|_{Y=H})/2 \tag{4.14}$$

Letting

$$\bar{F}=\frac{\lambda}{H}\int_o^H\left(\bar{u}\frac{\partial\bar{u}}{\partial X}+\bar{v}\frac{\partial\bar{u}}{\partial Y}\right)dY+\frac{d\bar{p}}{dX} \tag{4.15}$$

$$\bar{D}=\lambda\,P_r\,\bar{u}_m\frac{d\bar{T}_m}{dX} \tag{4.16}$$

---

3. $u\frac{\partial T}{\partial x}>>v\frac{\partial T}{\partial Y}$ i.e. $\bar{u}\frac{\partial\bar{T}}{\partial X}>>\bar{v}\frac{\partial\bar{T}}{\partial Y}$, see ref [89], page 702.

It may be noted that $\bar{F}$ and $\bar{D}$ are functions of x-alone. Solving equation (4.12) for $\bar{u}$, using boundary conditions given below :

$$\left.\begin{aligned} \frac{\partial \bar{u}}{\partial \bar{Y}} &= 0 \\ \bar{v} &= 0 \end{aligned}\right| \text{ at } Y = 0$$

$$\left.\begin{aligned} \bar{u} &= 1 \\ \bar{v} &= -2q + \frac{dH}{d\bar{X}} \end{aligned}\right| \text{at } Y = H \qquad (4.17)$$

One obtains

$$\bar{u} = 1 + \left(\frac{n}{n+1}\right)\left(\frac{\bar{F}}{A\bar{m}_1}\right)^{1/n} \left(Y^{(n+1)/n} - H^{(n+1)/n}\right), \quad -\infty \leq X \leq -X_1 \qquad (4.18)$$

The volume flux Q, defined by

$$Q = \int_0^H \bar{u}\, dY \qquad (4.19)$$

is obtained as

$$Q = H - \left(\frac{n}{2n+1}\right)\left(\frac{\bar{F}}{A\bar{m}_1}\right)^{1/n} H^{(2n+1)/n} \qquad (4.20)$$

Integration of continuity equation (4.8), using the boundary conditions (4.17) gives

$$\frac{\partial}{\partial \bar{X}} \int_0^H \bar{u}\, dY = -2q$$

or
$$Q = -2qX + d \qquad (4.21)$$

where d is the constant of integration.

Use of equations (4.18), (4.20) and (4.21) in equation (4.12) yields

$$I_n(X) + \frac{d\bar{p}_1}{dX} = J_f(X) \qquad (4.22)$$

where

$$f = H+2qX-d \ , \ J_f(X) = \bar{m}_1 f^n/H^{2n+1}$$

$$I_n(X) = \frac{\lambda}{H}\left[2X\left\{-1 + \frac{2B_n f}{H} - \frac{B_n f^2}{H^2}\right\} + 4q\left(\frac{B_n f}{H} - \frac{1}{2}\right)\right] \tag{4.23}$$

with

$$B_n = 2(2n+1)/(3n+2)$$

Now $\frac{\partial \bar{u}}{\partial Y} = 0$ at $X = -X_1 \Rightarrow$

$$f = X^2 - X_1^2 + 2q(X+X_1) \tag{4.24}$$

where the unknown X_1 is positive.

Similarly equation (4.13) can be solved for T. Using the boundary conditions

$$\frac{\partial \bar{T}}{\partial Y} = 0 \quad \text{at } Y = 0$$

$$\bar{T} = \bar{T}_h \text{ at } Y = H \tag{4.25}$$

the solution is obtained as

$$\bar{T}_1 = \bar{T}_h + \frac{\bar{D}}{2}(Y^2-H^2) + \frac{\gamma \bar{m}_1 f^{n+1}}{H\frac{(2n+1)(n+1)}{n}}\left(H^{(3n+1)/n} - Y^{(3n+1)/n}\right) \tag{4.26}$$

where $\gamma = P_r E_t\left(\frac{n}{3n+1}\right)$.

Averaging (4.26) using definition given in (4.11) , the expression for the mean temperature is obtained as follows :

$$\bar{T}_{m_1} = \bar{T}_h - \frac{H^2}{3}\bar{D} + \gamma_1 \bar{m}_1 f^{n+1}/H^{2n} \tag{4.27}$$

where $\gamma_1 = P_r E_t\left(\frac{n}{4n+1}\right)$.

Substituting the value of $\bar{D}$ from equation (4.16) into (4.27), one gets,

$$\lambda P_r \bar{u}_m \frac{H^2}{3} \frac{d\bar{T}_{m_1}}{dX} = \bar{T}_h - \bar{T}_{m_1} + \gamma_1 \bar{m}_1 f^{n+1}/H^{2n} \qquad (4.28)$$

The differential equations (4.22) and (4.28) are the final forms of Reynolds and energy equations giving pressure and the mean temperature distributions for the first region $-\infty \leq X \leq -X_1$, where f is given by (4.24) and $\bar{u}_m$ (using (4.14)) is given below:

$$\bar{u}_m = 1 - \left(\frac{2n+1}{n+1}\right) \frac{f}{2H} \qquad (4.29)$$

Similarly, for the other region, $-X_1 \leq X \leq 0$, equations corresponding to (4.22), (4.26) and (4.28) giving pressure, temperature and the mean temperature distributions are

$$I_n(X) + \frac{d\bar{p}_2}{dX} = J_{-f}(X) \qquad (4.30)$$

$$\bar{T}_2 = \bar{T}_h + \frac{\bar{D}}{2}(Y^2 - H^2) + \gamma \bar{m}_2 (-f)^{n+1} \left(H^{(3n+1)/n} - Y^{(3n+1)/n}\right)/H \frac{(2n+1)(n+1)}{n} \qquad (4.31)$$

$$\lambda P_r \bar{u}_m \frac{H^2}{3} \frac{d\bar{T}_{m_2}}{dX} = \bar{T}_h - \bar{T}_{m_2} + \gamma_1 \bar{m}_2 (-f)^{n+1}/H^{2n} \qquad (4.32)$$

where

$$J_{-f}(X) = -\bar{m}_2 (-f)^n / H^{2n+1} \qquad (4.33)$$

The final equations (4.22), (4.30), (4.26) and (4.31) are coupled through $\bar{m}$ and have to be solved simultaneously under the following boundary conditions :

$$\bar{p}_1 = 0, \ \bar{T}_1 = \bar{T}_o, \ \bar{T}_{m_1} = \bar{T}_o \text{ at } X = -\infty$$
$$\bar{p}_2 = 0 \quad \text{at } X = 0 \qquad (4.34)$$

The Reynolds equations (4.22,4.30) and the mean temperature equations (4.28,4.32) contain an unknown X_1 which is determined using the above conditions and the process mentioned earlier. Subsequently pressure and the mean temperature can be obtained by solving equations (4.22-4.28) and (4.30-4.32) simultaneously.

It may be noted at this stage that $\lambda \to 0$ corresponds to the case when inertia and convection terms have been ignored. For this case Reynolds and energy equations for the two specified regions reduce to

$$\frac{d\bar{p}_1}{dX} = J_f(X)$$

$$\frac{d\bar{p}_2}{dX} = J_{-f}(X) \qquad (4.35)$$

$$\bar{T}_1 = \bar{T}_h + \gamma\bar{m}_1 f^{n+1}(H^{(3n+1)/n} - Y^{(3n+1)/n})/H^{(2n+1)(n+1)/n} \qquad (4.36)$$

$$\bar{T}_2 = \bar{T}_h + \gamma\bar{m}_2(-f)^{n+1}(H^{(3n+1)/n} - Y^{(3n+1)/n})/H^{(2n+1)(n+1)/n}$$

$$\bar{T}_{m_1} = \bar{T}_h + \gamma_1\bar{m}_1 f^{n+1}/H^{2n} \qquad (4.37)$$

$$\bar{T}_{m_2} = \bar{T}_h + \gamma_1\bar{m}_2(-f)^{n+1}/H^{2n}$$

Equations similar to the last three sets of equations (4.35), (4.36), (4.37) were also obtained in chapter III. These can be solved by the process outlined earlier giving pressure and temperature distributions for the case $\lambda \to 0$.

Load and Traction : The non-dimensional load W_Y and the non-dimensional traction/drag T_F are obtained from the following expressions :

$$W_Y = \int_{-\infty}^{-X_1} \frac{\bar{m}_1 X f^n}{H^{2n+1}}\, dX - \int_{-X_1}^{o} \frac{\bar{m}_2 X(-f)^n}{H^{2n+1}}\, dX \qquad (4.38)$$

$$T_F = \int_{-\infty}^{-X_1} \frac{\bar{m}_1 f^n}{H^{2n}}\, dX - \int_{-X_1}^{o} \frac{\bar{m}_2 (-f)^n}{H^{2n}}\, dX \qquad (4.39)$$

4.3 RESULTS AND DISCUSSION :

The numerical values of the dimensionless pressure $\tilde{p}$ and the mean film temperature $\bar{T}_m$ are obtained by solving equations (4.22),(4.28) and (4.30),(4.32) simultaneously for various values of the flow behaviour index $n(.4 \leq n \leq 1.15)$ and squeeze velocity $q(-0.09 \leq q \leq +0.09)$. The other dimensionless parameters which are important in the present context are $\lambda(= \rho U^2 \alpha)$, $P_r(= \frac{ch_o}{4kU\alpha}(\frac{h_o}{2R})^{1/2})$ and $E_t(= \frac{U^2\beta}{c})$. The values of these parameters λ, P_r and E_t are chosen to be 26×10^{-5}, 52506×10^{-1} and 202×10^{-6} respectively. The other representative numerical values used in this analysis are the following :

$U = 450$ cm sec^{-1}, $h_o = 7\times10^{-4}$ cm, $R = 3$ cm, $\alpha = 1.6\times10^{-9}$ $dyne^{-1}cm^2$. All the parameters, especially n, q and λ have profound effects on various bearing characteristics. This has been elaborated through various graphs and tables. It may be noted at this

stage that for the case $\lambda \to 0$, it was not possible to plot curves for all n and q, because the differences were not discernible in the graphs. So graphs have been made for $\lambda \neq 0$ mainly and curves for only a few values of n and q in case of $\lambda \to 0$ have been drawn (denoted by -.-.-).

The present case may be considered to be a generalization of the previous chapter as well as the work done by Pascovici [156]. Pascovici's case may be obtained directly from this problem by letting $\lambda \to 0$, $n = 1$ in Reynolds and energy equations, and $\alpha = 0$ in the empirical relation for m given in (4.4).

Pressure Distribution : The lubricant pressure $\bar{p}$ which is a function of n and q has been computed numerically by solving Reynolds equations (4.22) and (4.30). The results have been presented in fig.(4.2). For both the cases of $\lambda \neq 0$ and $\lambda \to 0$ (as mentioned earlier), the qualitative behaviour of $\bar{p}$ for the different values of q (for fixed n) is identical. This is in conformity with the results of Dowson et al [121] and those obtained in the first and the third chapters. A similar trend for both the cases is displayed by the pressure curves when n is varied and q is held fixed. This kind of behaviour was observed by Safar and Shawki [63] for a thrust bearing and by Bukholz [73] for a journal bearing. The point of maximum pressure for the case $\lambda \neq 0$ is of special interest here. Mathematically speaking, the point of maximum pressure

for the present case is the point of intersection of the curves $I_n(X)$ and $J_f(X)$. This has been shown in fig.(4.1). Physically it is the point at which inertia and viscous forces balance each other. The point of maximum pressure for the case $\lambda \neq 0$ is different from the point $X = -X_1$ (at which $\frac{\partial u}{\partial y}$ is zero) and lies before $X = -X_1$. However, for the case $\lambda \to 0$, these two coincide i.e. the pressure gradient and the velocity gradient vanish simultaneously.

A comparison between the two cases can also be made from the same figure. It is seen from fig.(4.2) that for each fixed n and q, the pressure curves for $\lambda \neq 0$ lie above the corresponding curves for $\lambda \to 0$. One may therefore infer that the inclusion of inertia term leads to an increased pressure. It may be further noted that the inertia effect is less on the Newtonian fluid (n=1) in comparison to that for the dilatant fluid (n > 1). Increased pressure due to the presence of inertia has also been reported by Safar [166] and others [116].

Temperature Distribution : The mean film temperature $\bar{T}_m$ is computed from differential equations (4.28) and (4.32). The results for $\bar{T}_m$ are elaborated through figs. (4.3) and (4.4) for various values of n and q (for both the cases $\lambda \neq 0$ and $\lambda \to 0$). It is clear from fig. (4.3) that for a fixed n and $q(>0)$, $\bar{T}_m$ increases as the lubricant flows towards the pressure peak region. Subsequently, it decreases

till the pressure is zero (ambient). For a fixed n and $q \leq 0$, the behaviour of $\bar{T}_m$ is similar to that mentioned above, except near the centre line of contact ($X=0$) where it increases though only marginally. For a fixed n, $\bar{T}_m$ increases as q decreases whereas for a fixed q, $\bar{T}_m$ increases as n increases. A similar trend for temperature with respect to n and q has also been observed in the chapter I.

A comparison between the mean temperature for both the cases has also been made in fig. (4.4). It is observed from the figure that the mean temperature near the inlet for the case $\lambda \neq 0$, is less than that for the case $\lambda \to 0$. However, the trend is reversed in the pressure peak region. One may interpret these results from a physical view point. For the case $\lambda \neq 0$, the convection dominant region extends farther than that for the case $\lambda \to 0$. Thus the heat lost by convection for $\lambda \to 0$ is smaller as compared to that for $\lambda \neq 0$. This may cause the temperature rise there. However, as the lubricant flows towards the pressure peak region, the heat transported by conduction becomes more significant for the case $\lambda \to 0$. Consequently, $\bar{T}_m$ decreases continuously right up to the pressure peak region. Thus for the case $\lambda \neq 0$, $\bar{T}_m$ is higher than that for $\lambda \to 0$ near the pressure peak region.

Consistency Variation : The dimensionless consistency $\bar{m}$, given by the empirical relation viz.

$$\bar{m} = \bar{m}_o \, e^{\bar{p}-\bar{T}_m+\bar{T}_o}$$

is depicted in fig. (4.5) for various values of n and q. It is evident that the consistency variation depends on the combined effects of pressure $\bar{p}$ and the mean film temperature $\bar{T}_m$. Since $\bar{m}$ for the pseudoplastic fluids (n< 1) does not vary significantly with respect to q. Therefore, for this case, $\bar{m}$ is plotted for only one value of q(=-0.09). Moreover, the consistency variation for all the values of n and q have similar trends i.e. $\bar{m}$ decreases near the inlet marginally because increase in $\bar{T}_m$ is marginally higher than the corresponding increase in $\bar{p}$. Thereafter, $\bar{m}$ follows the pressure trend throughout the region i.e. $\bar{m}$ increases and then decreases near X = 0. For each q, $\bar{m}$ increases with n throughout the region. However for each n, $\bar{m}$ increases with q in the inlet region whereas the trend is reversed in whole of the pressure peak region. It is seen from the fig. (4.5) that variation in $\bar{m}$ for $n \leq 1$ (particularly $n < 1$) is very less. It may therefore be noted that $\bar{m}$ may be treated as constant for pseudoplastic fluids (n< 1).

The consistency variation for $\lambda \to 0$ has also been presented along with that for $\lambda \neq 0$. The qualitative behaviour of $\bar{m}$ versus X (for all n and q) in this case is similar to that for $\lambda \neq 0$. However, quantitatively , $\bar{m}$ for $\lambda \to 0$ is less than that for $\lambda \neq 0$ except in the pressure peak region where the trend is reversed. This is because of abnormal change in $\bar{T}_m$ and $\bar{p}$ in that region which has already been mentioned .

Load and Traction : The surface force W_Y and the traction force T_F are calculated from the expressions (4.38) and (4.39) for various values of n and q and for both the cases $\lambda \neq 0$ and $\lambda \to 0$. These results are presented in table (4.2). It is seen from the table that for a fixed q, W_Y and T_F both increase as n increases whereas for a fixed n, both of them increase as q decreases. This is in accordance with the view point that when the surfaces are approaching towards each other (i.e. q decreases) higher pressure is developed (see fig.(4.2)). Consequently, the load and the traction both will be more.

In order to study the effect of inertia on load and traction, results for $\lambda \to 0$ have also been presented in table (4.2). It is seen that the inclusion of the inertia force leads to increase in the load and the traction for all n and q. However, the increase in results is not very significant for the pseudoplastic fluids (n< 1).

Separated Regions : The Reynolds and the energy equations (4.22), (4.28), (4.30) and (4.32) contain X_1 ($X = -X_1$ is the point at which $\frac{\partial \bar{u}}{\partial \bar{y}}$ vanishes). This point $X = -X_1$ separates the region $-\infty \leq X \leq 0$ into two subregions $-\infty \leq X \leq -X_1$ and $-X_1 \leq X \leq 0$. The values of X_1 for different n and q, and for both the cases have been presented in table (4.1). It can be seen from the table that for a fixed n, X_1 increases as q increases whereas for a fixed q, X_1 decreases as n

increases. A similar trend was also obtained by Sinha et al [66] for $\lambda \to 0$ and $\tilde{m}$ constant.

4.4 CONCLUSION : A theoretical analysis of cylindrical rollers moving with equal velocity and lubricated with a power law fluid has been presented. Thermal and inertia effects have also been taken into account together with the squeezing motion. A simple model for m given in equation (4.4) has been considered. Average/mean values of the fluid inertia and the energy convection considered in the mometum and energy equations result in an anlytical solution for temperature and semi-analytical solutions for pressure and the mean temperature.

Fluid inertia causes a significant increase in pressure and thus the load and the traction. This effect has even more significant in case of squeezing motion. This effect however, does not have significant effect on the mean temperature. The fluid inertia tends to stretch the fluid film which results in a lubricating flow field larger than that of the inertialess case ($\lambda \to 0$) i.e. the point at infinity is shifted further away from the centre line of contact O. This also tends to shift the position of pressure peak away from the origin O.

Table 4.1 : Values of X_1

n/m_o	q			λ
	-0.09	0.0	+ 0.09	
1.15/0.56	0.507454	0.532187	0.564312	2×10^{-5}
1.00/0.75	0.542656	0.564640	0.593375	
0.545/86	0.615625	0.631562	0.652031	
0.40/128	0.656250	0.663531	0.680562	
1.15/0.56	0.528906	0.553437	0.585844	26×10^{-5}
1.00/0.75	0.548830	0.570569	0.598645	
0.545/86	0.618262	0.634101	0.654375	
0.40/128	0.656781	0.664062	0.681250	

Table 4.2 : Normal force component and traction

n/m_o	W_Y	T_F	q	
	0.840294	1.939247	-0.09	
1.15/0.56	0.751967	1.796557	0.00	
	0.661339	1.648009	+0.09	
	0.156338	0.398510	-0.09	
1.00/0.75	0.142047	0.372889	0.00	26×10^{-5}
	0.127634	0.347025	+0.09	
	0.053363	0.176291	-0.09	
0.545/86	0.050922	0.170916	0.00	
	0.048347	0.165351	+0.09	
	0.012929	0.047981	-0.09	
0.40/128	0.012440	0.046617	0.00	
	0.011919	0.045219	+0.09	
	0.700509	1.573574	-0.09	
1.15/0.56	0.632719	1.481634	0.00	
	0.563006	1.383317	+0.09	
	0.148747	0.374285	-0.09	
1.00/0.75	0.135689	0.352230	0.00	2×10^{-5}
	0.122407	0.329620	+0.09	
	0.051965	0.169671	-0.09	
0.545/86	0.049722	0.165095	0.00	
	0.047331	0.160291	+0.09	
	0.012412	0.044684	-0.09	
0.40/128	0.012027	0.043809	0.00	
	0.011607	0.042888	+0.09	

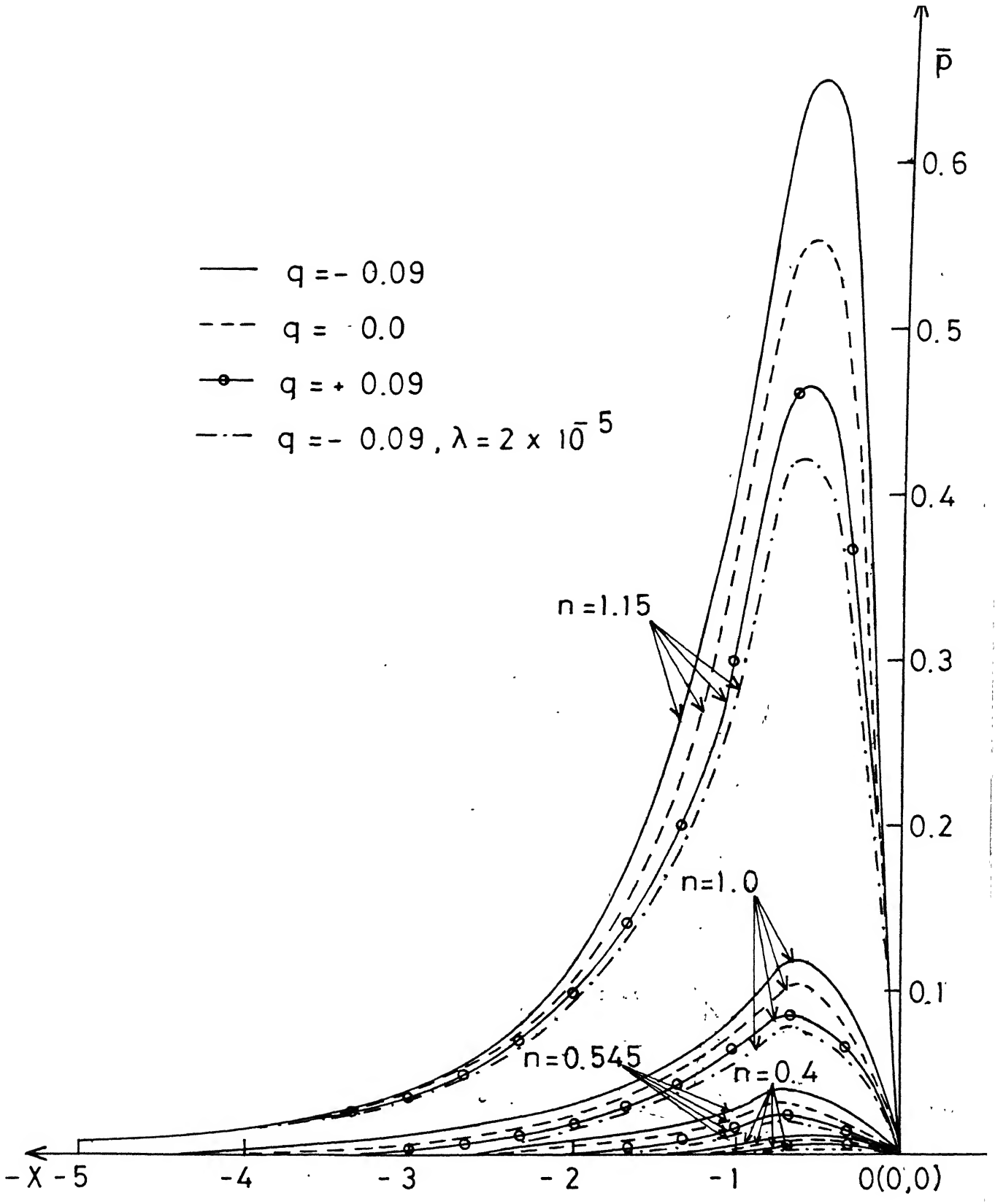

Fig. 4.2 Pressure profile $\bar{p}$ against X.

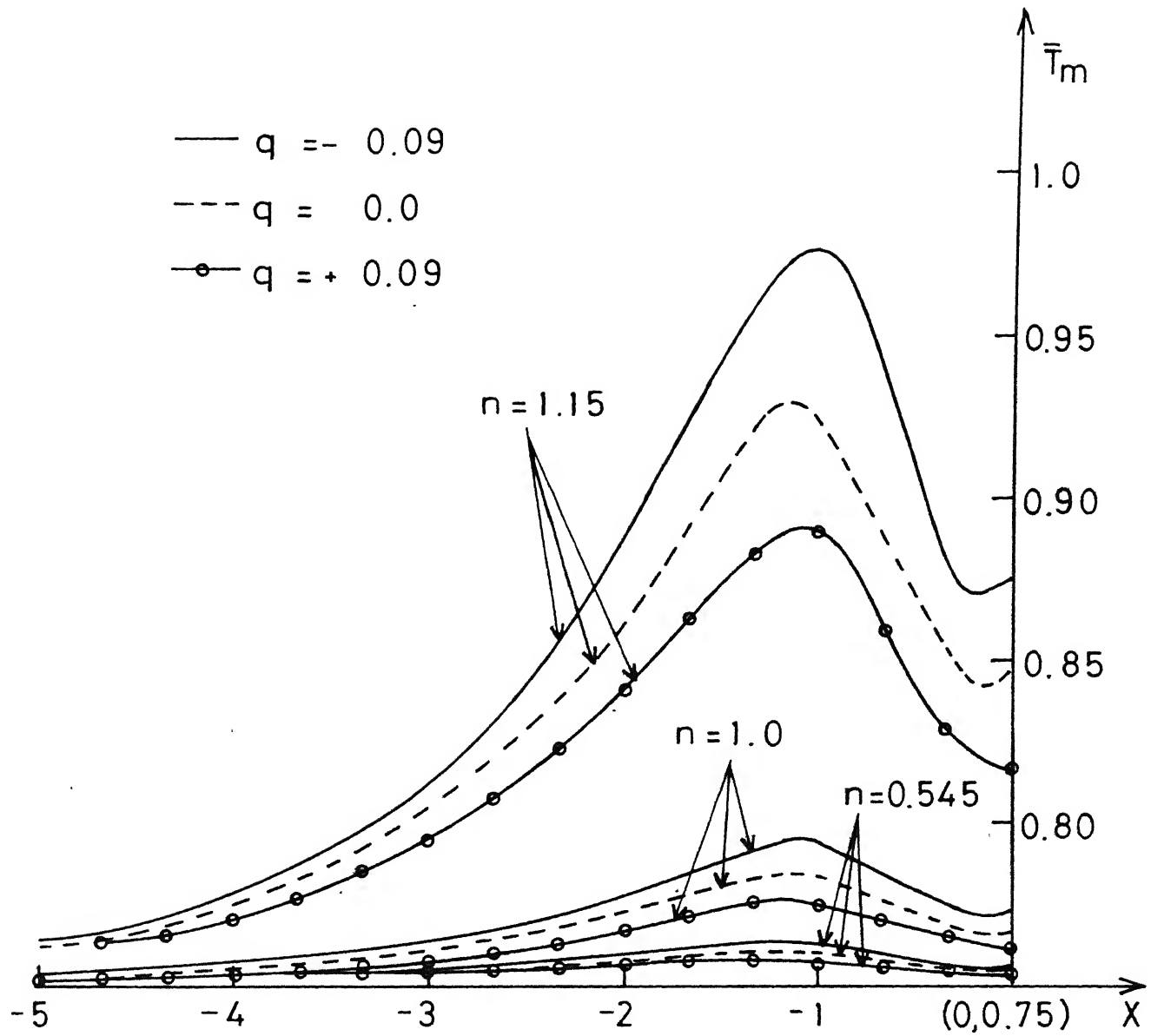

Fig. 4.3 The mean temperature distribution $\bar{T}_m$ against X.

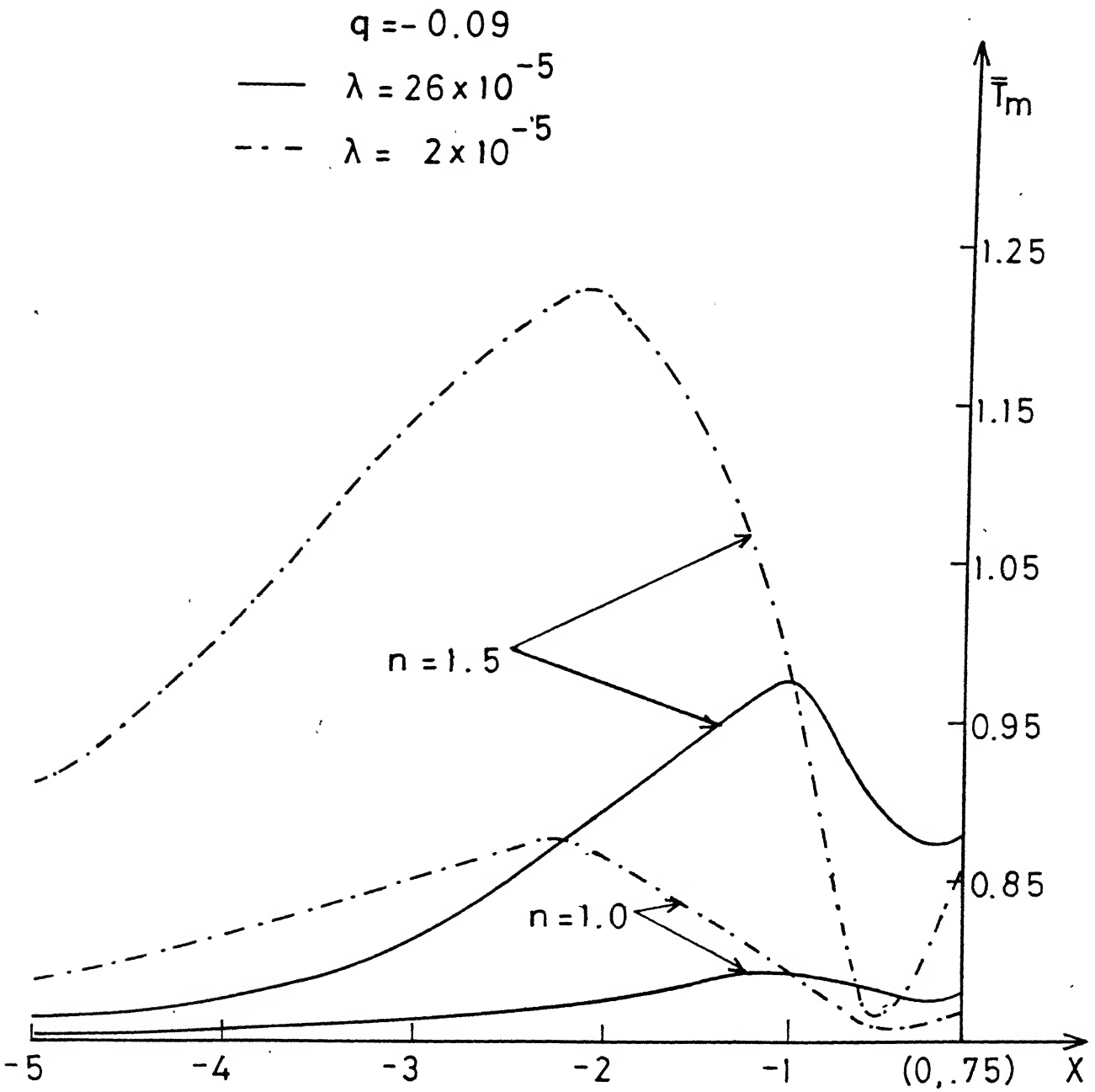

Fig. 4.4 Temperature distribution $\bar{T}_m$ against X.

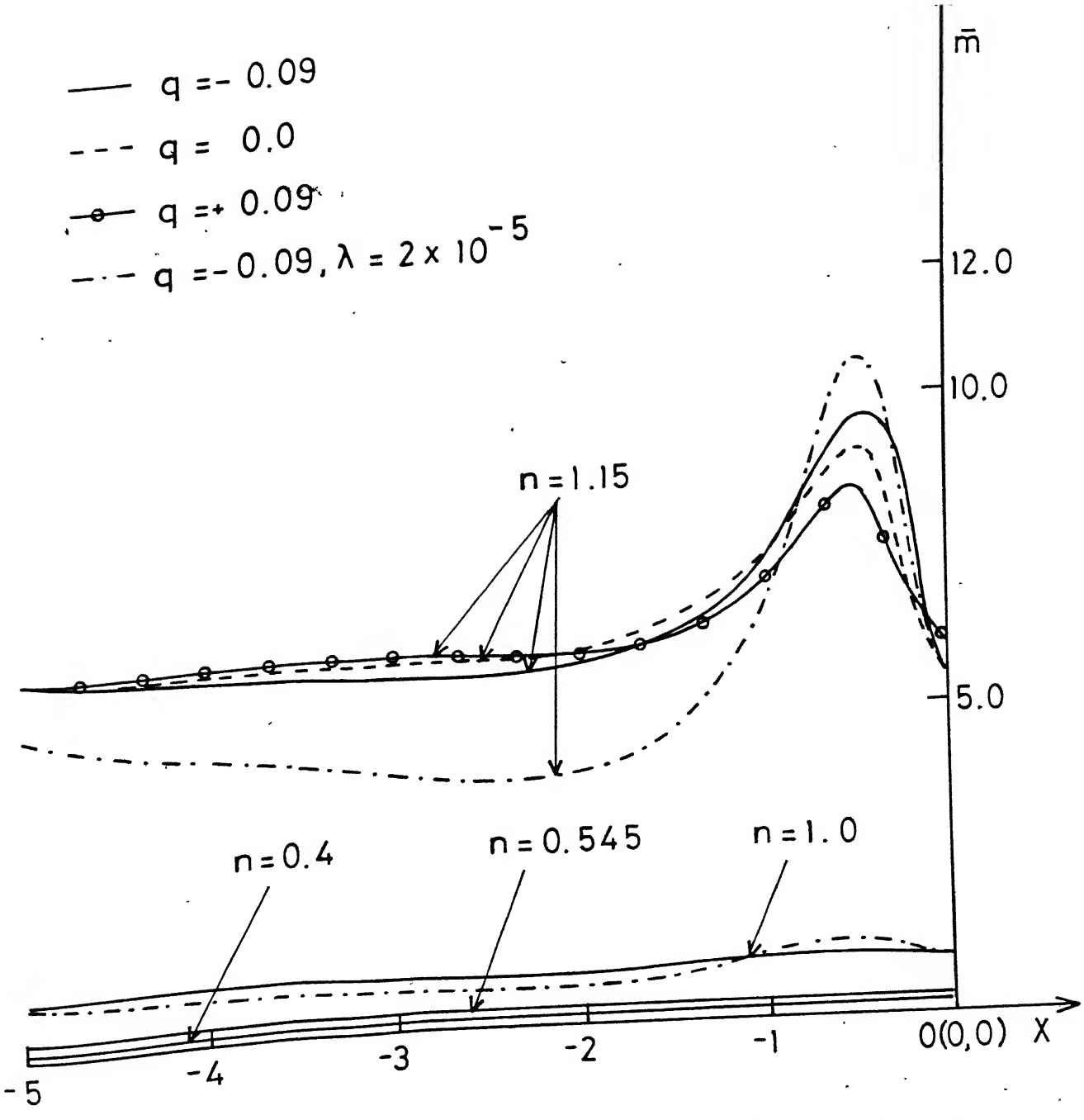

Fig. 4.5 The consistency distribution $\bar{m}$ against X.

CHAPTER V

THERMAL EFFECTS IN LUBRICATION OF ROLLING/SLIDING CONTACTS

5.1 INTRODUCTION :

Most of the roller bearing problems (pure rolling motion of cylinders) considering a power law lubricant have been studied using symmetric conditions i.e. both the rollers have the same dimension and velocity [30,33,57,66,67]. In all the preceding chapters also , the symmetric conditions for pure rolling were made. Particularly, the lubricant flow about x-axis was made symmetric (see chapter I). How far are theseidealized symmetric conditions true under actual operation is in fact a matter of investigation. An obvious generalization of the work presented earlier in this thesis would be the relaxation of the symmetric conditions.i.e. both the rollers may be assumed to have different dimensions and velocities (anti-symmetric case). Thus rolling/sliding operations come into picture.

Several investigations on rolling/sliding concentrated contacts have been reported. Some of the early important works in this direction have already been mentioned in the previous chapters [62,86,89,91,92]. More recently Sadeghi and Dow [160 presented a two dimensional solution to the problem of thermal EHL of rolling/sliding contacts. The Reynolds equation, the two dimensional energy equation and the elastic equation

have been solved simultaneously considering a pressure and temperature dependent viscosity for a synthetic hydrocarbon lubricant (XRM-109F). Sadeghi et al [175] subsequently studied the same problem using an approximate method for the prediction of mid-film temperature and sliding traction. Rashid and Seireg [176] elaborated heat partition and transient temperature distribution in dry and lubricated rolling/sliding contacts. They particularly commented on the existence of the non-Newtonian behaviour of the lubricant in the concentrated contacts. They felt that this happens because the lubricant is subjected to extremely high pressures and shear-stresses which act for a very short time, thus the Newtonian property of the lubricant may not be valid. Rashid and Seireg [177] further mentioned that the severe thermal environment occuring in this type of contacts due to the combination of high pressure and sliding speeds is one of the main factors in the malfunctioning of the machine elements such as gears, bearings, cams and drives. Bush et al [178] analysed surface roughness effects in a rolling/sliding line contact using non-Newtonian lubricants such as a power law, a non-linear sinh-law and a linear visco-elastic Maxwell model. Expressions for bearing traction along with numerical results have been presented. Apart from these, there are several other publications on lubricated rolling/sliding line contacts where Newtonian and different non-Newtonian models have been considered in the analysis. Pressure and temperature dependenc

on non-Newtonian and Newtonian viscosities of the lubricants have also been taken into account.

In most of the references cited above, anti-symmetric conditions have been used. It is also clear that the lubricant properties change with pressure and temperature during rolling/sliding concentrated contacts. Particularly, the lubricant-viscosity changes significantly. The non-Newtonian characteristic of the lubricant also seems to be important. Since the lubricant pressure and temperature in case of rolling/sliding are expected to be higher than those for the pure rolling case (as considered in the previous chapters), it becomes far important to incorporate the non-Newtonian behaviour of the lubricant together with variable viscosity/consistency.

In the present analysis, a power law fluid film lubrication of cylindrical rollers having different dimensions and velocities, is studied under cavitation boundary conditions. Since the rolling bearing geometry is equivalent to a cylinder-plane geometry, the latter is prefered for mathematical calculation. Lubricant consistency is allowed to vary in a manner similar to that mentioned in chapter III. The lubricant inertia which is generally small has been ignored , as this is likely to make the solutions extremely complicated. A very simple approach is adopted in the present analysis in order to separate the zones for positive and negative velocity gradients.

5.2 MATHEMATICAL ANALYSIS :

The governing equations with the usual assumptions of hydrodynamic lubrication for the problem under consideration, in which the two rollers are assumed to have different dimensions and velocities, are

$$\frac{dp}{dx} = \frac{\partial}{\partial y}\left(m\left|\frac{\partial u}{\partial y}\right|^{n-1}\frac{\partial u}{\partial y}\right) \tag{5.1}$$

$$\frac{\partial u}{\partial x} + \frac{\partial v}{\partial y} = 0 \tag{5.2}$$

where m follows the relation (3.2)

$$m = m_o e^{\alpha p - \beta(T_m - T_o)} \tag{5.3}$$

with

$$T_m = \frac{1}{h}\int_o^h T\, dy \tag{5.4}$$

From the point of view of mathematical analysis, the contact between two cylinders of radii R_a and R_b , as shown in fig. (5.1(a)) can be described by an equivalent cylinder near a plane, shown in fig. (5.1(b)) [126].

Film thickness h for the geometry given in fig.(5.1(b)) is expressed as

$$h = h_o + \frac{x^2}{2R} \tag{5.5}$$

where

$$\frac{1}{R} = \frac{1}{R_a} + \frac{1}{R_b} \tag{5.6}$$

The boundary conditions for the governing equations (5.1) and (5.2) are as follows :

$$u = U_1 \, , \; v = 0 \text{ at } y = 0 \tag{5.7}$$

$$u = U_2 \, , \; v = U_2 \frac{dh}{dx} \text{ at } y = h \tag{5.8}$$

$$p = 0 \text{ at } x = -\infty$$

$$p = 0 \, , \; \frac{dp}{dx} = 0 \text{ at } x = x_2 \tag{5.9}$$

In order to solve the system of equations (5.1) and (5.2) for various bearing characterics, one has to first of all determine the sign of the velocity gradient $\frac{\partial u}{\partial y}$ i.e. to eastablish the regions of positive or negative velocity gradients. Approximately, these regions can be obtained easily for the Newtonian fluid (n=1) and it is expected that there will not be a significant deviation for non-Newtonian fluids.

Equations (5.1) and (5.2) can be solved for n = 1 and m to be a constant or a function of x-alone , one can obtain [89]

$$u = U_1 + (U_2 - U_1) \frac{y}{h} - \left(\frac{y}{2m} \frac{dp}{dx}\right)(h-y) \tag{5.10}$$

$$\frac{dp}{dx} = 6(U_1 + U_2)m(h-h_1)/h^3 \tag{5.11}$$

It can be seen that u is a linear function of y at points where $\frac{dp}{dx} = 0$. At these points, the velocity gradient $\frac{\partial u}{\partial y} = \frac{(U_2 - U_1)}{h}$, which can never be equal to zero, since $U_2 \neq U_1$ It can also be seen from fig. (5.2) that for each x, $\frac{\partial u}{\partial y}$ can

vanish at only one point of $y(=\delta)$ in the regions $-\infty \leq X < -X_1$ and $-x_1 < x < x_2$. Thus these regions can be divided into four sub-regions separated by δ-profile, as shown in fig.(5.2).

Let u_1, u_2 and u_3, u_4 be the velocities in the respective regions (see fig.(5.2)), then according to the velocity profile, shown in the figure, one may observe the following :

$$\left.\begin{aligned} &\frac{\partial u_1}{\partial Y} \geq 0 \ , \ \delta \leq y \leq h \\ &\frac{\partial u_2}{\partial Y} \leq 0, \ 0 \leq y \leq \delta \\ &\frac{\partial u_1}{\partial Y} = \frac{\partial u_2}{\partial Y} = 0 \text{ at } y = \delta \end{aligned}\right\} -\infty \leq X < -x_1 \qquad (5.12)$$

$$\left.\begin{aligned} &\frac{\partial u_3}{\partial Y} \geq 0 \ , \ 0 \leq y \leq \delta \\ &\frac{\partial u_4}{\partial Y} \leq 0, \ \delta \leq y \leq h \\ &\frac{\partial u_4}{\partial Y} = \frac{\partial u_3}{\partial Y} = 0 \text{ at } y = \delta \end{aligned}\right\} -x_1 < x < x_2 \qquad (5.13)$$

It is expected that the nature of the velocity profiles for different n as well as variable m may remain unchanged but δ will certainly differ in each case.

Using the sign for the velocity gradients given in (5.12) and integrating equation (5.1) for the region $\delta \leq y \leq h$, one can obtain

$$\frac{\partial u_1}{\partial y} = \left(\frac{1}{m_1} \frac{dp_1}{dx}\right)^{1/n} (y-\delta)^{1/n}$$

Further integration of this, using condition (5.8), gives

$$u_1 = U_2 - \left(\frac{n}{n+1}\right)\left(\frac{1}{m_1}\frac{dp_1}{dx}\right)^{1/n}\{(h-\delta)^{(n+1)/n} - (y-\delta)^{(n+1)/n}\} \tag{5.14}$$

Similarly for the other regions, the following expressions can be obtained :

$$u_2 = U_1 - \left(\frac{n}{n+1}\right)\left(\frac{1}{m_1}\frac{dp_1}{dx}\right)^{1/n}\{\delta^{(n+1)/n} - (\delta-y)^{(n+1)/n}\} \tag{5.15}$$

$$u_3 = U_1 + \left(\frac{n}{n+1}\right)\left(-\frac{1}{m_2}\frac{dp_2}{dx}\right)^{1/n}\{\delta^{(n+1)/n} - (\delta-y)^{(n+1)/n}\} \tag{5.16}$$

$$u_4 = U_2 + \left(\frac{n}{n+1}\right)\left(-\frac{1}{m_2}\frac{dp_2}{dx}\right)^{1/n}\{(h-\delta)^{(n+1)/n} - (y-\delta)^{(n+1)/n}\} \tag{5.17}$$

Now the volume flux Q for the region $(-\infty \leq x < -x_1)$ is obtained as

$$Q = \int_0^h u\, dy$$

$$\text{or} \qquad Q = \int_0^\delta u_2\, dy + \int_\delta^h u_1\, dy$$

$$\text{or} \quad Q = U_1\delta + U_2(h-\delta) - \left(\frac{n}{2n+1}\right)\left(\frac{1}{m_1}\frac{dp_1}{dx}\right)^{1/n}\{\delta^{(2n+1)/n} + (h-\delta)^{(2n+1)/n}$$

(5.18)

Since the flux Q is constant through the every cross section, thus the flux Q may be equated to the flux through the point $x = -x_1$ [179]. This point is selected in order to enforce the continuity of flow.

The flux Q through the point $x = -x_1$ (where $\frac{dp}{dx} = 0$) can be evaluated directly from the equation (5.1), yielding

$$Q(-x_1) = \frac{(U_1+U_2)}{2} h_1 \qquad (5.19)$$

Finally, equating the fluxes given by (5.18) and (5.19) and simplifying, one can obtain the following Reynolds equation

$$\frac{dp_1}{dx} = m_1 \left(\frac{2n+1}{n}\right)^n \left[\frac{(U_1-U_2)\delta + U_2 h - \left(\frac{U_1+U_2}{2}\right) h_1}{\delta^{(2n+1)/n} + (h-\delta)^{(2n+1)/n}}\right]^n, \quad -\infty \leq x \leq -x_1 \qquad (5.20)$$

Similarly for the other region, the Reynolds equation may be written as

$$\frac{dp_2}{dx} = -m_2 \left(\frac{2n+1}{n}\right)^n \left[\frac{\left(\frac{U_1+U_2}{2}\right) h_1 - U_2 h - (U_1-U_2)\delta}{\delta^{(2n+1)/n} + (h-\delta)^{(2n+1)/n}}\right]^n, \quad -x_1 \leq x \leq x_2 \qquad (5.21)$$

Use of the matching conditions:

$$\begin{aligned} u_1 &= u_2 \\ u_3 &= u_4 \end{aligned} \quad \text{at } y = \delta \qquad (5.22)$$

into (5.14-5.17) yields

$$U_2 - U_1 - \left(\frac{n}{n+1}\right)\left(\frac{1}{m_1}\frac{dp_1}{dx}\right)^{1/n} \left\{(h-\delta)^{(n+1)/n} - \delta^{(n+1)/n}\right\} = 0, \quad -\infty \leq x < -x_1 \qquad (5.23)$$

$$U_2 - U_1 + \left(\frac{n}{n+1}\right)\left(-\frac{1}{m_2}\frac{dp_2}{dx}\right)^{1/n} \left\{(h-\delta)^{(n+1)/n} - \delta^{(n+1)/n}\right\} = 0, \quad -x_1 < x < x_2 \qquad (5.24)$$

Eliminating $\frac{dp_1}{dx}$ and $\frac{dp_2}{dx}$ from equations (5.23) and (5.24), using Reynolds equations (5.20) and (5.21), one can obtain a single relation as follows :

$$U_2-U_1-\left(\frac{2n+1}{n+1}\right)\frac{\{(h-\delta)^{(n+1)/n}-\delta^{(n+1)/n}\}\{(U_1-U_2)\delta+U_2h-\left(\frac{U_1+U_2}{2}\right)h_1\}}{[\delta^{(2n+1)/n}+(h-\delta)^{(2n+1)/n}]}=0 \tag{5.25}$$

It must be noted here that the equation (5.25) cannot be used to evaluate δ at $x = -x_1$ and $x = x_2$ since $\frac{\partial u}{\partial y} \neq 0$ there.

Energy equation : The energy equation for this problem is considered to be the same as that considered in chapter III i.e.

$$\frac{\partial^2 T}{\partial y^2} = -\left(\frac{m}{k}\right)\left|\frac{\partial u}{\partial y}\right|^{n-1}\left(\frac{\partial u}{\partial y}\right)^2 \tag{5.26}$$

where the heat of convection has been neglected.

The boundary conditions for this equation are

$$\begin{aligned} T &= T_{o1} \quad \text{at } y = 0 \\ T &= T_h \quad \text{at } y = h \end{aligned} \tag{5.27}$$

Integration of equation (5.26) twice for the region, $-\infty \leq x \leq -x_1$, gives

$$T_{11} = -\frac{n^2}{(2n+1)(3n+1)}\left(\frac{m_1}{k}\right)\left(\frac{1}{m_1}\frac{dp_1}{dx}\right)^{(n+1)/n}(y-\delta)^{(3n+1)/n}+c_1y+d_1 \tag{5.28}$$

$$T_{12} = -\frac{n^2}{(2n+1)(3n+1)}\left(\frac{m_1}{k}\right)\left(\frac{1}{m_1}\frac{dp_1}{dx}\right)^{(n+1)/n}(\delta-y)^{(3n+1)/n}+c_2y+d_2 \tag{5.29}$$

where T_{11} and T_{12} are the lubricant temperature in the regions, $\delta \leq y \leq h$ and $0 \leq y \leq \delta$ respectively, c_1, d_1 and c_2, d_2 are the integration constants.

Use of the temperature matching condition

$$T_{11} = T_{12} \text{ at } y = \delta$$

and the matching heat flux

$$k \frac{\partial T_{11}}{\partial y} = k \frac{\partial T_{12}}{\partial y} \text{ at } y = \delta$$

implies

$$c_1 = c_2 = c(\text{say})$$
$$d_1 = d_2 = d(\text{say}).$$

The constants c and d are evaluated using the boundary conditions (5.27) and are given below :

$$c = \frac{T_h - T_{ol}}{h} + \left(\frac{m_1 A_n}{hk}\right)\left(\frac{1}{m_1}\frac{dp_1}{dx}\right)^{(n+1)/n}\left[(h-\delta)^{(3n+1)/n} - \delta^{(3n+1)/n}\right]$$

$$d = T_{ol} + \left(\frac{m_1 A_n}{k}\right)\left(\frac{1}{m_1}\frac{dp_1}{dx}\right)^{(n+1)/n}\delta^{(3n+1)/n} \qquad (5.30)$$

where $A_n = \dfrac{n^2}{(2n+1)(3n+1)}$.

Thus T_{11} and T_{12} are explicitely known functions of x and y, giving temperature distribution in the region under consideration.

Finally the mean temperature T_{m_1}, as defined in equation (5.4), may be written as

$$T_{m_1} = \frac{1}{h} \int_o^h T \, dy$$

or $$T_{m_1} = \frac{1}{h} \left[\int_o^\delta T_{12} \, dy + \int_\delta^h T_{11} \, dy \right]$$

or $$T_{m_1} = \frac{T_h + T_{o1}}{2} + \frac{S_1}{2} \left[(h-\delta)^{(3n+1)/n} + \delta^{(3n+1)/n} \right]$$

$$- \frac{nS_1}{(4n+1)h} \left\{ (h-\delta)^{(4n+1)/n} + \delta^{(4n+1)/n} \right\} \qquad (5.31)$$

where

$$S_1 = \left(\frac{m_1 A^n}{k}\right) \left(\frac{1}{m_1} \frac{dp_1}{dx}\right)^{(n+1)/n} \qquad (5.32)$$

Proceeding in the same way, the mean temperature for the region $-x_1 \leq x \leq x_2$, can also be written as

$$T_{m_2} = \left(\frac{T_h + T_{o1}}{2}\right) + \frac{S_2}{2} \left[(h-\delta)^{(3n+1)/n} + \delta^{(3n+1)/n} \right]$$

$$- \frac{nS_2}{(4n+1)h} \left[(h-\delta)^{(4n+1)/n} + \delta^{(4n+1)/n} \right] \qquad (5.33)$$

where

$$S_2 = \left(\frac{m_2 A^n}{k}\right) \left(-\frac{1}{m_2} \frac{dp_2}{dx}\right)^{(n+1)/n} \qquad (5.34)$$

Using the non-dimensional scheme given in the previous chapter together with the following :

$$\bar{T}_m = \beta T_m \, , \; \bar{\delta} = \delta / h_o \, , \; \bar{U} = U_1 / U_2 \; (U_1 > U_2) \qquad (5.35)$$

equations (5.20), (5.21), (5.25), (5.31), (5.33) may be rewritten as

$$\frac{d\bar{p}_1}{d\bar{x}} = \bar{m}_1 (\bar{f}_x)^n \qquad (5.36)$$

$$\frac{d\bar{p}_2}{d\bar{X}} = -\bar{m}_2(-\bar{f}_X)^n \tag{5.37}$$

$$1-\bar{U}-\left(\frac{2n+1}{n+1}\right)\frac{\{(H-\bar{\delta})^{(n+1)/n} - \bar{\delta}^{(n+1)/n}\}\{(\bar{U}-1)\bar{\delta}+H-\left(\frac{1+\bar{U}}{2}\right)H_1\}}{[\bar{\delta}^{(2n+1)/n} + (H-\bar{\delta})^{(2n+1)/n}]} = 0 \tag{5.38}$$

$$\bar{T}_{m_1} = \frac{\bar{T}_n+\bar{T}_{o1}}{2} + \bar{m}_1\, d_n\, \bar{\gamma}_s\, (\bar{f}_X)^{n+1}\, \bar{g}_X \tag{5.39}$$

$$\bar{T}_{m_2} = \frac{\bar{T}_n+\bar{T}_{o1}}{2} + \bar{m}_2\, d_n\, \bar{\gamma}_s\, (-\bar{f}_X)^{n+1}\, \bar{g}_X \tag{5.40}$$

where

$$\bar{m}_1 = \bar{m}_o\, e^{\bar{p}_1-\bar{T}_{m_1}+\bar{T}_o}\ ,\ \bar{m}_2 = \bar{m}_o\, e^{\bar{p}_2-\bar{T}_{m_2}+\bar{T}_o} \tag{5.41}$$

$$\bar{\gamma}_s = \left(\frac{U_2 h_o \beta}{k\alpha}\right)\left(\frac{h_o}{2\bar{R}}\right)^{1/2} \tag{5.42}$$

$$d_n = n/((3n+1)2^{n+1}) \tag{5.43}$$

$$\bar{f}_X = \left[\frac{(\bar{U}-1)\bar{\delta} + H - \left(\frac{\bar{U}+1}{2}\right)H_1}{\bar{\delta}^{(2n+1)/n} + (H-\bar{\delta})^{(2n+1)/n}}\right] \tag{5.44}$$

$$\bar{g}_X = \frac{1}{2}\{(H-\bar{\delta})^{(3n+1)/n} + \bar{\delta}^{(3n+1)/n}\} - \frac{n}{(4n+1)H}\{(H-\bar{\delta})^{(4n+1)/n} + \bar{\delta}^{(4n+1)/n}\} \tag{5.45}$$

Equations (5.36), (5.39) and (5.37), (5.40) have to be solved simultaneously using the following conditions :

$$\bar{p}_1 = 0 \text{ at } X = -\infty \tag{5.46}$$

$$\left.\begin{aligned} \bar{p}_2 &= 0 \\ \frac{d\bar{p}_2}{dX} &= 0 \end{aligned}\right| \quad \text{at } X = X_2 \qquad (5.47)$$

From equation (5.37) , it may be observed that the condition

$$\frac{d\bar{p}_2}{dX} = 0 \text{ at } X = X_2$$

implies

$$(\bar{U}-1)\,\bar{\delta}_2 + H_2 - \frac{(\bar{U}+1)}{2}H_1 = 0 \qquad (5.48)$$

Since $\bar{\delta}_2$ comes out to be $H_2/2$ (for detail, see numerical calculation, section (5.3)) , it follows that

$$X_2 = X_1 \qquad (5.49)$$

Thus $X = X_1$ gives the point of cavitation.

5.3 : RESULTS AND DISCUSSION :

Numerical solutions of the Reynolds equations (5.36,5.37) and the energy equations (5.39,5.40) have been obtained for anti-symmetric , viscous incompressible flow of a power law fluid through the gap between a cylinder and a plane (see fig. (5.1)). The results of this investigation are assessed in terms of parameters n and $\bar{U}(= U_1/U_2,\ U_1 > U_2)$. The values of n have already been mentioned in earlier chapter. The sliding parameter $\bar{U}$ is chosen to lie between 1 and 1.2 (i.e. max of 20% slip). The parameter $\bar{U}$ arises due to

the consideration of anti-symmetric conditions and is important because the presence of sliding ($\bar{U} > 1$) is likely to yield more pressure and temperature as compared to that for pure rolling ($\bar{U}=1$). The significance of $\bar{U}$ along with n has been demonstrated through table and graphs. For the numerical calculation, the following representative values have been used :

$U_2 = 400$ cm sec^{-1}, $h_o = 5 \times 10^{-4}$ cm, $\alpha = 1.6 \times 10^{-9}$ $dyne^{-1}$ cm^2, $R = 3$ cm, $\bar{T}_h = 1.5$, $\bar{T}_{o1} = 1$. The thermal factor $\bar{\gamma}_s = (U_2 h_o \beta \sqrt{h_o/2R}/k\alpha)$ is chosen to be 5.

An important feature of this problem is that this reduces to (a) the exact problem done in [33] for $U_1 = U_2$ and m = constant , (b) a similar problem done in [156] for n = 1 and $\alpha = 0$ and (c) the exact problem done in chapter III for $U_1 = U_2$.

Numerical Solutions : The Reynolds and energy equations are coupled through $\bar{m}$ and contain two unknowns $\bar{\delta}$ (the locus of points at which $\frac{\partial u}{\partial y} = 0$) and X_1 ($X = -X_1$ is the point of maximum pressure). These unknowns are also present in equation (5.38). As there is no symmetry ($\bar{U} \neq 1$) for $\bar{\delta}$-distribution , it is necessary to solve equation (5.38) for $\bar{\delta}$ over the complete region under consideration, along with Reynolds and energy equations. The actual process followed for the numerical calculations is given below.

The algebraic equation (5.38) in $\bar{\delta}$ contains X and X_1 explicitly. First of all an initial value of X is assigned i.e. the point at minus infinity is replaced by a large but a finite negative value. An arbitrary value of X_1 is chosen. The value of $\bar{\delta}$ at the inlet is obtained by solving the algebraic equation (5.38) for $\bar{\delta}$ using the bisection method with a reasonable tolerance (say 10^{-4}). These values of X and $\bar{\delta}$ are substituted in the energy equation (5.39). $\bar{T}_{m_1}$ at the inlet is then obtained from solving the algebraic energy equation by prescribing $\bar{m}_o$ and $\bar{p}_1$ (=0 at $X = -\infty$) and using the earlier numerical technique. The same X, $\bar{m}_o$ and the computed $\bar{\delta}$ and $\bar{T}_{m_1}$ are used in the differential equation (5.36). Fourth order Runga-Kutta method is used to evaluate $\bar{p}_1$ at $X = X+\Delta X$. For this value of X ($=X+\Delta X$), equation (5.38) is solved for $\bar{\delta}$. These new X, $\bar{\delta}$ and $\bar{p}_1$ are substituted in the energy equation which again yields $\bar{T}_{m_1}$. X and $\bar{\delta}$ are used to calculate $\bar{p}_1$ as a solution of equation (5.36) at another point $X = X+2\Delta X$. This process is repeated for further values of X till such time that equation (5.38) yields values of $\bar{\delta}$ satisfying $0 \leq \bar{\delta} \leq H$ (because $\bar{\delta}$ cannot exceed H). It may be noted that at $X = -X_1$, $\bar{\delta}$ does not exist (see previous section). Further in the neighbour-hood (n'-hood) of $X = -X_1$, the determined values of $\bar{\delta}$ do not lie in the interval $0 \leq \bar{\delta} \leq H$. Hence in the n' hood of $X = -X_1$, $\bar{\delta}$ (=say $\bar{\delta}^*$) has to be determined solely

on the basis of physical consideration. It should be emphasized here that $\bar{\delta}^*$ does not refer to the locus of points at which the velocity gradient vanishes. Let one consider an ε-n'hood $(-X_1-\varepsilon \leq X \leq -X_1+\varepsilon,\ \varepsilon > 0)$ of the point $X = -X_1$ where there exists no $\bar{\delta}$ lying in the interval $0 \leq \bar{\delta} \leq H$ and satisfying equation (5.38). To ease the mathematical complexity, a linear profile for $\bar{\delta}$ given below

$$\bar{\delta}^*(X) = -\frac{H}{2\varepsilon}(X + X_1 - \varepsilon) \qquad (5.50)$$

is assumed. This profile was chosen in such a manner that it not only satisfies the Reynolds equations at $X = -X_1$, but also makes the pressure curve continuous. Having determined $\bar{\delta} = \bar{\delta}^*$ using equation (5.50) in the n'hood of the point $X = -X_1$, the procedure outlined earlier is adopted to evaluate $\bar{p}_1$ and $\bar{T}_{m_1}$ for the region $-X_1-\varepsilon \leq X \leq -X_1$ and $\bar{p}_2$, $\bar{T}_{m_2}$ for the region $-X_1 \leq X \leq -X_1+\varepsilon$. Since in the interval $-X_1+\varepsilon \leq X \leq X_2-\varepsilon$, $\bar{\delta}$ (roots of equation (5.38)) satisfies the inequality $0 \leq \bar{\delta} \leq H$, so $\bar{\delta}$ in the region $-X_1+\varepsilon \leq X \leq X_2-\varepsilon$ is determined (by the same procedure followed near the inlet) along with $\bar{p}_2$ and $\bar{T}_{m_2}$. Subsequently in the interval $X_2-\varepsilon \leq X \leq X_2$ (since equation (5.38) is not valid at $X = X_2$), the same type of linear profile given below

$$\bar{\delta}^*(X) = \frac{H_2}{2\varepsilon}(X-X_2+\varepsilon),\ X_2-\varepsilon \leq X \leq X_2 \qquad (5.51)$$

is assumed (The complete $\bar{\delta}$-profile has been shown in fig. (5.2)).

This will satisfy the Reynolds cavitation boundary condition (5.47) i.e. $\frac{d\bar{p}_2}{dX} = 0$ at $X = X_2$ (5.52)

iff $X_2 = X_1$

$\bar{\delta}$ in the region $X_1 - \varepsilon \leq X \leq X_1$ is calculated using relation (5.48) together with $\bar{p}_2$ and $\bar{T}_{m_2}$. If the computed value of $\bar{p}_2$ at $X = X_1$ satisfies the condition (5.47) (i.e. $\bar{p}_2 = 0$ at $X = X_1$), the assumed arbitrary value of X_1 was correct. Otherwise another value of X_1 is assigned and the whole process is repeated so long as $\bar{p}_2$ vanishes at $X = X_1$. Thus X_1 and $\bar{\delta}$ (as a function of X) are computed along with pressures $\bar{p}_1, \bar{p}_2$ and the mean temperatures $\bar{T}_{m_1}, \bar{T}_{m_2}$. The complete pressure and the mean temperature profiles as functions of n and $\bar{U}$ have been presented in the following sections.

Pressure Profile : The pressure profile $\bar{p}$ has been presented for various values of n and $\bar{U}$ in fig.(5.3). It can be seen that for each fixed n and $\bar{U}$, the pattern of the pressure profile with respect to X is exactly similar to that shown in previous chapters. It can also be noted that for a fixed $\bar{U}$, the qualitative behaviour of $\bar{p}$ with respect to n remains unaltered (see earlier chapters) i.e. $\bar{p}$ increases with n. For a fixed n, $\bar{p}$ increases with $\bar{U}$. This can be seen through the fig. (5.3) for values of $n \geq 1$. $\bar{p}$ depicts the same trend for $n < 1$, also, however it has not been shown because of overlapping of curves. $\bar{p}$ increases with $\bar{U}$ which implies that

hydrodynamic pressure due to sliding is higher than that for the pure rolling. This is justified also because the rolling friction is always less than the sliding friction.

Temperature Profile : The mean temperature distribution has been depicted in fig. (5.4) as a function of n and $\bar{U}$. It is clear that the qualitative behaviour of the mean temperature $\bar{T}_m$ versus X is quite similar to that obtained in chapter III. For a fixed $\bar{U}$, $\bar{T}_m$ increases with increasing value of n. This pattern also is in accordance with the results mentioned in that chapter (for $q = 0$). For a fixed n, $\bar{T}_m$ increases with $\bar{U}$ (its behaviour is similar to that of the pressure profile). Hence the same geometrical interpretation may follow here. It may be easily concluded that the sliding temperature is higher than that for the pure rolling.

Consistency Profile : The characteristic behaviour of the consistency $\bar{m}$ i.e. over all change in $\bar{m}$ due to the combined effect of pressure $\bar{p}$ and the temperature $\bar{T}_m$ (see relation (5.41)) has been demonstrated through the fig. (5.5). It is seen that the consistency distribution $\bar{m}$ versus X is qualitatively almost similar to the pressure profile. The difference appears (in case of $n > 1$) near the inlet as well as outlet. However , for $n \leq 1$, the difference appears only near the outlet. Near the inlet (for $n > 1$), $\bar{m}$ decreases

because the increase in $\bar{p}$ is unable to compensate for the temperature rise. After that it is almost flattened because of equal contribution of $\bar{p}$ and $\bar{T}_m$. Again at the outlet (for all n), $\bar{m}$ increases (though very marginal) since the impact of the reduced temperature is higher than that of the reduced pressure. Further the consistency peak in the low pressure gradient region is quite sharp. This happens due to sharp increase in $\bar{p}$ and decrease in $\bar{T}_m$ (when $X \to X_1$) simultaneously. For a fixed $\bar{U}$, $\bar{m}$ increases with n. Similarly for a fixed $n(> 1)$, it increases with $\bar{U}$ except near the inlet where the trend is reversed. For a fixed $n(\leq 1)$, a similar trend has been obtained, however it has not be shown due to overlapping of curves.

Load and Traction : Load W_Y and traction T_F have been computed for various values of n and $\bar{U}$ and have been presented in table (5.1). For a fixed value of $\bar{U}$, W_Y as well as T_F both have similar trend with respect to n as discussed in the previous chapters. For each fixed n, W_Y and T_F increase with $\bar{U}$. Hence it follows that load and traction increase due to sliding.

Film Rupture : Film cavitation points have also been calculat and have been displayed in the same table (5.1). It may be seen from the table that for a fixed value of $\bar{U}$, the cavitati points follow the same trend as mentioned earlier (i.e. X_1 increases as n decreases). Similarly for each fixed n, X_1

increases as $\bar{U}$ decreases. It seems that cavitation during the sliding motion occurs earlier to that of the pure rolling case.

5.4 CONCLUSION :

With the usual assumptions of hydrodynamic lubrication, an endeavour is made to study thermal lubrication of rolling/sliding contacts by an incompressible power law fluid. The thermal Reynolds and energy equations which are functions of consistency ($\bar{m}$) , sliding velocity ($\bar{U}$) and the location of points at which the velocity gradients vanish ($\bar{\delta}$), are derived. Semi-analytical solutions for pressure $\bar{p}$ and the mean temperature $\bar{T}_m$ are obtained for the isothermal boundaries. It may be concluded from the results obtained that

(a) there is a significant increase in pressure (hence the load and traction) with flow index n for a fixed value of $\bar{U}$. A similar trend follows when $\bar{U}$ is varied (from 1 to 1.2) and n is held fixed.

(b) there is also a significant change in the mean temperature with respect to n and $\bar{U}$.

(c) In addition , the consistency variation resulting from $\bar{p}$ and $\bar{T}_m$ is also important. Particularly, this variation is quite significant in the pressure peak region for Newtonian and dilatant fluids.

Table 5.1 : Bearing characteristics for various values of n and $\bar{U}$

n/m_o	$\bar{U}$	$X_1 = X_2$	W_Y	T_F
	1.20	0.420500	1.802456	1.160597
	1.15	0.423172	1.789505	1.148427
1.15/0.56	1.10	0.425062	1.774255	1.133527
	1.05	0.426737	1.756257	1.115375
	1.01	0.427515	1.740753	1.100124
	1.20	0.457812	0.460492	0.253302
	1.15	0.461625	0.453943	0.250487
1.00/0.75	1.10	0.463750	0.446638	0.246039
	1.05	0.464625	0.439343	0.241624
	1.01	0.465000	0.433326	0.237861
	1.20	0.474590	0.157524	0.076426
	1.15	0.481500	0.156369	0.076375
0.545/86	1.10	0.485725	0.155055	0.076145
	1.05	0.489300	0.153657	0.075812
	1.01	0.495125	0.152522	0.075730
	1.20	0.483750	0.037372	0.0175410
	1.15	0.485000	0.037140	0.0175131
0.400/128	1.10	0.495750	0.036910	0.0174810
	1.05	0.511500	0.036672	0.0174570
	1.01	0.514062	0.036458	0.0174290

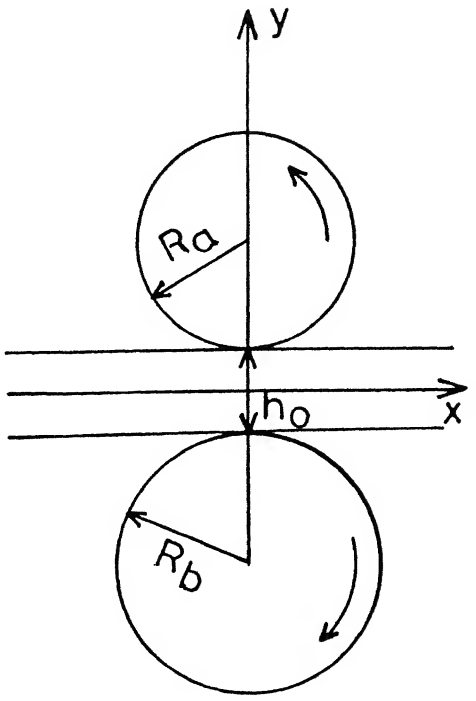

Fig. 5.1(a) Lubrication of two cylindrical rollers having different dimensions and velocities.

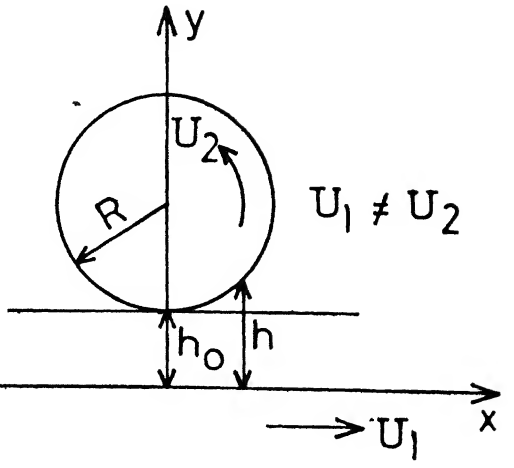

Fig. 5.1(b) Lubrication of a cylinder on a plane.

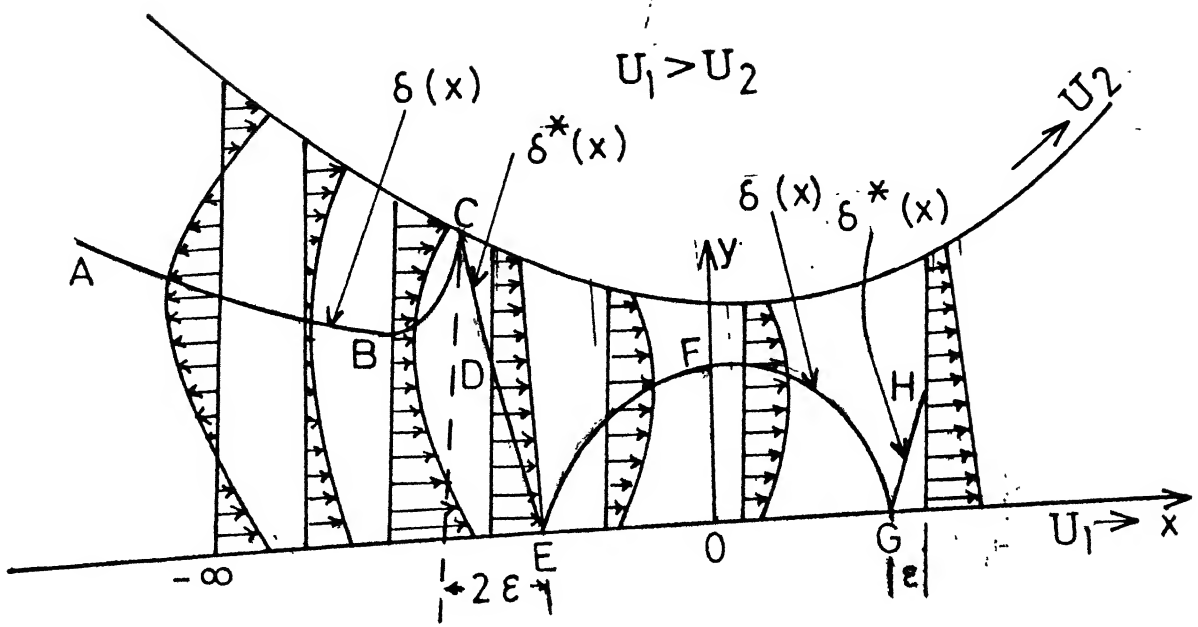

Fig. 5.2 Velocity profiles by arrow mark, δ-profiles by ABC and EFG, and δ^*-profiles by CD, DE and GH, D being the middle point of height of the film thickness at $x = -x_1$.

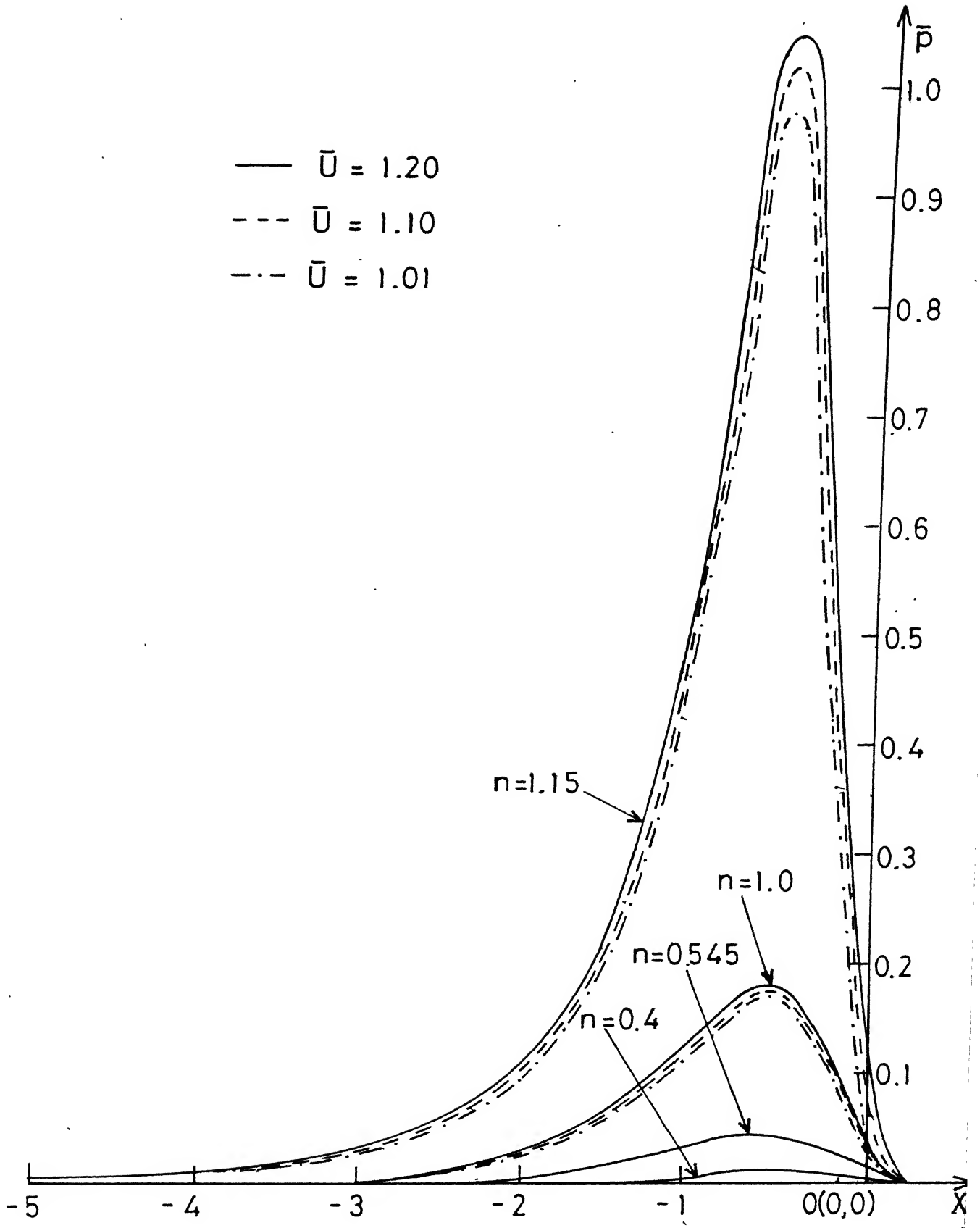

Fig. 5.3 Pressure distribution $\bar{p}$ vs. X.

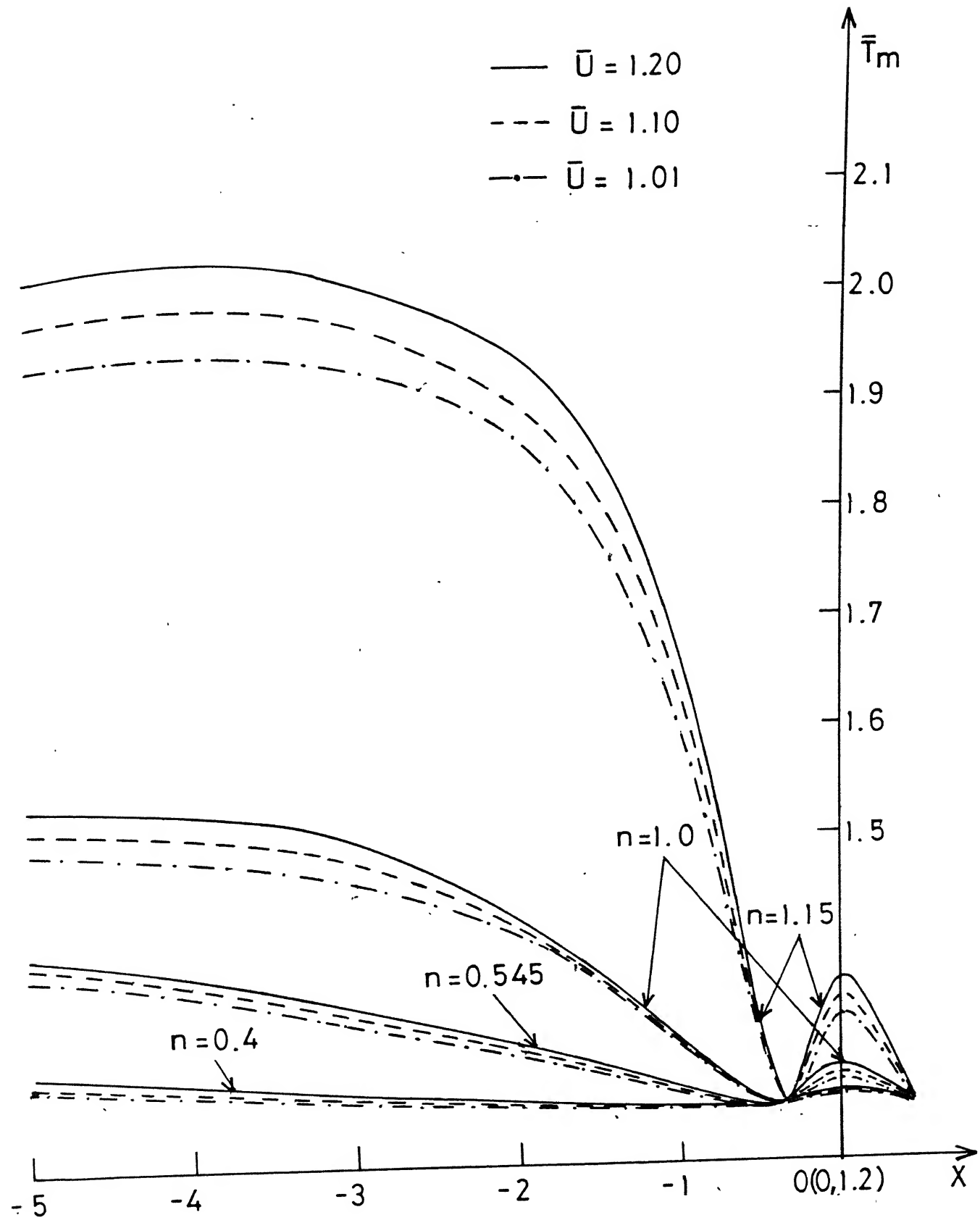

Fig. 5.4 The mean temperature distribution $\bar{T}_m$ vs. X.

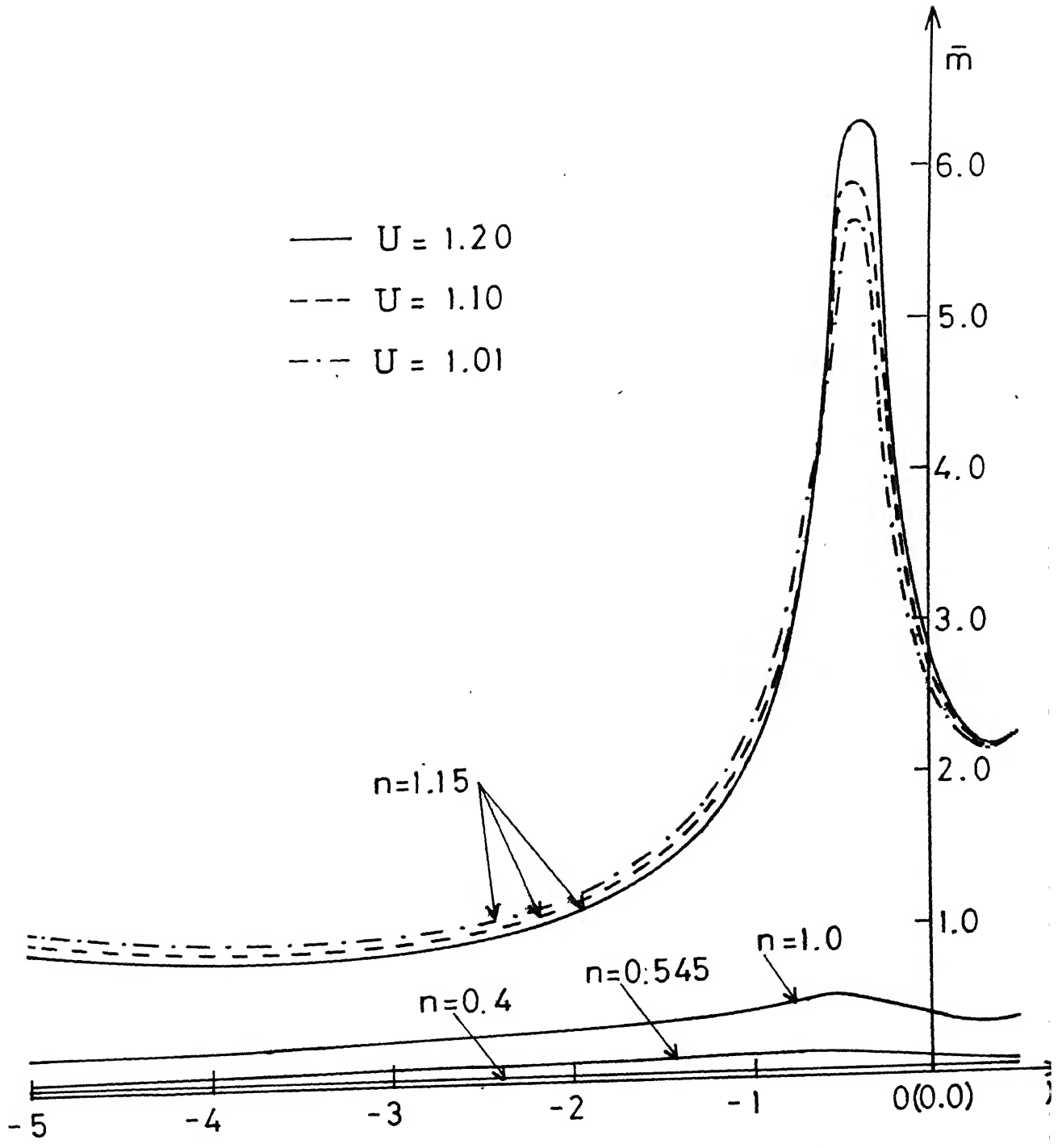

Fig. 5.5 The consistency distribution $\bar{m}$ vs. X.

REFERENCES

[1] Halling, J., Principle of tribology, The MacMillan Press Ltd. (1975) 1.

[2] Radzimovsky, E.I., Lubrication of bearings, The Ronald Press Company, New York (1959)3.

[3] Wilcock, D.F. and Booser, E. R., Bearing design and applications, McGraw-Hill Book Company, Inc, (1957)V.

[4] Harris, T.A, Rolling bearing analysis, John Wiley and Sons (1984)2.

[5] Parish, W.F., Lubrication Encylopedia Britanica, 14th. Ed.,14(1929)451.

[6] Walowit, J.A. and Anno, J., Modern development in lubrication mechanics, Applied Science publishers Ltd. London (1975)1

[7] Hirn, G.A., Bull. Soc. Indust. Mulhous, 26(1954)188.

[8] Bowden, P. and Tabor, D., The friction and lubrication of solids, part I (1950).

[9] Tower, B., First report on friction experiment, Proc. Instn. Mech. Engrs, 34(1883)362.

[10] Reynolds, O., On the theory of lubrication and its application to Mr. Beauchamp Tower's experiment including an experimental determination of the viscosity of the oil, Phil. Trans., Roy. Soc. London., 177A(1886)13

[11] Sommerfeld, A., Zur hydrodynamischen theroie der Schmiermi-Helreiburg, Z. Angew. Math. U. Phys., 50(1904)97.

[12] Davenport, T.C., The rheology of lubricants, John Wiley and Sons (1973) 1.

[13] Dayson, A., Thickness of very thin film in EHD lubrication, Discussion of the Faraday society, No. 1(1971)231.

[14] Prasad, K.R., Effects of surface roughness and additives in lubrication, Ph.D. Thesis, IIT Kanpur (India), 1980.

[15] Barwell, F.T., Additives for lubricants and operational fluids, conference report, Trib. international, 19(1986)104.

[16] Kingsbury,A., A new oil testing machine and some of its results, Trans. ASME, 24(1903)144.

[17] Needs, S.J ., Boundary film investigations, Trans. ASME, 62(1940)331.

[18] Fuks, G.I., The properties of solutions of organic acids in liquids hydrocarbons at solid surface, Research in surface forces, Edt. Derjaguin, B.V., 1(1960)79.

[19] Fuks, G.I., The polymolecular component of the lubricating boundary layer, Research in surface forces, Edt. Derjaguin, 2(1964)159.

[20] Hayward, A.T. J. and Isdale, J.D., The rheology of liquids very near to solid boundaries, Brit. J. Appl. Phys. 2(1969)251.

[21] Cameron, A. and Crouch, R.F., Interaction of hydrocarbon and surface active agent, Nature, 198(1963)475.

[22] Gohar, R. and Cameron, A., Optical measurement of oil film thickness under EHL, Nature, 200(1963)458.

[23] Askwith, T.C., Cameron, A. and Crouch, R.F., Chain length of additives in relation to lubricants in thin film and boundary lubrication, Proc. Roy. Soc. London, Ser. A 291(1966)500.

[24] Cameron, A. and Gohar, R., Theoretical and experimental studies of the oil film in lubricated point contact, Proc. Roy. Soc. London, Ser. A 291(1966)520.

[25] Gentle, C.R., Paul, G.R. and Cameron, A., Some evidence of granular behavior in EHD traction, Trans. ASLE, 23(1980)155.

[26] Paul, G.R., Density changes at high pressure with an impact viscometer, Wear, 49(1978)79.

[27] Paul, G.R., Time dependent viscosity following a pressure rise measured on an impact viscometer, Trans. ASLE, 19(1976)17.

[28] King, V.W. and Lauer, J.L., Temperature gradient through EHD films and molecular alignment evidence by Infrared Spectroscopy, J. Lub. Tech., 103(1981)65.

[29] Booth, M.J. and Hirst, W., The rheology of oils during impact, Proc. Roy. Soc. London, Ser A 316(1970) 391-429.

[30] Hirst, W. and Lewis, M.G., The rheology of oils during impact, Proc. Roy. Soc. London, Ser. A334(1973)1.

[31] Walters, K., New concepts in theoretical and experimental rheology of lubricants, from Rheology of lubricants, Edt. Devenport, T.C., Wiley (1973)1.

[32] Yousif, A.E. and Bogi, K.D., The rheological behaviour of a new high temperature synthetic grease, Proc. Instn. Mech. Engrs., London, (1970).

[33] Sinha, P. and Singh C., Lubrication of cylinder on a plane with a non-Newtonian fluid considering cavitation, J. Lub. Tech., 104(1982)168.

[34] Yousif, A.E.T., and Ibrhim, M., Lubrication of a slider bearing with oils containing additives and contaminants, Wear, 81(1982)33.

[35] Hirst, W. and Moore, A.J., Non-Newtonian behaviour in EHL, Proc. Roy. Soc. London, Ser.A 337(1974)101.

[36] Johnson, K.L., General thermal effects, Thermal effects in tribology, Proc. 6th Leeds-Lyon Symposium on tribology (1979)175.

[37] Milne, A.A., A theory of grease lubrication of a slider bearing, Proc. 2nd Intl. Congr. on Rheology, (1953) 427.

[38] Sasaki, T., Mori, H. and Okino, N., Theory of grease lubrication of cylindrical roller bearing, Bull. JSME, 3(1960)212.

[39] Wada, S., Hayashi, H., Haga, K., Kawakami, Y. and Okajima, M., EHD lubrication of Bingham solid, Bull. JSME, 20(1977)110.

[40] Mutuli, S., Bonneau, D. and Frene, J., Velocity measurements in the grease lubricating film of a sliding contact, Trans. ASLE, 29(1986)515.

[41] Burton, R.A., An analytical investigation of viscoelast effects in the lubrication of rolling contact, Trans. ASLE, 3(1960)1.

[42] Johnson, K.L. and Tevaarwerk, J.L., Shear behaviour of EHD oil films, Proc. Roy. Soc. London, Ser.A 156(1977)215.

[43] Houpert, L., Fast numerical calculations of EHD sliding Traction forces, An application to rolling bearings, J. Tribology, 107(1985)234.

[44] Bair, S. and Winer, W.O., A rheological model for EHD contacts based on primary laboratory data, J. Lub. Tech., 101(1979)258.

[45] Heyes, D.M. and Montroso, C.J., The use of line and point contacts in determining lubricant rheology under low slip EHD conditions, J. Lub. Tech., 105(1983)28

[46] Phan-Thien, N., The transmission loss in squeeze film flow of Newtonian and some viscoelastic fluids, J. Tribology, 109(1987)93.

[47] Phan-Thien, N. and Tainer, R.I, Viscoelastic squeeze film flows-Maxwell fluids, J. Fluid Mech., 129(1983)265.

[48] Phan-Thien, N. and Walsh, W., Squeezing film flow of an Oldroyd-B fluid: Similarity solution and limiting Weissenberg number, ZAMP, 35(1984)747.

[49] Phan-Thien, N. Dudec, J., Boger, D. V. and Tirtaatmadja, V., Squeezing film flow of ideal elastic liquids, J. non-Newtonian Fluid Mech., 18(1985)227.

[50] Hsu, Y.C. and Saibel, E., Slider bearing performance with non-Newtonian lubricant, Trans. ASLE,8(1965)191.

[51] Wada, S. and Hayasi, H., Hydrodynamic lubrication of journal bearings by pseudo-plastic lubricants, Part I and II, Bull. JSME, 14(1971)268.

[52] Wada, S., Hayasi, H. and Hashimoto, H., EHL of rollers between two lubricated cylinders with non-Newtonian fluids, Bull. JSME, 21(1978)730.

[53] Hashimoto, H. and Wada, S., The effects of fluid inertia forces in parallel circular squeeze film bearings lubricated with pseudo-plastic fluids, J. Tribology, 108(1986)282.

[54] Scott, J.R., Theory and application of the parallel plate plastic meter, Trans. Inst. Rubber Ind.,7(1931)16

[55] Acharya, A., Mashelkar, R.A. and Ulbrecht, J., Rheologi Acta,15(1976) 454.

[56] Bhavaraju, S.M., Mashelkar, R. A. and Blanch , H.W., Buble motion and mass transfer in non-Newtonian fluids, AICHE J., 24(1978)1063.

[57] Sinha, P., Shukla, J.B., Singh, C. and Prasad, K.R., Non-Newtonian lubrication theory for rough surfaces: Application to rough and elastic rollers, J. Mech. Engr. Sci., 24(1982)147.

[58] Kawase, Y. and Moo-Young, M., Approximate solutions for power law fluid flow past particle at low Reynolds numbers, J. Non-Newtonian fluid Mech.21(1986)16

[59] Schowalter, W.R., Mechanics of non-Newtonian fluids, Pergamon press, (1978)139.

[60] Riddle, M.J., Narvaez, C. and Bird, R.B., Interactions between two spheres falling along their line of centres in a viscoelastic fluid, J. Non-Newtonian Fluid Mech.,2(1977)23.

[61] Griskey, R. G. and Green, R.G., Flow of dilatant (shear-thickening) fluids, AICHE J., 17(1971)725.

[62] Dayson, A. and Wilson, A.R., Film thickness in EHD lubrication by Silicon fluids, Proc. Instn. Mech. Engrs., Lubrication and wear fourth convection, 180(1965-66) Pt-3K,97.

[63] Safar, Z.S. and Shawki, G., Performance of thrust bearings operating with non-Newtonian lubricating films, Trib. International 12(1979)31.

[64] Safar, Z.S., Journal bearing operating with non-Newtonia lubricating films, Wear, 53(1979)95.

[65] Safar, Z.S., Dynamical loaded bearings operating with non-Newtonian lubricating films, Wear, 55(1979)295.

[66] Sinha, P., Shukla, J.B., Prasad, K., R. and Singh, C., Non-Newtonian power law fluid lubrication of lightly loaded cylinders with normal and rolling motion, Wear, 89(1983)313.

[67] Sinha, P. and Raj, A., Exponential viscosity variation in the non-Newtonian lubrication of rollers considerin cavitation, Wear, 87(1983)29.

[68] Salem, E. A., Khalil, M.F. and Bedewi, M.A., Analysis of externally pressurized spherical bearings lubricated with non-Newtonian fluids, Wear, 91(1983)1.

[69] Salem, E. A., Khalil, M.F. and Bedewi, M.A., Thermal and inertia effects in externally pressurized spherical bearing lubricated with non-Newtonian fluids, Wear, 91(1983)15.

[70] Dein, I. K. and Elrod, H.G., A generalized steady Reynolds equation for non-Newtonian fluids with application to journal bearings, J. Lub. Tech., 105(1983)385.

[71] Elkouh., A.F., Nigro, N. J. and Liou, Y.S., Non-Newtonian squeeze film between two plane annuli, J. Lub. Tech., 104(1982)275.

[72] Elkouh, A.F., Nigro, N. J. and Glowacz, A., A generalized squeezing flow of a power low fluid between two plane annuli, J. Tribology, 108(1986)80.

[73] Buckholz, R.H., On the role of a non-Newtonian fluid in short journal bearing theory, J. Tribology, 107(1985)68.

[74] Buckholz, R.H. and Hwang, B., The accuracy of short bearing theory for non-Newtonian lubricants, J. Tribology, 108(1986)73,

[75] Raj, A., Effects of consistency variation on Non-Newtonian lubrication, Ph.D. Thesis, I.I.T. Kanpur(India 1984.

[76] Nailwal, T.S., Some Newtonian and non-Newtonian aspects of radial face seals, Ph.D. Thesis, I.I.T. Kanpur(India), 1983.

[77] Safar, Z. and Szeri, A.Z., THD lubrication in laminar and turbulent regimes, J. Lub. Tech., 96(1974)48.

[78] Tipei, N., Theory of lubrication, Stanford University Press, Standford, CA, USA, (1962)177.

[79] Raimondi, A.A., An adiabatic solution for the finite slider bearing (L/B=1), Trans. ASLE, 9(1966)283.

[80] Ripple, H.C., Simplified design of thrust bearings, Part 3, Lubricant temperature and heat balance techniques, Machine Design, 38(1966)209.

[81] Ettles, C. and Cameron, A., Action of Parallel surfaces thrust bearings, presented at the Institution of Mechanical Engineers Lubrication and Wear fourth convention, Schaveningen, The Netherlands, May 12-14,1966.

[82] Barwell, F.T., Bearing data--Can they be made more useful to designers, lubrication and wear third convention , proceedings of the Institution of Mechanical Engineers, 179 part 3J (1965)85.

[83] Tipei, N. and Nica, A., Temperature field in lubricating film of journal bearing, Revue Romanie des Sciences Technique Serie de Mechanique Applique, 11(1966)383.

[84] Tipei, N. and Nica, A., On field of temperature in lubricating films, J. Lub. Tech., 89(1967)483.

[85] McCallion, H., Yousif, F. and Lloyd, T., The analysis of thermal effects in a full journal bearing, J. Lub. Tech.,92(1970)578.

[86] Crook, A.W., The lubrication of rollers III, A theoretical discusssion of friction and the temperatur in the oil film, Phil. Trans., Roy. Soc. London, 254(1961)237.

[87] Crook, A.W., The lubrication of rollers 4 : Measuremen of friction and effective viscosity, Phil. Trans., Roy. Soc. London, 255(1963)281.

[88] Cheng, H.S., A refined solution to THD lubrication of rolling and sliding cylinders., Trans. ASLE, 8(1965)397.

[89] Cheng, H.S. and Sternlicht, B., A numerical solution for pressure temperature and film thickness between two infinitely long lubricated rolling and sliding cylinders, under heavy loads, J. Basic Engr. 87(1965)695.

[90] Davson, A., Friction traction and lubricant rheology in EHL, Phil. Trans., Roy. Soc. London, 266(1970)1.

[91] Kannel, J.W. and Walowit, J. A., Simplified analysis for traction between rolling sliding EHD contacts, J. Lub. Tech., 93(1971)39.

[92] Johnson, K.L. and Greenwood, J. A., Thermal analysis of an Eyring fluid in EHD traction, Wear, 61(1980)353.

[93] Conry. T.F., Thermal effects on traction in EHD lubrication, J. Lub. Tech., 103(1981)533.

[94] Ghose, M.K. and Hamrock, J., Trans. ASLE, 28(1985)159.

[95] Houpert, L., Flamand, L. and Berthe, D., Rheological and thermal effects in lubricated EHD contacts, J. Lub. Tech. 103(1981)526.

[96] Houpert, L., New results of traction force calculation in EHD contacts, 107(1985)241. J. Tribology.

[97] Roelands, C.J.A., Correlation aspects of the viscosity temperature pressure relationship of oils, Ph.D. Thesis, Technische Hogeschool, Delft, Netherland, 1966.

[98] Szeri, A.Z., Some extensions of the lubrication theory of Osborne Reynolds, J. Tribology, 109(1987)21.

[99] Dowson, D. and March, C.N.A., THD analysis of journal bearing, Proc. Instn. Mech. Engr 181(1967)30.

[100] Ezzat, H. A. and Rhode, S.M., A study of THD performence of finite slider bearing, J. Lub. Tech., 95(1973)298.

[101] Salem, E. and Khalil, F., Variable viscosity effect in externally pressurized spherical oil bearing, Wear, 50(1978)221.

[102] Shih-I Pai, Viscous flow theory II, D. Van Nostrand Company, Inc. (1957) 94.

[103] Dowson, D., Higginson, G. R. and Whitaker, A.V., EHL-a survey of isothermal solutions, J. Mech. Engr. Sci., 4(1962)121.

[104] Milne, A. A., Inertia effects in self-acting bearing lubrication, theory, Proc. Inter. symposium on lubrication wear and friction (1965)491.

[105] Houpert, L. and Hamrock, J., Fast approach for calculating film thicknesses and pressures in EHD lubricated contacts at high loads, J. Trobology, 108(1986)411.

[106] Archard, G.D., Gair, F.C. and Hirst, W., The EHL of rollers, Proc. Roy. Soc. London, Ser. A 262(1961)51.

[107] Dowson, D. and Whitaker, A.V., The isothermal lubrication of cylinders, Trans. ASLE, 8(1965)224.

[108] Adams, D.R. and Hirst, W., Frictional traction in EHL, Proc. Roy. Soc. London, Ser. A 332(1973)505.

[109] Rodkiewicz, C.M. and Srinivasan, V., EHL in rolling and sliding contacts, J. Lub. Tech., 94(1972)324.

[110] Cheng, H.S., Isothermal EHD theory for the full ranges of pressure viscosity coefficient, J. Lub. Tech. 94(1972)35.

[111] Evans, H.P. and Snidle, R.W., The isothermal EHD lubrication of spheres, J. Lub. Tech. 103(1981)547.

[112] Hirst, W. and Moore, J., The effect of temperature on traction in EHL, Phil. Trans., Roy. Soc. London, 293(1980)183.

[113] Mazumdar, B.C., The THD solution of oil journal bearing, Wear, 31(1975)287.

[114] Hartung, H.A. and Philadelphia, P.A., Density temperature pressure relations for liquid lubricants, Trans. ASME, 78(1950)941.

[115] Smalley, A.J., Vohr, J.H., Castelli, V. and Wachmann, C., An analytical and experimental investigation of turbulent flow in bearing films including convective fluid inertia forces, J. Lub. Tech. 96(1974)151.

[116] Elkouh, A.F., Fluid inertia effects in non-Newtonian squeeze film, J. Lub. Tech., 98(1976)409.

[117] Kreminsky, H. and Raczynsky, A., Selection of lubricant-viscosity for sliding lubricants, Tashkent, May 22-26, Scientific council on friction and lubrication, Moscow, 3/1(1985)314.

[118] Hashimato, H. and Wada, S., Turbulent lubrication of tilting pad thrust bearings with thermal and elastic deformations, J. Tribology, 107(1985)82.

[119] Floberg, L., Lubrication of two cylindrical surfaces considering cavitation, Trans. Chalmers University Tech., Gothenberg, Inst. Machine element 14(1961)234.

[120] Sasaki, T., Mori, H. and Okino, N., Fluid lubrication theory of roller bearings, J. Basic Engr. 84(1962)166.

[121] Dowson, D., Markho, P.H. and Jones, D.A., The lubrication of lightly loaded cylinders in combined rolling, sliding and normal motion, Part I, Theory. J. Lub. Tech., 98(1976)509.

[122] Conry. T.F., An analytical solution for the normal load carrying capacity of lightly loaded cylinder in combined rolling , sliding and normal motion, J. Lub. Tech., 103(1981)467.

[123] Gatcombe, E.K., Lubrication characteristics of involute spur-gears - a theoretical investigation, Trans. ASME, 67(1945)177.

[124] Hersey, M.D. and Lowdenslager, D.B., Film thickness between gear teeth, Trans. ASME, 72(1950)1035.

[125] Blok , H., Discussion , Gear lubrication symposium, Part I, The lubrication of gears, J. Inst. Petrol. 38(1952)673.

[126] Dowson, D. and Higginson, G.R., The fundamentals of roller gear lubrication EHD, Pergamon Press , (1966)3.

[127] Cameron, A., Basic theory of lubrication, 2nd Edtn. John Wiley and Sons (1976)13.

[128] Mostofi, A. and Gohar, R., Oil film thickness and pressure distributions in EHD point contacts, J. Mech. Engr. Sci., 24(1982)173.

[129] Karami, G., Evans, H.P. and Snidle, R.W., EHL of circumferentially finished rollers having sinusoidal roughness, Proc. Instn. Mech. Engr., 201(1987)29.

[130] Gould, P., High pressure spherical squeeze film, J. Lub. Tech., 93(1971)207.

[131] Rohde, S.M. and Ezzat, H. A., A study of THD squeeze films, J. Lub. Tech., 96(1974)198.

[132] Zienkiewicz, O.C., Temperature distribution within lubrication film between parallel surfaces and its effect on pressure developed, Proc. Conf. Lubrication and Wear, Istn. Mech. Engr.81(1957)135.

[133] Dowson, D. and Whitaker, A.V., A numberical procedure for the solution of the EHD problem of rolling and sliding contacts lubrication by Newtonian fluids, Symposium on EHD lubrication, Leeds, 1965, Proc. Instn. Mech. Engr., 180 3B(1965-66)47.

[134] Agrawal, B.B. and Wilson, W.R.D., Improved thermal Reynolds equations, Proc. 6th Leeds-Neyon symposium on tribology, from Thermal effects in tribology, (1980)153.

[135] Heshmat, H. and Pinkus, O., Mixing inlet temperatures in hydrodynamic bearings, J. Tribology, 108(1986)231.

[136] Giordano, M. and Boudet, R., THD flow of a piezo viscous fluid between two parallel discs, Proc. 6th Leeds-Neyon symposium on tribology, from Thermal effects in tribology, (1980)127.

[137] Dowson, D., Hudson, J.D., Hunter, B. and March, C.N., An experimental investigation of the thermal equilbrium of steadily loaded journal bearings, Proc. Instn. Mech. Engr., 3B 181(1966)70.

[138] Tonneson, J. and Hansen, P.K., Some experiment on the steady state characteristics of a cylindrical fluid film, 103(1981)237, J. Lub. Tech.

[139] Pinkus, O. and Sternlicht, B., Theory of hydrodynamic lubrication, McGraw Hill, New York, (1961) 287,289.

[140] Wilkinson, W.L., Non-Newtonian fluids, Pergamon Press, London (1960).

[141] Buckholz, R.H. and Lin, J.F., The effect of journal bearing misalignment on load and cavitation for non-Newtonian lubricants, J. Tribology, 108(1986)645.

[142] Curnlor, A.R. and Taylor, R.L., A thermomechanical formulation and solution of lubricated contacts, J. Lub. Tech., 104(1982)109.

[143] Shukla, J.B. and Isa, M., Thermal effects in squeeze films and externally pressurized bearing with power law lubricants, Wear, 51(1978)237.

[144] Shih - I Pai, Viscous flow theory, Laminar flow, Vol.1., D. Van Nostrand Company, Inc.(1956)42.

[145] Jarzebsky, A.B. and Wilkinson, W.L., Non-isothermal developing flow of power law fluid in a converging slit, J. Non-Newtonian Fluid Mech., 12(1983)1.

[146] Pinkus, D. and Wilcock, D.F., Thermal effects in fluid film bearings, Proc. 6th Leeds-Nyon symposium on tribology, from thermal effects in tribology, (1980)8.

[147] Barwell, F.T., Lubrication of bearings, Butterworths scientific publications (1956)148.

[148] Markho, P.H., A study of the lubrication and dynamics of cylindrical rollers, Ph.D. Thesis, The University of Leeds, England (1972).

[149] Murch, L.E., A thermal EHD zone analysis, J. Lub. Tech., 97(1975)212.

[150] Jacobson, B. and Vinet, P., A model for the influence of pressure on the bulk modulus and the influence of temperature on the solidification pressure for liquid lubricants, J. Tribology, 109(1987)709.

[151] Hamrock, B.J. and Jacobson, B.O., EHL of line contact, Trans. ASLE, 27(1984)275.

[152] Dowson, D. and Higginson, G.R., New roller bearing lubrication formula, Engineering (London) 4972, 192(1961)158.

[153] Lubrecht, A.A, Napel, W.E.T, and Bosma, R., Multigrid, an alternative method for calculating film thickness and pressure profiles in EHD lubricated line contacts, J. Tribology, 108(1986)551.

[154] Lebeck, A.O., Parallel sliding load support in the mixed friction regime, Part I-The experimental data and part II-Evaluation of the mechanisms, J. Tribology, 109(1987)189-203.

[155] Gross, W.A., Gas film lubrication, John Wiley and Sons, Inc. New York, London, (1962)46.

[156] Pascovici, M.D., Temperature distribution in lubricant film of slider bearing under intensive lubricant wall heat transfer conditions, Wear, 29(1974)227.

[157] Pascovici, M.D., Experimental study of the influence of heat transfer on the temperature distribution in a lubricant film, Wear, 29(1974)59.

[158] Malik, M., Dass, B. and Sinhasan, R., The analysis of hydrodynamic journal bearings using non-Newtonian lubricants by viscosity averaging across the film. Trans. ASLE, 26(1983)459.

[159] Heyes, D.M. and Montroso, C.J., Non-linear shear stress and thermal effects in fully flooded EHD line contact, Trans. ASME, J. Lub. Tech. 102(1980)459.

[160] Sadeghi, F. and Dow, T.A., Thermal effects in rolling sliding contacts, Trans. ASME, J. Tribology, 109(1987)512.

[161] Ramanaiah, G., Inertia effects in hydromagnetic lubrication, App. Sci. Res., 19(1968)213.

[162] Mori, A., Tanaka, K. and Mori, H., Effects of fluid inertia forces on the performance of plane annular thrust bearing under laminar condition, J. Tribology, 107(1985)46.

[163] Zuk, J., Storm, T.N. Ludwig, L.P. and Johnson, R.L., Convective inertia and gas ingestion effects on flow regimes of the visco-seal theory and experiment, Trans. ASLE, 10(1967)273.

[164] Osterle, F. and Saibel, E., On the effect of lubricant inertia in hydrodynamic lubrication, ZAMP, 6(1965)334.

[165] Kettleborough, C.F., Turbulent and inertia flow in slider bearings, Trans. ASLE, 8(1965)286.

[166] Safar, Z.S., Inertia and thermal effects in turbulent flow journal bearings, Wear, 53(1979)325.

[167] Kuzma, D.C., Fluid inertia in squeeze film, Appl. Sci. Res., 18(1967)15.

[168] Milne, A.A., Inertia effects in self acting bearing lubrication theory, Proc. Intl. Symp. on lubr. and Wear, (1965)433.

[169] Ting, L.L. and Mayer, J.E., The effect of temperature and inertia on hydrostatic thrust bearing performance, J. Lub. Tech., 93(1971)307.

[170] Coombs, J.A. and Dowson, D., An experimental investigation of the effects of lubricant inertia in a hydrostatic thrust bearing, Proc. Instn. Mech. Engr., 179 Part 3 (1964)96.

[171] Dowson, D., Smith, E.H. and Taylor, C.M., An experimental study of hydrodynamic film rupture in a steadily loaded non-conformal contact, J. Mech. Engr. Sci., 22(1980)71.

[172] You, H.I. and Lu, S., Inertia effect in hydrodynamic lubrication with film rupture, J. Tribology, 109(1987)86.

[173] Elkouh, A.F., Fluid inertia effects in a squeeze film between two plane annuli, Trans. ASME, J. Tribology, 106(1984)223.

[174] Tichy, J.A., Effect of fluid inertia and viscoelasticity on one dimensional squeeze film, Trans. ASLE, 27(1984)167.

[175] Sadeghi, F., Dow, T.A. and Johnson, R.R., Thermal effects in rolling/sliding contacts : Part-3 Approximate method for prediction of mid-film temperature and sliding traction, J. Tribology, 109(1987)519.

[176] Rashid, M. and Seireg, A., Heat partition and transient temperature distribution in layered concentrated contacts: Part 1-Theoretical model, J. Tribology, 109(1987)487.

[177] Rashid, M. and Seireg, A., Heat partition and transient temperature distribution in layered concentrated contacts : Part 2-Dimensionless relationships and numerical results, J. Tribology, 109(1987)496.

[178] Bush, A.W., Hughes, G.D. and Skinner, P.H., The influence of surface roughness and non-Newtonian effects in elastohydrodynamic lubrication, presented at 10th Leeds/Nyon Symposium on tribology, Leeds 1984.

[179] Shew, S. and Wilson, W.R.D., Viscoplastic lubrication of asperities, J. Lub. Tech., 104(1982)568.